Oxidative Medicine and Cellular Longevity

NRF2 as an Emerging Therapeutic Target

Guest Editors: Ian M. Copple, Albena T. Dinkova-Kostova, Thomas W. Kensler, Karen T. Liby, and W. Christian Wigley

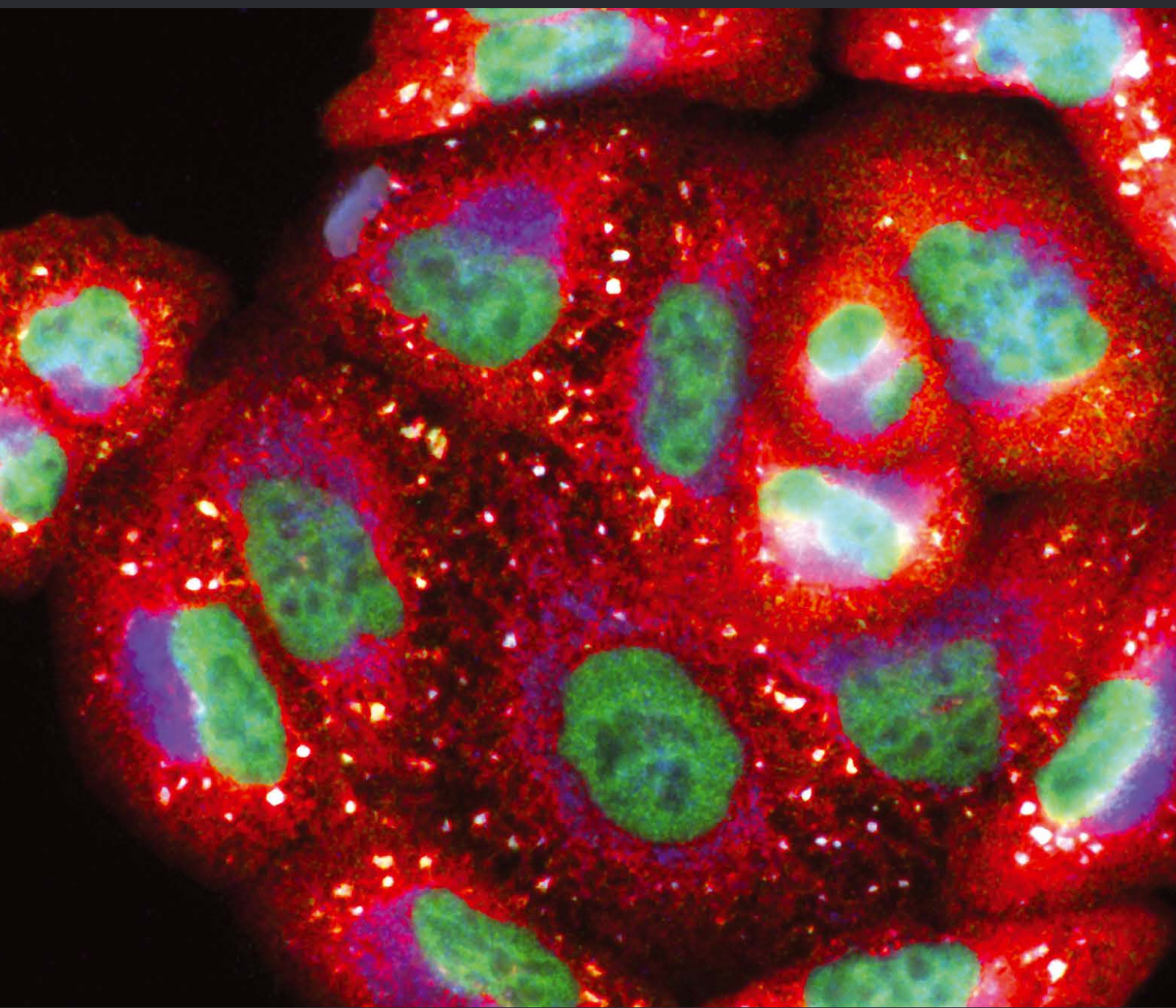

NRF2 as an Emerging Therapeutic Target

Oxidative Medicine and Cellular Longevity

NRF2 as an Emerging Therapeutic Target

Guest Editors: Ian M. Copple, Albena T. Dinkova-Kostova, Thomas W. Kensler, Karen T. Liby, and W. Christian Wigley

Editorial Board

Contents

Hindawi Publishing Corporation
Oxidative Medicine and Cellular Longevity
Volume 2017, Article ID 8165458, 2 pages
http://dx.doi.org/10.1155/2017/8165458

Editorial

NRF2 as an Emerging Therapeutic Target

Ian M. Copple,[1] Albena T. Dinkova-Kostova,[2] Thomas W. Kensler,[3] Karen T. Liby,[4] and W. Christian Wigley[5]

[1]*MRC Centre for Drug Safety Science, Department of Molecular and Clinical Pharmacology, University of Liverpool, Liverpool L69 3GE, UK*
[2]*Division of Cancer Research, School of Medicine, University of Dundee, Dundee DD1 9SY, UK*
[3]*Department of Pharmacology and Chemical Biology, University of Pittsburgh, Pittsburgh, PA 15261, USA*
[4]*Department of Pharmacology and Toxicology, Michigan State University, East Lansing, MI 48824, USA*
[5]*Reata Pharmaceuticals Inc., 2801 Gateway Drive, Irving, TX 75063, USA*

Correspondence should be addressed to Ian M. Copple; icopple@liverpool.ac.uk

Received 21 December 2016; Accepted 22 December 2016; Published 31 January 2017

The transcription factor nuclear factor erythroid 2 related factor 2 (NRF2) is the master regulator of the basal and inducible expression of a large network of cytoprotective genes. As a result, NRF2 plays a key role in antagonising a range of pathological insults including reactive oxygen species and toxic xenobiotics [1]. Consistent with this, dysregulation of NRF2 signalling is associated with an increased susceptibility to and/or accelerated progression of a range of experimental diseases in mice. In recent years, NRF2 has shown promise as a novel therapeutic target in human diseases, particularly those with underlying oxidative and inflammatory stress components [2]. Indeed, several NRF2 inducers have recently entered the clinic and a number of pharmaceutical companies have NRF2-based programs. The goal of this special issue is to highlight the promise of NRF2 as a novel therapeutic target in a number of disease settings and in turn foster further research in this burgeoning field.

NRF2 is dysregulated in numerous human pathologies and thus represents an attractive drug target. A number of electrophilic NRF2 activators, including naturally occurring isothiocyanates and semisynthetic triterpenoids, are currently in clinical trials, and an oral preparation of dimethyl fumarate (DMF, Tecfidera) is used in clinical practice to reduce disease progression in patients with relapsing remitting multiple sclerosis. In multiple sclerosis, neuronal degeneration is linked to glutamate-induced excitotoxicity and oxidative stress, and it has been reported that DMF protects cells against the neurotoxicity of glutamate [3, 4]. In this special issue, C. Hoffmann et al. show that one of the consequences of exposure of cells to DMF is an increase in glutathione recycling by induction of the NRF2 transcriptional target glutathione reductase, the enzyme which catalyzes the regeneration of oxidized glutathione (GSSG) to its reduced (GSH) form. Curiously, however, inhibition (genetic or pharmacological) of glutathione reductase has a synergistic protective effect to that of DMF. The authors further show that this protection correlates with activation of a number of NRF2-dependent genes. These findings confirm the critical cytoprotective role of glutathione, the most abundant intracellular antioxidant, and illustrate the versatility and robustness of NRF2-mediated cytoprotection.

Two papers in this special issue highlight the protective effect of NRF2 in the eye. K. Takayama et al. describe a role for NRF2 in protection against blue light retinal pigment epithelial (RPE) cell damage. Specifically, the authors show that blue light exposure (450 nm) stimulates reactive oxygen species generation and NRF2 signalling in a human RPE cell line, and that primary RPE cells from transgenic Nrf2 knockout mice are more sensitive to blue light induced cell death compared with cells from wild type mice.

Using a pharmacological approach, X. Xu et al. show that the flavonoid apigenin protects a human RPE cell line against tert-butyl hydroperoxide-induced oxidative stress and cell death via the stimulation of NRF2 signalling, with

the protective effect abolished following siRNA knockdown of NRF2. The findings of these studies are consistent with previous work showing that aged Nrf2 knockout mice develop ocular pathology with similar features to human age-related muscular degeneration, a leading cause of blindness [5]. These and other preclinical studies highlight the potential of NRF2 as a novel therapeutic target in ocular disease, and may inform future clinical trials in this area.

Angiotensin II (Ang II) is a vasoconstrictive hormone and a key component of the renin-angiotensin system, which regulates vascular tone and blood pressure. Although largely associated with effects on vascular smooth muscle and kidney epithelia, receptors for Ang II are present in testes, suggesting a potential role in male fertility. S.-J. Wang et al. have contributed with an interesting study assessing the effects of Ang II on testicular cell viability and the potential impact of Nrf2 induction with the isothiocyanate sulforaphane. In wild type and Nrf2 knockout mice, treatment with Ang II was associated with testicular weight loss, oxidative and endoplasmic reticulum stress, inflammation, and apoptotic cell death. Treatment with sulforaphane was protective in wild type mice but not in those lacking Nrf2, demonstrating the Nrf2-dependence of the efficacy. These results further illustrate the importance of Nrf2 in male fertility and provide additional insights into the influence of Ang II signalling on testicular health and function.

Our expanding knowledge of the regulatory influences on NRF2 activity continues to inform new strategies for targeting the transcription factor beyond the use of electrophilic agents that have the ability to modify critical cysteine residues in KEAP1, the redox-sensitive repressor of NRF2. Indeed, compounds and peptides that disrupt the binding interface between NRF2 and KEAP1 have been described [6] and may represent an important alternative therapeutic approach given the propensity of some electrophiles to react with unintended targets. In their review, H. Yukitake et al. highlight the role of macrophage migration inhibitory factor (MIF) as a regulator of NRF2-driven gene expression. The authors describe how a chemical screening process identified the cardioprotective agent BTZO-1, which was subsequently found to augment the expression of NRF2-regulated genes in a MIF-dependent manner, similarly to recombinant MIF protein. In proposing that MIF is an alternative sensor for electrophilic NRF2 activators, H. Yukitake et al. highlight the importance of appreciating the selectivity of small molecules that target NRF2 and other signalling pathways, particularly for understanding the role of NRF2 per se in the therapeutic effects of a given compound.

Zebrafish (*Danio rerio*) are an important and widely used vertebrate model organism for studies on development and gene function. Using this model, the Kobayashi laboratory has described previously the evolutionary conservation of Keap1-Nrf2 signalling in defence against oxidative and electrophilic stresses. Herein, V. T. Nguyen et al. describe the conduct of a microarray analysis of zebrafish embryos that either overexpressed Nrf2 or were challenged with small molecule activators of the pathway. These genetic and pharmacologic approaches demonstrate that additional functions of the Nrf2 pathway, namely, the regulation of protein turnover and glucose metabolism that have been observed in higher vertebrates, are conserved in zebrafish. These results provide further support for the notion that the key actions of Nrf2 extend far beyond, evolutionarily and functionally, its canonical actions of affecting xenobiotic metabolism. Indeed, actions on protein turnover and glucose metabolism may be central to the evolutionary development of this important signalling pathway.

In summary, this special issue highlights recent advances in our understanding of the regulatory mechanisms, physiological roles, and cytoprotective effects of NRF2 in a range of preclinical models. At present, the benefits and risks of modulating NRF2 pathway activity in patients are not fully understood, and it is known that NRF2 and KEAP1 may cross-talk with other signalling pathways, such as NF-κB. Indeed, many NRF2 inducers directly influence the activities of these pathways, and thus it will be important to establish the true therapeutic value of modulating NRF2 per se in man. However, with an expanding number of compounds entering clinical trials, the field should be well-placed to answer these and other pertinent questions.

Acknowledgments

We thank the authors and referees for their contributions to the realization of this special issue.

Ian M. Copple
Albena T. Dinkova-Kostova
Thomas W. Kensler
Karen T. Liby
W. Christian Wigley

References

[1] J. L. Clarke, J. B. Murray, B. K. Park, and I. M. Copple, "Roles of Nrf2 in drug and chemical toxicity," *Current Opinion in Toxicology*, vol. 1, pp. 104–110, 2016.

[2] T. Suzuki, H. Motohashi, and M. Yamamoto, "Toward clinical application of the Keap1-Nrf2 pathway," *Trends in Pharmacological Sciences*, vol. 34, no. 6, pp. 340–346, 2013.

[3] P. Albrecht, I. Bouchachia, N. Goebels et al., "Effects of dimethyl fumarate on neuroprotection and immunomodulation," *Journal of Neuroinflammation*, vol. 9, article 163, 2012.

[4] D. Luchtman, R. Gollan, E. Ellwardt et al., "In vivo and in vitro effects of multiple sclerosis immunomodulatory therapeutics on glutamatergic excitotoxicity," *Journal of Neurochemistry*, vol. 136, no. 5, pp. 971–980, 2016.

[5] Z. Zhao, Y. Chen, J. Wang et al., "Age-related retinopathy in NRF2-deficient mice," *PLoS ONE*, vol. 6, no. 4, Article ID e19456, 2011.

[6] G. Wells, "Peptide and small molecule inhibitors of the Keap1-Nrf2 protein-protein interaction," *Biochemical Society Transactions*, vol. 43, pp. 674–679, 2015.

Hindawi Publishing Corporation
Oxidative Medicine and Cellular Longevity
Volume 2017, Article ID 8584930, 6 pages
http://dx.doi.org/10.1155/2017/8584930

Review Article

Macrophage Migration Inhibitory Factor as an Emerging Drug Target to Regulate Antioxidant Response Element System

Hiroshi Yukitake, Masayuki Takizawa, and Haruhide Kimura

Pharmaceutical Research Division, Takeda Pharmaceutical Company Ltd., 26-1 Muraoka-Higashi 2-Chome, Fujisawa, Kanagawa 251-8555, Japan

Correspondence should be addressed to Haruhide Kimura; haruhide.kimura@takeda.com

Received 25 August 2016; Accepted 13 December 2016; Published 16 January 2017

Academic Editor: Ian Copple

Oxidative stress is involved in pathophysiology and pathological conditions of numerous human diseases. Thus, understanding the mechanisms underlying the redox homeostasis in cells and organs is valuable for discovery of therapeutic drugs for oxidative stress-related diseases. Recently, by applying chemical biology approach with an ARE activator, BTZO-1, we found macrophage migration inhibitory factor (MIF) as a new regulator of antioxidant response element- (ARE-) mediated gene transcription. BTZO-1 and its active derivatives bound to MIF and protected cells and organs from oxidative insults via ARE activation in animal models with oxidative stress such as ischemia/reperfusion injury, inflammatory bowel diseases, and septic shock. In this review, we briefly highlight key findings in understanding the MIF-ARE system.

1. Introduction

Reactive oxygen species (ROS) and reactive nitrogen species (RNS) play a dual role, beneficial and deleterious functions, in living systems [1, 2]. ROS at low or moderate physiological concentrations mainly work as important signal mediators in multiple systems, including cellular defensive response and induction of a mitogenic response [1]. Excessive level of ROS/RNS, that is, oxidative stress and nitrosative stress, is harmful and damages cell structures, including lipids and membranes, proteins, and DNA [1, 3, 4]. Overproduction of ROS occurs due to dysregulation of mitochondrial electron transport chain or excessive stimulation of NAD(P)H. Oxidative stress and nitrosative stress are associated with imbalance between production of ROS and a function of enzymatic/nonenzymatic antioxidant reaction system in living organisms, and disturbance of this homeostasis plays a critical role in pathophysiology of human diseases, such as cardiovascular diseases, inflammatory bowel diseases, septic shock, rheumatoid arthritis, Alzheimer's disease, Parkinson's disease, multiple sclerosis, amyotrophic lateral sclerosis, schizophrenia, ischemia/reperfusion, atherosclerosis, diabetes mellitus, cancer, and other diseases, and in aging [1, 5–12]. Therefore, regulation of redox homeostasis would be a promising approach in the treatment and/or prevention of these diseases.

Antioxidant response element (ARE) is one of the control batteries for redox homeostasis. Induction of ARE-regulated gene expression is an intrinsic defense system and decreases oxidative stress in cells and organs [13–16]. ARE is a cis-acting DNA regulatory element located in the regulatory regions of multiple genes encoding phase II detoxifying enzymes and cytoprotective proteins, including glutathione S-transferases (GSTs), heme oxygenase-1 (HO-1), reduced nicotinamide adenine dinucleotide phosphate (NAD(P)H), quinone oxidoreductases (NQOs), UDP-glucuronosyl transferase (UDP-GT), epoxide hydrase, γ-glutamylcysteine synthetase (γ-GCS), and peroxiredoxin 1 [13–17]. Thus, activation of the ARE is of critical importance to cellular protection against oxidative stress and could be a therapeutic target for oxidative stress-related diseases.

2. Macrophage Migration Inhibitory Factor (MIF) as a Key Regulator of Antioxidant Response Element (ARE) System

ARE is an enhancer element having the consensus sequence TGACnnnGC [17, 18]. Many studies have supported the hypothesis that activation of ARE-mediated gene expression is mainly regulated by the transcription factor Nrf2, a member of the cap'n'collar family of basic region-leucine zipper transcription factor [19–22]. Nrf2 is a cytoplasmic protein sequestered by direct binding with the actin-bound protein Keap1 (Kelch ECH associating protein), a Cul3-based E3 ligase [23–25]. Under normal conditions, Nrf2 protein, via direct binding with Keap1, is strictly maintained at low levels by ubiquitination and consequent 26S proteasome degradation [23–29]. Under some pathological conditions, oxidative factors dissociate Keap1-Nrf2 complex, and that leads to increase in Nrf2 protein levels and nuclear translocation of Nrf2. Nrf2 in nucleus dimerizes with small Maf proteins and binds to the ARE, resulting in expression of many phase II detoxyfying and cytoprotective genes [30, 31]. Thus, Keap1-Nrf2 system is an attractive target for the induction of ARE-mediated gene expression.

We recently identified macrophage migration inhibitory factor (MIF) as a key regulator of ARE-mediated gene expression by chemical biology approach using BTZO-1, a 1,3-benzothiazin-4-on derivative, as chemical probe [32]. MIF, also named as glycosylation-inhibiting factor or phenylpyruvate tautomerase, was originally identified as a soluble factor with macrophage migration-inhibiting properties in the culture medium of activated T lymphocytes [33–37]. MIF has been considered as a cytokine regulating innate and acquired immune responses [37–39]. However, molecular behavior and expression pattern of MIF are different from those of conventional cytokines. For example, MIF is produced by a variety of cells, such as monocytes, macrophages, granulocytes, lymphocytes, eosinophils, neutrophils, endocrine cells, epithelial cells, endothelial cells, and smooth muscle cells, and exists as ubiquitous protein both intra- and extracellular [37, 40–46]. MIF has been reported to have a wide variety of other biological functions, such as counterregulation of glucocorticoid in inflammation, negative regulation of p53-mediated growth arrest and apoptosis, and activation of component of the mitogen-activated protein kinase and Jun-activation domain-binding protein-1 (Jab-1) pathway [47–50]; however, its precise function in the majority of cells is not known.

BTZO-1 was originally discovered from our chemical library as a cardiomyocyte-protective agent; BTZO-1 protected rat primary cardiomyocyte from serum deprivation-induced cell death [32]. Investigation of the mode of action of BTZO-1 revealed that BTZO-1 and its active derivatives activated ARE-mediated gene expression. Drug-affinity chromatography and surface plasmon resonance (SPR) biosensor technique showed that BTZO-1 and its active derivatives in both protection of rat primary cardiomyocyte from serum deprivation-induced cell death and ARE activation directly and selectively bound to MIF [32]. The structure-activity relationship of BTZO-1 derivatives in binding to MIF agreed well with that in ARE-mediated gene expression, as well as cardioprotection. Thus, MIF was considered as a molecular target of BTZO-1. In line with this hypothesis, recombinant purified MIF protein induced ARE-mediated gene expression and suppressed nitric oxide- (NO-) induced cardiomyocyte death in vitro [32]. Furthermore, BTZO-1 promoted MIF-induced ARE activation in H9c2 cells, while BTZO-1-induced ARE activation was decreased in the MIF-reduced H9c2 cells transfected with MIF siRNA [32]. The reduction of ARE-mediated gene expression by BTZO-1 in the MIF-reduced H9c2 cells was restored by applying recombinant MIF to the culture medium. Although the precise intracellular signaling pathway to activate ARE-mediated gene expression after BTZO-1-MIF interaction is unknown, our chemical biological approach with BTZO-1 derivatives suggested that MIF has a pivotal role in ARE-mediated gene regulation [32].

Recently, it was reported that MIF antagonized apoptosis induced by cigarette smoke, a generator of oxidative stress, in human pulmonary endothelial cells, and MIF knockout mice potentiated the toxicity of cigarette smoke exposure via increased apoptosis of endothelial cells [51]. Another study demonstrated that MIF expression levels and cellular antioxidant activity levels were age-dependently decreased in lung, and the analysis with MIF knockout mice revealed that the reductions in MIF expression levels contribute to age-related radiation-induced lung injury in mice [52], and the decrease in MIF appears to lead to the dysregulation of Nrf2, antioxidant activities, and Nrf2 nuclear concentrations [52]. Moreover, another group demonstrated that MIF provided cardioprotection during ischemia/reperfusion by reducing oxidative stress [53].

These studies support our discovery that MIF works, at least in part, as an upstream signal node for ARE-mediated gene transcription.

3. Is MIF a Sensor for ARE Activation?

ARE is also named electrophile/xenobiotic response element, and ARE-mediated gene expression is activated by not only oxidative stress but also electrophilic molecules and heavy metals [17, 25]. Keap1 is also known as a sensitive sensor not only for oxidative stress but also for xenobiotics such as electrophilic molecules in cytosol [15, 16, 20–28]. Keap1 is a cysteine-rich protein and its cysteine residues have essential roles in Keap1-dependent ubiquitination of Nrf2 [54, 55]. Oxidative/electrophilic molecules modified these cysteine residues, and these modifications resulted in disruption of efficient ubiquitination of Nrf2 and Nrf2 degradation by proteasome. Following the saturation of Keap1 by dysregulation of degradation of Nrf2, newly synthesized Nrf2 proteins accumulate within the cell and translocate to the nucleus, leading to ARE activation [15, 16, 20–28, 54, 55].

Our binding assays using both wild type and mutant MIFs demonstrated that BTZO-1-MIF interaction required the intact N-terminal Pro1 in MIF [32]. Interestingly, Pro1 is nucleophilic due to its location in a hydrophobic environment and has been reported to interact with electrophiles and alkylating agents [56, 57]. In fact, some of the known ARE

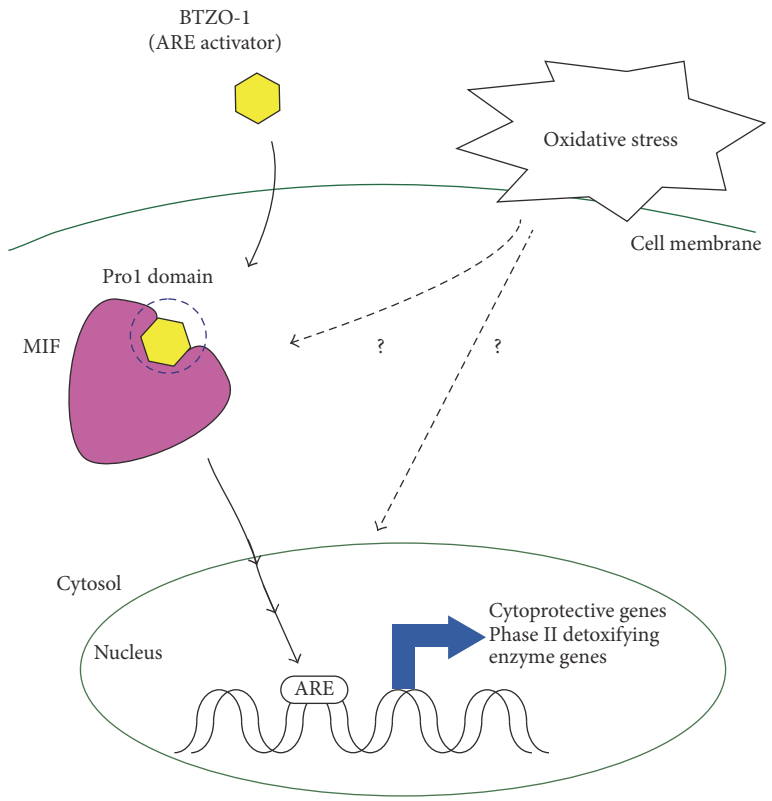

Figure 1: BTZO-1 induces ARE-mediated gene expression via MIF under oxidative conditions. MIF has nucleophilic part around N-terminal Pro1 region and BTZO-1 bound to the Pro1 region.

activators, such as 15-deoxy-Δ12,14-prostaglandin J2 (15d-PGJ2) a lipid-derived electrophilic molecule, bound to Pro1 site in MIF in the scintillation proximity assay using radiolabeled BTZO-1 as a ligand. Known ARE activators with binding affinity to MIF might activate ARE via binding to MIF [32]. Based on these observations, we propose a hypothesis that MIF N-terminal Pro1 domain functions as a sensor for deleterious electrophiles. Further studies to investigate this hypothesis are worth trying.

4. Potential of MIF-ARE System as Therapeutic Target

Disturbance of redox homeostasis plays a critical role in pathophysiology of several human diseases [1, 5–12]. MIF seems to be a sensor for oxidative stress and/or upstream regulator for ARE as described above; thus, MIF-ARE system may become a new therapeutic target for many diseases caused by excessive oxidative stress. In fact, our recent preclinical studies demonstrated that BTZO-2, a BTZO-1 analog with a better ADME profile, protected heart tissues during ischemia/reperfusion injury in rats [32]. BTZO-2 also protected lipopolysaccharide-induced endotoxic shock in mice [58]. BTZO-15, another active BTZO-1 derivative, ameliorated chemically induced colitis in rats [59]. In addition, 15d-PGJ2, which showed MIF binding affinity in a scintillation proximity assay (SPA) [32], exerts anti-inflammatory activity through activation of ARE and suppressed carrageenan-induced pleurisy [60]. Further screenings for ARE activators via MIF are worthwhile, and MIF-ARE system may be a high-value therapeutic target for wider oxidative stress-related diseases beyond Nrf2-ARE system.

5. Development of ARE Activators as Therapeutic Drugs

As discussed, induction of ARE-mediated gene expression is promising as a therapeutic target. However, there are few ARE activators with acceptable safety profiles for therapeutic drugs. ARE system is an intrinsic system against oxidative stress and/or xenobiotics; thus, toxic compounds might show strong efficacy in some drug screening campaigns aiming for ARE-transcriptional activator. These "false-positive toxic compounds" may hinder discovery of safer ARE activators. Therefore, new approaches and/or breakthrough for discovery of safer ARE activators are needed. BTZO-1 was identified in a cell-based and phenotypic screening program aiming for cardioprotective agents. Interestingly, BTZO-1 induced ARE-mediated gene expression without exhibiting cytotoxicity. One unique feature of BTZO-1 is that it activated ARE-mediated gene induction only under oxidative stress conditions, but not under normal conditions (Figure 1) [32]. It is unclear why BTZO-1 induced ARE activation only under

the oxidative stresses conditions, but this aspect of the unique profile of BTZO-1 could provide a novel avenue for understanding regulation of ARE activation and also for discovery of safer ARE activators. Furthermore, MIF-ARE activators like BTZO-1 may have different pharmacodynamics (PD) profiles compared with Keap1-modifying inducers of Nrf2. The difference in PD profiles will depend on Keap1 and MIF expression patterns and their signal contribution in the target tissues for therapy. And if MIF and Keap1 may capture different stresses/ligands, it may also lead to different PD profiles.

6. Future Directions

Clinical development of ARE activators as therapeutic drugs is an active area. For example, dimethyl fumarate (DMF) (Tecfidera™), the effects of which are believed, at least in part, to be mediated via Nrf2-ARE system, has been approved by the U.S. Food and Drug Administration as a therapy for multiple sclerosis [61]. CDDO-Me (2-cyano-3,12-dioxooleana-1,9 (11)-diene-28-oic acid methyl ester), also named as bardoxolone methyl, has been clinically studied against a variety of disorders [62]. Although phase III trials of CDDO-Me for chronic kidney disease in the USA failed because of a high rate of cardiovascular adverse events in subpopulation of susceptible patients with an increased risk for heart failure at baseline [63], several clinical trials, such as for treatment of pulmonary hypertension in the US and for chronic kidney disease associated with type 2 diabetes in Japan, are still ongoing. In cancer, the Nrf2-ARE system has emerged as a new therapeutic target [21, 22]. It was reported that Nrf2-ARE system was constitutively activated in some solid tumors, such as lung cancer and esophageal carcinoma, and it contributed to unfavorable prognosis [21, 64–66]. It was traditionally thought that the cancer cells took over and utilized Nrf2-ARE system for survival and malignant growth [21, 64–66]. However, recent reports suggested that Nrf2-ARE activation by CDDO-Me abrogates the immune-suppressive effects of myeloid-derived suppressor cells (MDSCs) and improves immune responses in cancer patients, and Nrf2 activation in MDSCs prevents cancer cell metastasis [22, 67–71]. There seems to be room to apply ARE activator to cancer therapy. Some reviews and papers have also pointed out that targeting the Nrf2-ARE system is a promising strategy to tackle neurodegenerative disorders [16, 19, 25, 72].

Here, we propose that MIF could be a critical regulator of ARE-mediated gene expression. Quite interestingly, BTZO-1 activated the ARE-mediated gene expression under oxidative stress conditions without showing cytotoxicity. This unique profile of BTZO-1 may open the door for the discovery of new and safer ARE activators as therapeutic drugs for multiple disorders. Drug screening campaigns using radiolabeled BTZO-1 and MIF protein are worth trying to identify novel MIF binders with potential to activate ARE-mediated transcription. Further studies using BTZO-1 derivatives will be needed to narrow down the best indications for ARE activators using the MIF-ARE system.

Competing Interests

All authors are employees of Takeda Pharmaceutical Company Limited.

References

[1] M. Valko, C. J. Rhodes, J. Moncol, M. Izakovic, and M. Mazur, "Free radicals, metals and antioxidants in oxidative stress-induced cancer," *Chemico-Biological Interactions*, vol. 160, no. 1, pp. 1–40, 2006.

[2] M. Valko, D. Leibfritz, J. Moncol, M. T. D. Cronin, M. Mazur, and J. Telser, "Free radicals and antioxidants in normal physiological functions and human disease," *International Journal of Biochemistry and Cell Biology*, vol. 39, no. 1, pp. 44–84, 2007.

[3] W. Dröge, "Free radicals in the physiological control of cell function," *Physiological Reviews*, vol. 82, no. 1, pp. 47–95, 2002.

[4] K. B. Beckman and B. N. Ames, "The free radical theory of aging matures," *Physiological Reviews*, vol. 78, no. 2, pp. 547–581, 1998.

[5] I. Dalle-Donne, R. Rossi, R. Colombo, D. Giustarini, and A. Milzani, "Biomarkers of oxidative damage in human disease," *Clinical Chemistry*, vol. 52, no. 4, pp. 601–623, 2006.

[6] N. S. Dhalla, R. M. Temsah, and T. Netticadan, "Role of oxidative stress in cardiovascular diseases," *Journal of Hypertension*, vol. 18, no. 6, pp. 655–673, 2000.

[7] P. Jenner, "Oxidative stress in Parkinson's disease," *Annals of Neurology*, vol. 53, no. S3, pp. S26–S38, 2003.

[8] L. M. Sayre, G. Perry, and M. A. Smith, "Oxidative stress and neurotoxicity," *Chemical Research in Toxicology*, vol. 21, no. 1, pp. 172–188, 2008.

[9] F. E. Emiliani, T. W. Sedlak, and A. Sawa, "Oxidative stress and schizophrenia: recent breakthroughs from an old story," *Current Opinion in Psychiatry*, vol. 27, no. 3, pp. 185–190, 2014.

[10] A. Paschos, R. Pandya, W. C. M. Duivenvoorden, and J. H. Pinthus, "Oxidative stress in prostate cancer: changing research concepts towards a novel paradigm for prevention and therapeutics," *Prostate Cancer and Prostatic Diseases*, vol. 16, no. 3, pp. 217–225, 2013.

[11] M. T. Elnakish, H. H. Hassanain, P. M. Janssen, M. G. Angelos, and M. Khan, "Emerging role of oxidative stress in metabolic syndrome and cardiovascular diseases: important role of Rac/NADPH oxidase," *Journal of Pathology*, vol. 231, no. 3, pp. 290–300, 2013.

[12] N. A. Simonian and J. T. Coyle, "Oxidative stress in neurodegenerative diseases," *Annual Review of Pharmacology and Toxicology*, vol. 36, pp. 83–106, 1996.

[13] T. Nguyen, P. J. Sherratt, and C. B. Pickett, "Regulatory mechanisms controlling gene expression mediated by the antioxidant response element," *Annual Review of Pharmacology and Toxicology*, vol. 43, pp. 233–260, 2003.

[14] X.-L. Chen and C. Kunsch, "Induction of cytoprotective genes through Nrf2/antioxidant response element pathway: a new therapeutic approach for the treatment of inflammatory diseases," *Current Pharmaceutical Design*, vol. 10, no. 8, pp. 879–891, 2004.

[15] J. W. Kaspar, S. K. Niture, and A. K. Jaiswal, "Nrf2:INrf2 (Keap1) signaling in oxidative stress," *Free Radical Biology and Medicine*, vol. 47, no. 9, pp. 1304–1309, 2009.

[16] H. E. de Vries, M. Witte, D. Hondius et al., "Nrf2-induced antioxidant protection: a promising target to counteract ROS-mediated damage in neurodegenerative disease?" *Free Radical Biology and Medicine*, vol. 45, no. 10, pp. 1375–1383, 2008.

[17] T. H. Rushmore and C. B. Pickett, "Transcriptional regulation of the rat glutathione S-transferase Ya subunit gene. Characterization of a xenobiotic-responsive element controlling inducible expression by phenolic antioxidants," *Journal of Biological Chemistry*, vol. 265, no. 24, pp. 14648–14653, 1990.

[18] T. H. Rushmore, M. R. Morton, and C. B. Pickett, "The antioxidant responsive element. Activation by oxidative stress and identification of the DNA consensus sequence required for functional activity," *The Journal of Biological Chemistry*, vol. 266, no. 18, pp. 11632–11639, 1991.

[19] D. A. Johnson and J. A. Johnson, "Nrf2—a therapeutic target for the treatment of neurodegenerative diseases," *Free Radical Biology and Medicine*, vol. 88, pp. 253–267, 2015.

[20] Y. Huang, W. Li, Z.-Y. Su, and A.-N. T. Kong, "The complexity of the Nrf2 pathway: beyond the antioxidant response," *Journal of Nutritional Biochemistry*, vol. 26, no. 12, pp. 1401–1413, 2015.

[21] A. L. Furfaro, N. Traverso, C. Domenicotti et al., "The Nrf2/HO-1 axis in cancer cell growth and chemoresistance," *Oxidative Medicine and Cellular Longevity*, vol. 2016, Article ID 1958174, 14 pages, 2016.

[22] T. Suzuki and M. Yamamoto, "Molecular basis of the Keap1-Nrf2 system," *Free Radical Biology and Medicine*, vol. 88, pp. 93–100, 2015.

[23] K. Itoh, N. Wakabayashi, Y. Katoh et al., "Keap1 represses nuclear activation of antioxidant responsive elements by Nrf2 through binding to the amino-terminal Neh2 domain," *Genes and Development*, vol. 13, no. 1, pp. 76–86, 1999.

[24] L. M. Zipper and R. Timothy Mulcahy, "The Keap1 BTB/POZ dimerization function is required to sequester Nrf2 in cytoplasm," *Journal of Biological Chemistry*, vol. 277, no. 39, pp. 36544–36552, 2002.

[25] I. Buendia, P. Michalska, E. Navarro, I. Gameiro, J. Egea, and R. León, "Nrf2-ARE pathway: an emerging target against oxidative stress and neuroinflammation in neurodegenerative diseases," *Pharmacology and Therapeutics*, vol. 157, pp. 84–104, 2016.

[26] K. Itoh, N. Wakabayashi, Y. Katoh, T. Ishii, T. O'Connor, and M. Yamamoto, "Keap1 regulates both cytoplasmic-nuclear shuttling and degradation of Nrf2 in response to electrophiles," *Genes to Cells*, vol. 8, no. 4, pp. 379–391, 2003.

[27] M. McMahon, K. Itoh, M. Yamamoto, and J. D. Hayes, "Keap1-dependent proteasomal degradation of transcription factor Nrf2 contributes to the negative regulation of antioxidant response element-driven gene expression," *The Journal of Biological Chemistry*, vol. 278, no. 24, pp. 21592–21600, 2003.

[28] Y. Katoh, K. Iida, M.-I. Kang et al., "Evolutionary conserved N-terminal domain of Nrf2 is essential for the Keap1-mediated degradation of the protein by proteasome," *Archives of Biochemistry and Biophysics*, vol. 433, no. 2, pp. 342–350, 2005.

[29] M. McMahon, N. Thomas, K. Itoh, M. Yamamoto, and J. D. Hayes, "Dimerization of substrate adaptors can facilitate Cullin-mediated ubiquitylation of proteins by a 'tethering' mechanism: *a two-site interaction model for the Nrf2-Keap1 complex*," *Journal of Biological Chemistry*, vol. 281, no. 34, pp. 24756–24768, 2006.

[30] T. W. Kensler, N. Wakabayashi, and S. Biswal, "Cell survival responses to environmental stresses via the Keap1-Nrf2-ARE pathway," *Annual Review of Pharmacology and Toxicology*, vol. 47, pp. 89–116, 2007.

[31] G. P. Sykiotis and D. Bohmann, "Stress-activated cap'n'collar transcription factors in aging and human disease," *Science Signaling*, vol. 3, no. 112, p. re3, 2010.

[32] H. Kimura, Y. Sato, Y. Tajima et al., "BTZO-1, a cardioprotective agent, reveals that macrophage migration inhibitory factor regulates are-mediated gene expression," *Chemistry and Biology*, vol. 17, no. 12, pp. 1282–1294, 2010.

[33] J. R. David, "Delayed hypersensitivity in vitro: its mediation by cell-free substances formed by lymphoid cell-antigen interaction," *Proceedings of the National Academy of Sciences of the United States of America*, vol. 56, no. 1, pp. 72–77, 1966.

[34] B. R. Bloom and B. Bennett, "Mechanism of a reaction in vitro associated with delayed-type hypersensitivity," *Science*, vol. 153, no. 3731, pp. 80–82, 1966.

[35] W. Y. Weiser, P. A. Temple, J. S. Witek-Giannotti, H. G. Remold, S. C. Clark, and J. R. David, "Molecular cloning of a cDNA encoding a human macrophage migration inhibitory factor," *Proceedings of the National Academy of Sciences of the United States of America*, vol. 86, no. 19, pp. 7522–7526, 1989.

[36] E. Rosengren, R. Bucala, P. Åman et al., "The immunoregulatory mediator macrophage migration inhibitory factor (MIF) catalyzes a tautomerization reaction," *Molecular Medicine*, vol. 2, no. 1, pp. 143–149, 1996.

[37] T. Calandra and T. Roger, "Macrophage migration inhibitory factor: a regulator of innate immunity," *Nature Reviews Immunology*, vol. 3, no. 10, pp. 791–800, 2003.

[38] J. Bernhagen, R. Krohn, H. Lue et al., "MIF is a noncognate ligand of CXC chemokine receptors in inflammatory and atherogenic cell recruitment," *Nature Medicine*, vol. 13, no. 5, pp. 587–596, 2007.

[39] D. Rajasekaran, S. Zierow, M. Syed, R. Bucala, V. Bhandari, and E. J. Lolis, "Targeting distinct tautomerase sites of D-DT and MIF with a single molecule for inhibition of neutrophil lung recruitment," *The FASEB Journal*, vol. 28, no. 11, pp. 4961–4971, 2014.

[40] J. Nishihira, Y. Koyama, and Y. Mizue, "Identification of macrophage migration inhibitory factor (MIF) in human vascular endothelial cells and its induction by lipopolysaccharide," *Cytokine*, vol. 10, no. 3, pp. 199–205, 1998.

[41] T. Calandra, J. Bernhagen, R. A. Mitchell, and R. Bucala, "The macrophage is an important and previously unrecognized source of macrophage migration inhibitory factor," *Journal of Experimental Medicine*, vol. 179, no. 6, pp. 1895–1902, 1994.

[42] A. G. Rossi, C. Haslett, N. Hirani et al., "Human circulating eosinophils secrete macrophage migration inhibitory factor (MIF). Potential role in asthma," *The Journal of Clinical Investigation*, vol. 101, no. 12, pp. 2869–2874, 1998.

[43] K. Imamura, J. Nishihira, M. Suzuki et al., "Identification and immunohistochemical localization of macrophage migration inhibitory factor in human kidney," *Biochemistry and Molecular Biology International*, vol. 40, no. 6, pp. 1233–1242, 1996.

[44] A. Daryadel, R. F. Grifone, H.-U. Simon, and S. Yousefi, "Apoptotic neutrophils release macrophage migration inhibitory factor upon stimulation with tumor necrosis factor-α," *Journal of Biological Chemistry*, vol. 281, no. 37, pp. 27653–27661, 2006.

[45] T. Shimizu, "Role of macrophage migration inhibitory factor (MIF) in the skin," *Journal of Dermatological Science*, vol. 37, no. 2, pp. 65–73, 2005.

[46] L. Verschuren, J. H. N. Lindeman, J. Van Hajo Bockel, H. Abdul-Hussien, T. Kooistra, and R. Kleemann, "Up-regulation and coexpression of MIF and matrix metalloproteinases in human abdominal aortic aneurysms," *Antioxidants and Redox Signaling*, vol. 7, no. 9-10, pp. 1195–1202, 2005.

[47] T. Calandra, J. Bernhagen, C. N. Metz et al., "MIF as a glucocorticoid-induced modulator of cytokine production," *Nature*, vol. 377, no. 6544, pp. 68–71, 1995.

[48] J. D. Hudson, M. A. Shoaibi, R. Maestro, A. Carnero, G. J. Hannon, and D. H. Beach, "A proinflammatory cytokine inhibits p53 tumor suppressor activity," *Journal of Experimental Medicine*, vol. 190, no. 10, pp. 1375–1382, 1999.

[49] R. A. Mitchell, C. N. Metz, T. Peng, and R. Bucala, "Sustained mitogen-activated protein kinase (MAPK) and cytoplasmic phospholipase A2 activation by macrophage migration inhibitory factor (MIF). Regulatory role in cell proliferation and glucocorticoid action," *The Journal of Biological Chemistry*, vol. 274, no. 25, pp. 18100–18106, 1999.

[50] R. Kleemann, A. Hausser, G. Geiger et al., "Intracellular action of the cytokine MIF to modulate AP-1 activity and the cell cycle through Jab1," *Nature*, vol. 408, no. 6809, pp. 211–216, 2000.

[51] J. Fallica, L. Boyer, B. Kim et al., "Macrophage migration inhibitory factor is a novel determinant of cigarette smoke-induced lung damage," *American Journal of Respiratory Cell and Molecular Biology*, vol. 51, no. 1, pp. 94–103, 2014.

[52] B. Mathew, J. R. Jacobson, J. H. Siegler et al., "Role of migratory inhibition factor in age-related susceptibility to radiation lung injury via NF-E2-related factor-2 and antioxidant regulation," *American Journal of Respiratory Cell and Molecular Biology*, vol. 49, no. 2, pp. 269–278, 2013.

[53] K. Koga, A. Kenessey, S. R. Powell, C. P. Sison, E. J. Miller, and K. Ojamaa, "Macrophage migration inhibitory factor provides cardioprotection during ischemia/reperfusion by reducing oxidative stress," *Antioxidants and Redox Signaling*, vol. 14, no. 7, pp. 1191–1202, 2011.

[54] I. M. Copple, "The Keap1-Nrf2 cell defense pathway—a promising therapeutic target?" *Advances in Pharmacology*, vol. 63, pp. 43–79, 2012.

[55] K. I. Tong, A. Kobayashi, F. Katsuoka, and M. Yamamoto, "Two-site substrate recognition model for the Keap1-Nrf2 system: a hinge and latch mechanism," *Biological Chemistry*, vol. 387, no. 10-11, pp. 1311–1320, 2006.

[56] P. D. Senter, Y. Al-Abed, C. N. Metz et al., "Inhibition of macrophage migration inhibitory factor (MIF) tautomerase and biological activities by acetaminophen metabolites," *Proceedings of the National Academy of Sciences of the United States of America*, vol. 99, no. 1, pp. 144–149, 2002.

[57] E. Lolis and R. Bucala, "Macrophage migration inhibitory factor," *Expert Opinion on Therapeutic Targets*, vol. 7, no. 2, pp. 153–164, 2003.

[58] H. Yukitake, H. Kimura, Y. Tajima et al., "BTZO-2, an antioxidant response element-activator, provides protection against lethal endotoxic shock in mice," *European Journal of Pharmacology*, vol. 700, no. 1–3, pp. 80–85, 2013.

[59] H. Yukitake, H. Kimura, H. Suzuki et al., "BTZO-15, an ARE-activator, ameliorates DSS- and TNBS-induced colitis in rats," *PLoS ONE*, vol. 6, no. 8, Article ID e23256, 2011.

[60] K. Itoh, M. Mochizuki, Y. Ishii et al., "Transcription factor Nrf2 regulates inflammation by mediating the effect of 15-Deoxy-$\Delta^{12,14}$-prostaglandin J_2," *Molecular and Cellular Biology*, vol. 24, no. 1, pp. 36–45, 2004.

[61] M. Stangel and R. A. Linker, "Dimethyl fumarate (BG-12) for the treatment of multiple sclerosis," *Expert Review of Clinical Pharmacology*, vol. 6, no. 4, pp. 355–362, 2013.

[62] P. E. Pergola, P. Raskin, R. D. Toto et al., "Bardoxolone methyl and kidney function in CKD with type 2 diabetes," *New England Journal of Medicine*, vol. 365, no. 4, pp. 327–336, 2011.

[63] M. P. Chin, D. Wrolstad, G. L. Bakris et al., "Risk factors for heart failure in patients with type 2 diabetes mellitus and stage 4 chronic kidney disease treated with bardoxolone methyl," *Journal of Cardiac Failure*, vol. 20, no. 12, pp. 953–958, 2014.

[64] X.-J. Wang, Z. Sun, N. F. Villeneuve et al., "Nrf2 enhances resistance of cancer cells to chemotherapeutic drugs, the dark side of Nrf2," *Carcinogenesis*, vol. 29, no. 6, pp. 1235–1243, 2008.

[65] H. M. Leinonen, E. Kansanen, P. Pölönen, M. Heinäniemi, and A.-L. Levonen, "Dysregulation of the Keap1-Nrf2 pathway in cancer," *Biochemical Society Transactions*, vol. 43, pp. 645–649, 2015.

[66] E. J. Moon and A. Giaccia, "Dual roles of NRF2 in tumor prevention and progression: possible implications in cancer treatment," *Free Radical Biology and Medicine*, vol. 79, pp. 292–299, 2015.

[67] D. S. Hong, R. Kurzrock, J. G. Supko et al., "A phase I first-in-human trial of bardoxolone methyl in patients with advanced solid tumors and lymphomas," *Clinical Cancer Research*, vol. 18, no. 12, pp. 3396–3406, 2012.

[68] Y.-Y. Wang, Y.-X. Yang, H. Zhe, Z.-X. He, and S.-F. Zhou, "Bardoxolone methyl (CDDO-Me) as a therapeutic agent: an update on its pharmacokinetic and pharmacodynamic properties," *Drug Design, Development and Therapy*, vol. 8, pp. 2075–2088, 2014.

[69] S. Nagaraj, J.-I. Youn, H. Weber et al., "Anti-inflammatory triterpenoid blocks immune suppressive function of MDSCs and improves immune response in cancer," *Clinical Cancer Research*, vol. 16, no. 6, pp. 1812–1823, 2010.

[70] H. Satoh, T. Moriguchi, K. Taguchi et al., "Nrf2-deficiency creates a responsive microenvironment for metastasis to the lung," *Carcinogenesis*, vol. 31, no. 10, pp. 1833–1843, 2010.

[71] K. Hiramoto, H. Satoh, T. Suzuki et al., "Myeloid lineage-specific deletion of antioxidant system enhances tumor metastasis," *Cancer Prevention Research*, vol. 7, no. 8, pp. 835–844, 2014.

[72] M. Dumont, E. Wille, N. Y. Calingasan et al., "Triterpenoid CDDO-methylamide improves memory and decreases amyloid plaques in a transgenic mouse model of Alzheimer's disease," *Journal of Neurochemistry*, vol. 109, no. 2, pp. 502–512, 2009.

Hindawi Publishing Corporation
Oxidative Medicine and Cellular Longevity
Volume 2017, Article ID 5374897, 12 pages
http://dx.doi.org/10.1155/2017/5374897

Research Article

Sulforaphane Prevents Angiotensin II-Induced Testicular Cell Death via Activation of NRF2

Yonggang Wang,[1,2] Hao Wu,[3] Ying Xin,[2,4] Yang Bai,[2,5] Lili Kong,[2,6] Yi Tan,[2,7] Feng Liu,[8] and Lu Cai[2,7]

[1]*Department of Urology, China-Japan Union Hospital of Jilin University, 126 Xiantai St, Changchun, Jilin 130033, China*
[2]*Pediatric Research Institute, Department of Pediatrics, Wendy L. Novak Diabetes Care Center, University of Louisville, 570 S Preston St, Louisville, KY 40202, USA*
[3]*Department of Nephrology, The Second Hospital of Jilin University, 218 Ziqiang St, Changchun, Jilin 130041, China*
[4]*The Key Laboratory of Pathobiology, Ministry of Education, The Norman Bethune Medical College, Jilin University, Changchun, Jilin 130021, China*
[5]*Cardiovascular Center, The First Hospital of Jilin University, 71 Xinmin St, Changchun, Jilin 130021, China*
[6]*Department of Nephrology, The First Hospital of Jilin University, 71 Xinmin St, Changchun, Jilin 130021, China*
[7]*Chinese-American Research Institute for Diabetic Complications, School of Pharmaceutical Science, Wenzhou Medical University, Wenzhou, Zhejiang, China*
[8]*Department of Nephrology, China-Japan Union Hospital of Jilin University, Changchun, China, 126 Xiantai St, Changchun, Jilin 130033, China*

Correspondence should be addressed to Hao Wu; wuhaobaha@jlu.edu.cn, Feng Liu; jdliufeng@163.com, and Lu Cai; l0cai001@louisville.edu

Received 31 July 2016; Revised 28 November 2016; Accepted 12 December 2016; Published 16 January 2017

Academic Editor: Christian Wigley

Although angiotensin II (Ang II) was reported to facilitate sperm motility and intratesticular sperm transport, recent findings shed light on the efficacy of Ang II in stimulating inflammatory events in testicular peritubular cells, effect of which may play a role in male infertility. It is still unknown whether Ang II can induce testicular apoptotic cell death, which may be a more direct action of Ang II in male infertility. Therefore, the present study aims to determine whether Ang II can induce testicular apoptotic cell death and whether this action can be prevented by sulforaphane (SFN) via activating nuclear factor (erythroid-derived 2)-like 2 (NRF2), the governor of antioxidant-redox signalling. Eight-week-old male C57BL/6J wild type (WT) and *Nrf2* gene knockout mice were treated with Ang II, in the presence or absence of SFN. In WT mice, SFN activated testicular NRF2 expression and function, along with a marked attenuation in Ang II-induced testicular oxidative stress, inflammation, endoplasmic reticulum stress, and apoptotic cell death. Deletion of the *Nrf2* gene led to a complete abolishment of these efficacies of SFN. The present study indicated that Ang II may result in testicular apoptotic cell death, which can be prevented by SFN via the activation of NRF2.

1. Introduction

Infertility affects 6.1 million US couples, representing 10% of reproductive-age adults and 15% of all couples trying to conceive. Half of the time, infertility is the result of an abnormal semen analysis or other male factors [1]. Therefore, there remains an urgent need to identify novel targets and develop novel medicines to prevent male infertility.

Although angiotensin II (Ang II) exerts significant functions in multiple organs and systems [2–4], little is known about Ang II action in male infertility. Both Ang II type 1 and type 2 receptors are found in testis [5], indicating that Ang II may have an important impact on male reproductive function. Previous findings showed that Ang II facilitated human sperm motility [5, 6]. Hence, Ang II may play a beneficial role in male fertility. However, a recent study by Welter et al. showed that Ang II also generated inflammatory events in testicular peritubular cells, in addition to the cell contraction [7]. Consequently, the induction of inflammation by Ang II may exert negative effects in male fertility.

Ang II is found to induce oxidative stress [8, 9]. Previously we reported that Ang II played a critical role in cardiac alcohol-induced cardiac nitrosative damage, cell death, remodelling, and cardiomyopathy [10]. We also found that Ang II activated NADPH oxidase-mediated nitrosative damage to induce pulmonary fibrosis [11]. Notably, oxidative stress contributes to testicular apoptotic cell death [12–16]. Oxidative stress is also known to induce endoplasmic reticulum (ER) stress [17, 18], which has also been demonstrated to play an important role in testicular apoptotic cell death [19–23]. Moreover, a crosstalk has been established between oxidative stress and ER stress [24, 25]. NRF2 controls cellular defence mechanisms against oxidative stress [26] by turning on the transcription of antioxidant genes, such as *Ho1* and *Nqo1* [27, 28]. Notably, NRF2 plays a critical role in prevention of male infertility, since *Nrf2*-null male mice developed infertility in an age-dependent manner [29]. Therefore, NRF2 activation may be a promising strategy to ameliorate Ang II-induced testicular apoptotic cell death.

SFN is a potent activator of NRF2 [30, 31]. We have demonstrated the critical role of NRF2 in SFN protection against diabetes-induced testicular apoptosis [32], diabetic nephropathy [31], and diabetic cardiomyopathy [33]. However, it is unclear whether or how much NRF2 may contribute to the effect of SFN on Ang II-induced testicular injury. The present study aims to answer the following questions: (1) does Ang II induce testicular apoptotic cell death? (2) Does SFN have protective effect on Ang II-induced testicular injury? (3) Does NRF2 contribute to the protective effect of SFN? And if so, how much? To these ends, *Nrf2*-null mice and their WT controls were subjected to Ang II, in the presence or absence of SFN.

2. Methods

2.1. Animal Treatment. *Nrf2*-null ($Nrf2^{-/-}$) mice with C57BL/6J background (WT) were obtained through breeding of homozygote ($Nrf2^{-/-}$) with heterozygote ($Nrf2^{+/-}$) following the mating system suggested by Jackson Laboratory (Bar Harbor, ME, USA). C57BL/6J male mice ($Nrf2^{+/+}$) were also purchased from the Jackson Laboratory. All mice were housed in University of Louisville Research Resources Center at 22°C, on a 12 h light-dark cycle, with free access to standard rodent feed and tap water. The Institutional Animal Care and Use Committee at University of Louisville approved all experimental procedures for these animals, and all procedures complied with the Guide for the Care and Use of Laboratory Animals by the US National Institutes of Health (2011, eighth edition). To test the preventive effect of SFN on Ang II-induced testis injury, as well as the role of NRF2 in SFN action, eight-week-old WT or *Nrf2*-null mice were randomized into the following groups, respectively ($n = 5$ per group): control (Ctrl), SFN-treated control (Ctrl/SFN), Ang II-treated mice (Ang II), and mice treated with Ang II and SFN in combination (Ang II/SFN). Mice received subcutaneous injections of Ang II (Sigma-Aldrich, St Louis, MO, USA, 0.5 mg/Kg) every other day for two months and SFN (Sigma-Aldrich, St Louis, MO, USA, 0.5 mg/Kg) five days each week for three months as previously described [11, 31, 32, 34, 35]. Mice were then killed with their testis and caudae epididymis harvested for analysis. Experimenters of this study were blind to group assignment and outcome assessment.

2.2. Sperm Density Assessment. Caudae epididymis from each mouse was placed in 2 mL Earle's balanced salt solution (Sigma-Aldrich, St. Louis, MO, USA) supplemented with 0.1% bovine serum albumin (Sigma-Aldrich). The epididymis was gently teased with a bent needle to release spermatozoa under observation through a stereomicroscope (Olympus). Sperm density was assessed with a haemocytometer and was presented by spermatozoa count per epididymis [36, 37].

2.3. Western Blot Analysis. Western blot was performed using testis tissue as described in our previous study [38]. The primary antibodies included anti-3-NT (Millipore, Temecula, CA, USA; 1 : 1,000), anti-4-HNE (Alpha Diagnostic, San Antonio, TX, USA; 1 : 3,000), anti-Actin (Santa Cruz Biotechnology, Dallas, TX, USA, 1 : 2,000), anti-ATF4 (Cell Signaling Technology, Danvers, MA, USA, 1 : 1000), anti-Bax (Cell Signaling Technology, 1 : 1000), anti-Bcl-2 (Santa Cruz Biotechnology, 1 : 2,000), anti-caspase-3 (Cell Signaling Technology, 1 : 1000), anti-caspase-8 (Cell Signaling Technology, 1 : 1000), anti-caspase-12 (Cell Signaling Technology, 1 : 1000), anti-CHOP (Cell Signaling Technology, 1 : 1000), anti-Histone H3 (Santa Cruz Biotechnology; 1 : 500), anti-IL-6 (Cell Signaling Technology, 1 : 1000), anti-NRF2 (Santa Cruz Biotechnology, 1 : 1000), anti-TNF-α (Abcam, 1 : 2,000), and anti-VCAM-1 (Santa Cruz Biotechnology, 1 : 500)

2.4. Quantitative Reverse Transcription PCR (qPCR). qPCR was performed as described in our previous studies [39, 40]. Primers for *Ho1* and *Nqo1* were purchased from Life Technologies (Grand Island, NY, USA).

2.5. Histological, Immunohistochemical Staining and Terminal Deoxynucleotidyl Transferase-Mediated dUTP Nick End Labeling (TUNEL) Assay. Testis tissues were fixed immediately in 10% buffered formalin solution after harvesting and were embedded in paraffin and sectioned into 5 μm thick sections onto glass slides. The sections were processed for hematoxylin and eosin (H&E) staining. To test the status of testicular cell apoptosis, TUNEL assay was performed as previously described [32].

2.6. Isolation of Nuclei. Testicular nuclei were isolated using a nuclei isolation kit (Sigma-Aldrich) as previously described [41]. Briefly, testis tissue (30 mg) from each mouse was homogenised for 45 s in 150 μL of cold lysis buffer containing 0.5 μL of dithiothreitol (DTT) and 0.1% Triton X-100. After that, 300 μL of cold 1.8 mol/L cushion solution (Sucrose cushion solution: sucrose cushion buffer: DTT = 900 : 100 : 1) was added to the lysis solution. The mixture was transferred to a new tube preloaded with 150 μL of 1.8 mol/L sucrose cushion solution followed by centrifugation at 30,000 g for 45 min. The supernatant fraction, containing cytosolic components, was aspirated and the nuclei were visible as a thin pellet at the bottom of the tube.

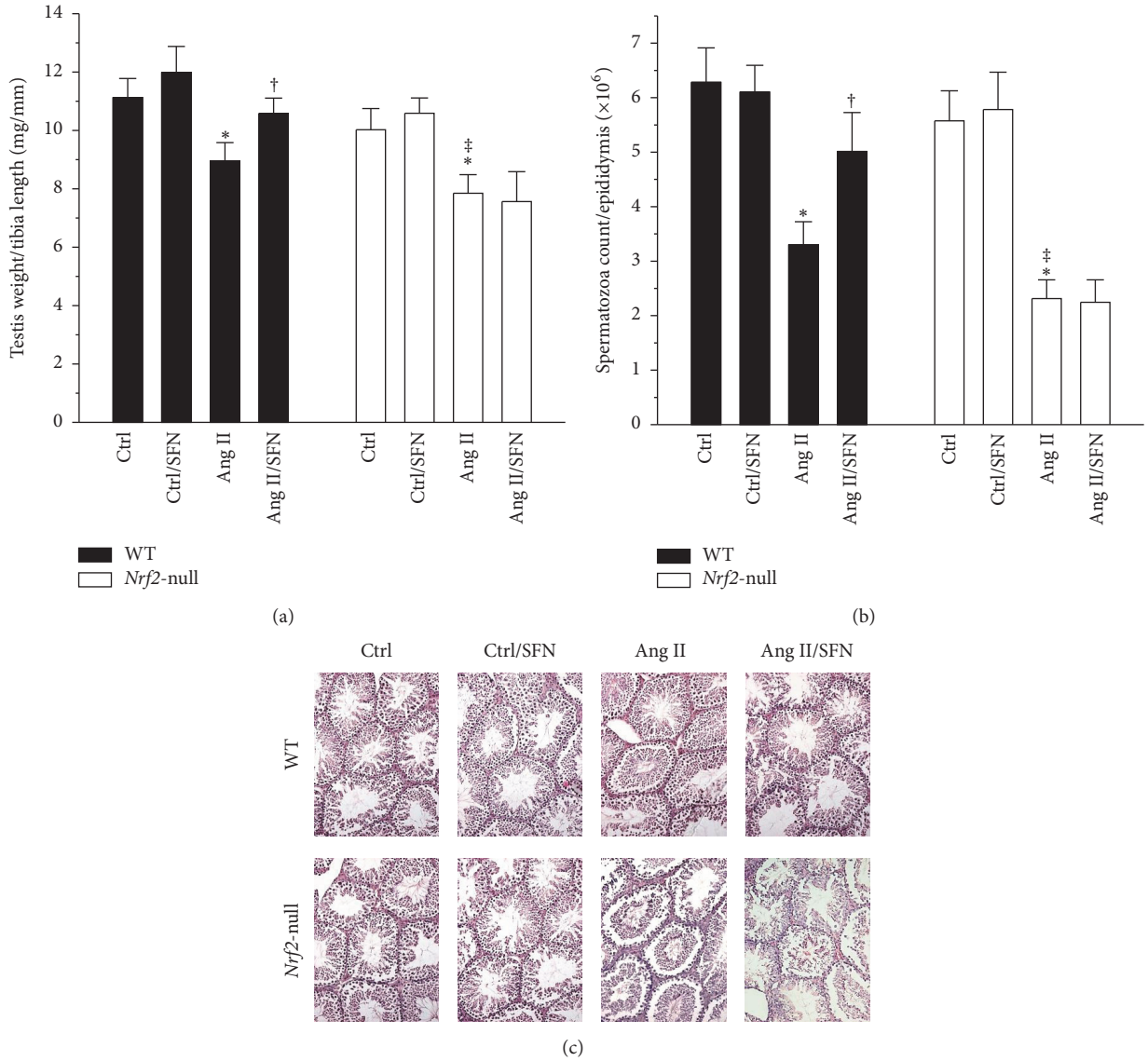

Figure 1: Deletion of the *Nrf2* gene completely abolished SFN protection against Ang II-induced decrease in testicular weight and spermatozoa count. (a) Testis weight to tibia length ratio was calculated after WT and *Nrf2-null* mice were killed. (b) Sperm density assessment was done by performing spermatozoa count. (c) H&E staining was conducted for observation of morphological change. Data are presented as means ± SD ($n = 5$). $^{*}p < 0.05$ versus Ctrl; $^{\dagger}p < 0.05$ versus Ang II. $^{\ddagger}p < 0.05$ versus WT mice treated with Ang II.

2.7. Statistical Analysis. Five mice per group were studied. The measurements for each group were summarised as means ± SD. Image Quant 5.2 (GE Healthcare Bio-Sciences, Pittsburgh, PA, USA) was used to analyse Western blots. One-way ANOVA was performed for comparisons among different groups, followed by post hoc pairwise comparisons using Tukey's test with Origin 8.6 data analysis and graphing software Lab (OriginLab, Northampton, MA, USA). Differences were significant if $p < 0.05$.

3. Results

3.1. Deletion of the Nrf2 Gene Completely Abolished SFN Protection against Ang II-Induced Decrease in Testicular Weight and Spermatozoa Count. *Nrf2*-null mice suffered from a more significant decrease in Ang II-induced testicular weight (Figure 1(a)) and spermatozoa count (Figure 1(b)). WT mice, but not *Nrf2*-null mice, benefited from SFN protection against these injuries (Figures 1(a) and 1(b)). H&E staining showed no significant changes between the groups (Figure 1(c)). These results implicate that testicular apoptotic cell death may play an important role in Ang II-induced testicular weight loss, and NRF2 is required in the protective effect of SFN.

3.2. SFN Alleviated Ang II-Induced Testicular Apoptotic Cell Death through the Activation of NRF2. Ang II resulted in a marked increase in the number of apoptotic cells in the testis of WT mice (Figure 2(a), left panel). Moreover, this effect of Ang II was more prominent in *Nrf2*-null mice (Figure 2(a), right panel). Mitochondrial pathway was further evaluated by determining the protein levels of Bax, Bcl-2, and caspase-3.

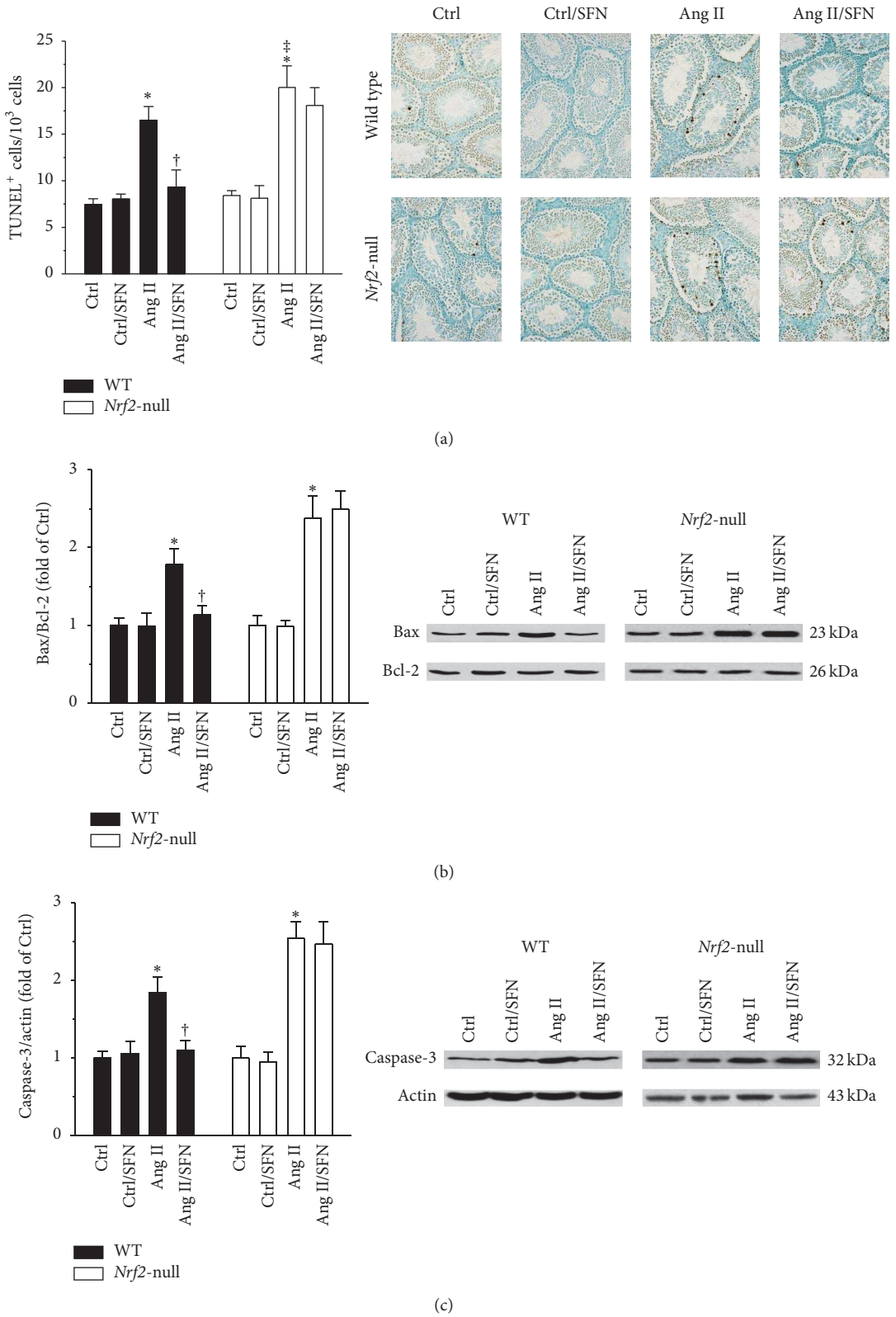

FIGURE 2: SFN alleviated Ang II-induced testicular apoptotic cell death through the activation of NRF2. (a) TUNEL staining was performed to evaluate the effect of SFN on Ang II-induced testicular apoptotic cell death. Mitochondrial pathway was further evaluated by determining (b) the ratio of Bax to Bcl-2 and (c) the protein level of Caspase-3. For (b) and (c), data were normalised by respective Ctrl and presented as means ± SD ($n = 5$). $^{*}p < 0.05$ versus Ctrl; $^{\dagger}p < 0.05$ versus Ang II; $^{\ddagger}p < 0.05$ versus WT mice treated with Ang II.

Ang II produced a significant increase in the ratio of Bax to Bcl-2 (Figure 2(b)) and caspase-3 protein (Figure 2(c)). SFN prevented these effects of Ang II in WT mice (Figures 2(a)–2(c), left panels). However, deletion of the *Nrf2* gene abrogated all these protective effects of SFN (Figures 2(a)–2(c), right panels).

3.3. ER Stress, But Not Receptor Cell Death Pathway, Was Involved in Ang II-Induced Testicular Injury. In the following studies, we defined whether or not ER stress and receptor cell death pathways were involved in Ang II-induced testicular injury. In WT mice, Ang II increased the protein levels of ER stress pathway factors CHOP, caspase-12, BIP, and ATF4, effects of which were markedly prevented by SFN (Figures 3(a)–3(d), left panels). SFN failed to protect the testis from Ang II-induced ER stress in the absence of *Nrf2* (Figures 3(a)–3(d), right panels). No alteration in receptor cell death pathway by either Ang II or SFN was observed, as shown by TNF-α and caspase-8 protein levels (Figures 3(e) and 3(f)).

3.4. NRF2 Was Required for SFN Amelioration of Ang II-Induced Testicular Inflammation. Given that Ang II stimulated testicular inflammation in vitro [7], we tested whether or not Ang II could cause testicular inflammation in vivo. Testicular IL-6 and VCAM-1 proteins were elevated by Ang II, effects of which were significantly inhibited by SFN in WT mice, but not in *Nrf2*-null mice (Figures 4(a) and 4(b)).

3.5. NRF2 Played a Key Role in SFN Protection against Ang II-Induced Testicular Oxidative Stress. The status of testicular oxidative stress was evaluated since NRF2 is known to be the governor of cellular antioxidant activity. 3-NT and 4-HNE, the indicators of nitrosative and oxidative damage, were determined by Western blot. As shown in Figures 5(a) and 5(b), SFN almost completely prevented the Ang II-induced increase in testicular 3-NT and 4-HNE in WT mice (Figures 5(a) and 5(b), left panels), but not in *Nrf2*-null mice (Figures 5(a) and 5(b), right panels).

3.6. Nrf2 Gene Deletion Led to a Complete Loss of SFN Function in Activating Testicular Antioxidant Gene Transcription. NRF2 exerts its function through activation of the transcription of its downstream antioxidant genes. t-NRF2 and n-NRF2 proteins, as well as *Ho1* and *Nqo1* mRNAs, were determined. In WT mice, SFN significantly upregulated testicular t-NRF2 and n-NRF2 proteins (Figures 6(a) and 6(b), left panels), which were not detectable in *Nrf2*-null mice (Figures 6(a) and 6(b), right panels). *Nrf2*-null testis expressed lower *Ho1* and *Nqo1* mRNAs, as compared to WT testis (Figures 6(c) and 6(d)). *Nrf2* gene deletion disabled the efficacy of SFN in increasing the transcription of *Ho1* and *Nqo1* (Figures 6(c) and 6(d)).

4. Discussion

The present study explored the protective effect of SFN on Ang II-induced testicular apoptotic cell death. By using *Nrf2*-null mice, NRF2 was found to play a critical role in this protection, since deletion of the *Nrf2* gene led to a complete abolishment of SFN efficacies in the induction of NRF2 downstream targets and in the amelioration of Ang II-induced testicular oxidative damage, ER stress, inflammation, and apoptotic cell death (Figure 7).

In the present study, Ang II increased *Nrf2* expression and function in WT mice (Figures 6(a)–6(d), left panels). The administration of Ang II turned on NRF2 activation as an adaptive response to oxidative stress induced by Ang II. However, the mild increase of NRF2 by Ang II (Figures 6(a) and 6(b), left panels) was not sufficient to block Ang II-induced testicular oxidative damage (Figures 5(a) and 5(b), left panels). The enhanced oxidative damage was almost completely prevented by SFN (Figures 5(a) and 5(b), left panels) via a more significant increase in *Nrf2* expression and function (Figures 6(a)–6(d), left panels). Although the mild increase of NRF2 by Ang II (Figures 6(a) and 6(b), left panels) failed to block Ang II-induced oxidative damage (Figures 5(a) and 5(b), left panels), NRF2 still exerted protective effect, since Ang II produced more severe testicular injuries in *Nrf2*-null mice, as compared to WT mice (Figures 1(a), 1(b), 2(a)–2(c), 3(a)–3(d), 4(a), 4(b), 5(a) and 5(b)).

Ang II is reported to facilitate sperm motility [5, 6]. However, in addition to this beneficial effect of Ang II, Ang II was also found to account for increased inflammation, according to a recent study by Welter et al. [7]. Therefore, a detrimental aspect of Ang II has been unveiled. Inflammation is positively associated with oxidative stress, which plays a key role in testicular cell death [42]. In line with this notion, we found an increase in these indices, along with reduced sperm density and testicular weight in Ang II-treated mice. Our study could be an in vivo support for the previous findings by Welter et al. [7]. Hormesis is defined by a biphasic dose response with specific quantitative features for the amplitude and width of the stimulation [43]. The induction of hormesis by low level stressor agents could rapidly upregulate adaptive processes to repair damage [43, 44]. Therefore, we assume that the discrepancy between the present study and the study by Rossi et al. [6] could possibly be due to the dose difference of Ang II used between the two studies: Ang II concentration used in the previous publication [6] was 0.2 nM. However, we tested toxicological effect of Ang II at 0.5 mg/kg (roughly equal to 0.96 nM, 4.8-fold the value of 0.2 nM), for a long period in mice. In the latter, the toxicity was prominent, as shown by enhanced testicular oxidative damage (Figures 5(a) and 5(b)), inflammation (Figures 4(a) and 4(b)), ER stress (Figures 3(a)–3(d)), apoptosis (Figure 1(b); Figures 2(a)–2(c)), and weight loss (Figure 1(a)). Secondly, results observed in vitro and in vivo may be different since, under the in vivo condition, systemic responses to chronic exposure of Ang II may generate a more complicate outcome in the testis. These important issues will be further explored in the future study.

NRF2 activators have been applied to clinical trials [45, 46]. Although a phase III study of bardoxolone methyl in the treatment of patients with diabetic nephropathy was terminated due to heart complications [47], NRF2 remains a promising drug target, as evidenced by the approval of dimethyl fumarate (also known as BG-12) for use in

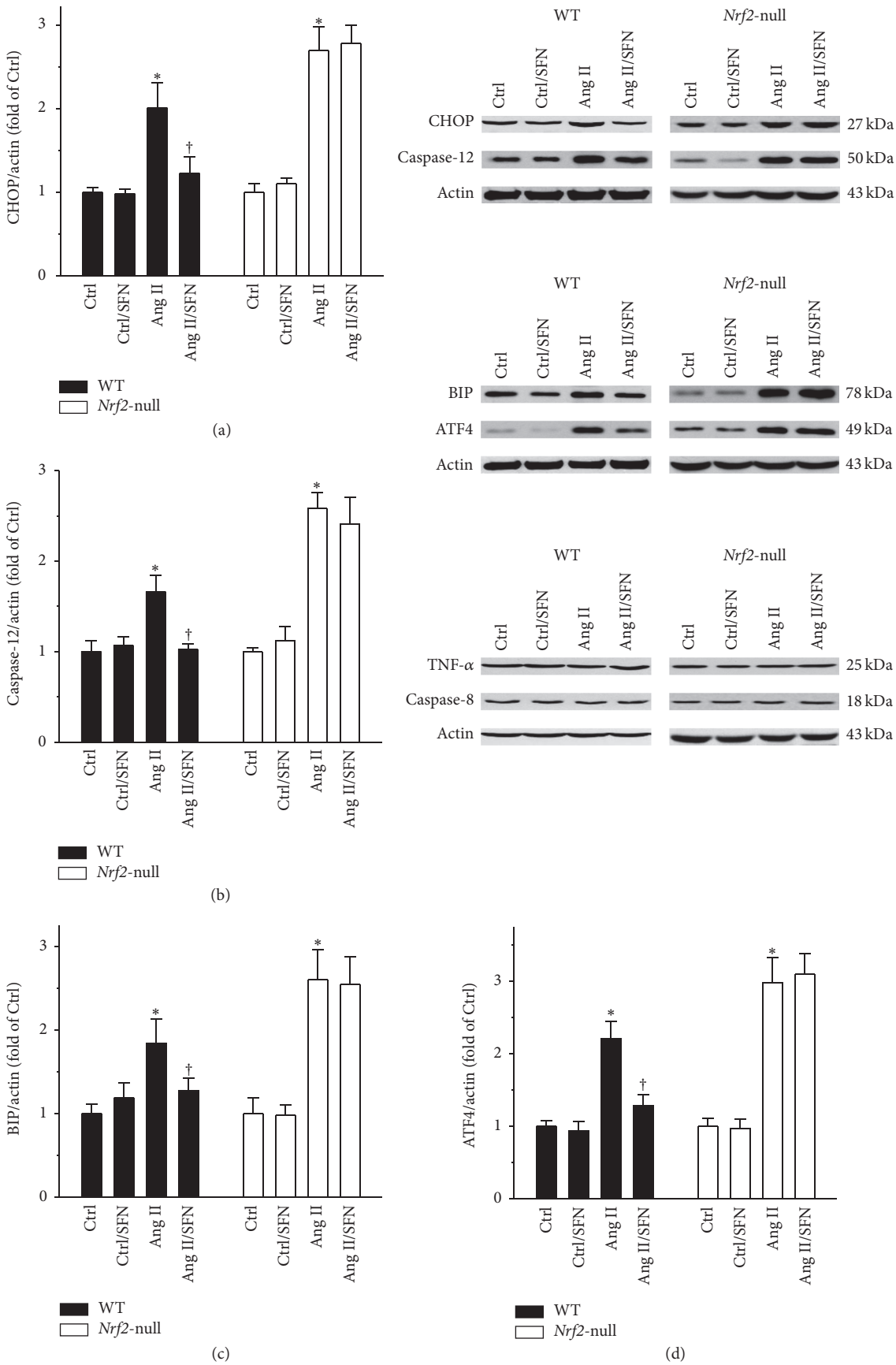

Figure 3: Continued.

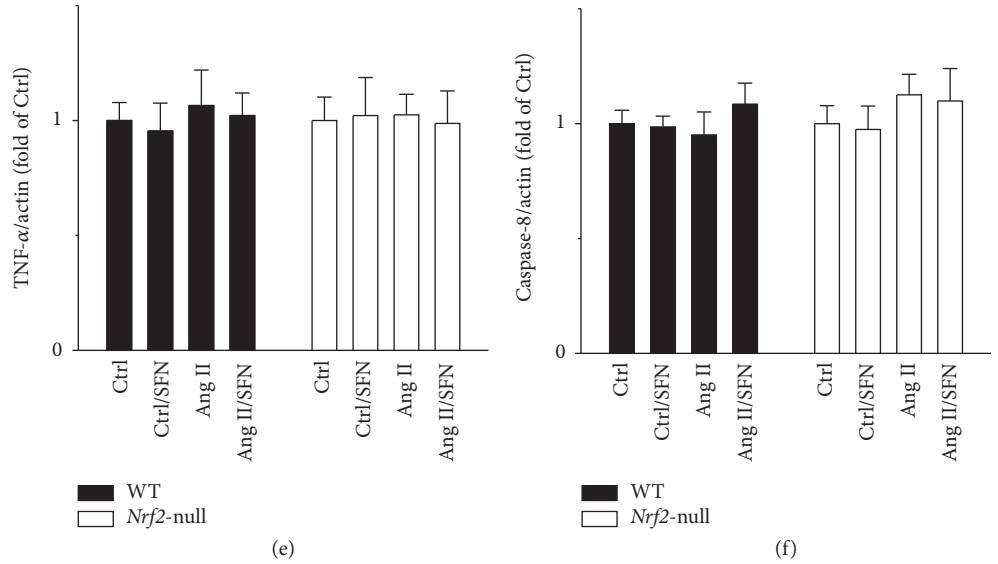

Figure 3: ER stress, but not receptor cell death pathway, was involved in Ang II-induced testicular injury. ER stress was reflected by determining the protein levels of (a) CHOP, (b) caspase-12, (c) BIP, and (d) ATF4. Receptor cell death pathway was also evaluated by determining the protein levels of (e) TNF-α and (f) caspase-8. Data were normalised by respective Ctrl and presented as means ± SD ($n = 5$). $^{*}p < 0.05$ versus Ctrl; $^{\dagger}p < 0.05$ versus Ang II.

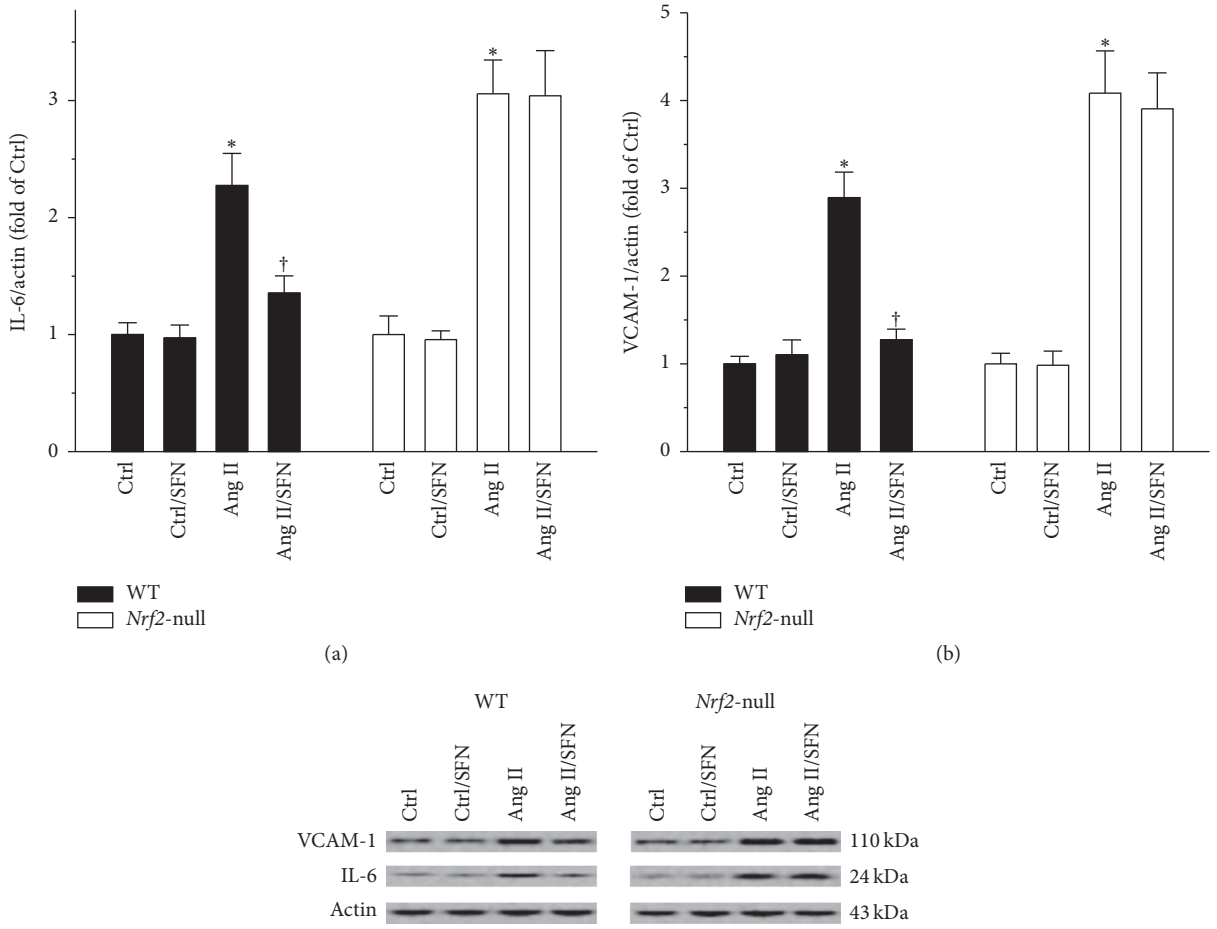

Figure 4: NRF2 was required for SFN amelioration of Ang II-induced testicular inflammation. Testicular inflammatory markers (a) IL-6 and (b) VCAM-1 were measured by Western blot. Data were normalised by respective Ctrl and presented as means ± SD ($n = 5$). $^{*}p < 0.05$ versus Ctrl; $^{\dagger}p < 0.05$ versus Ang II.

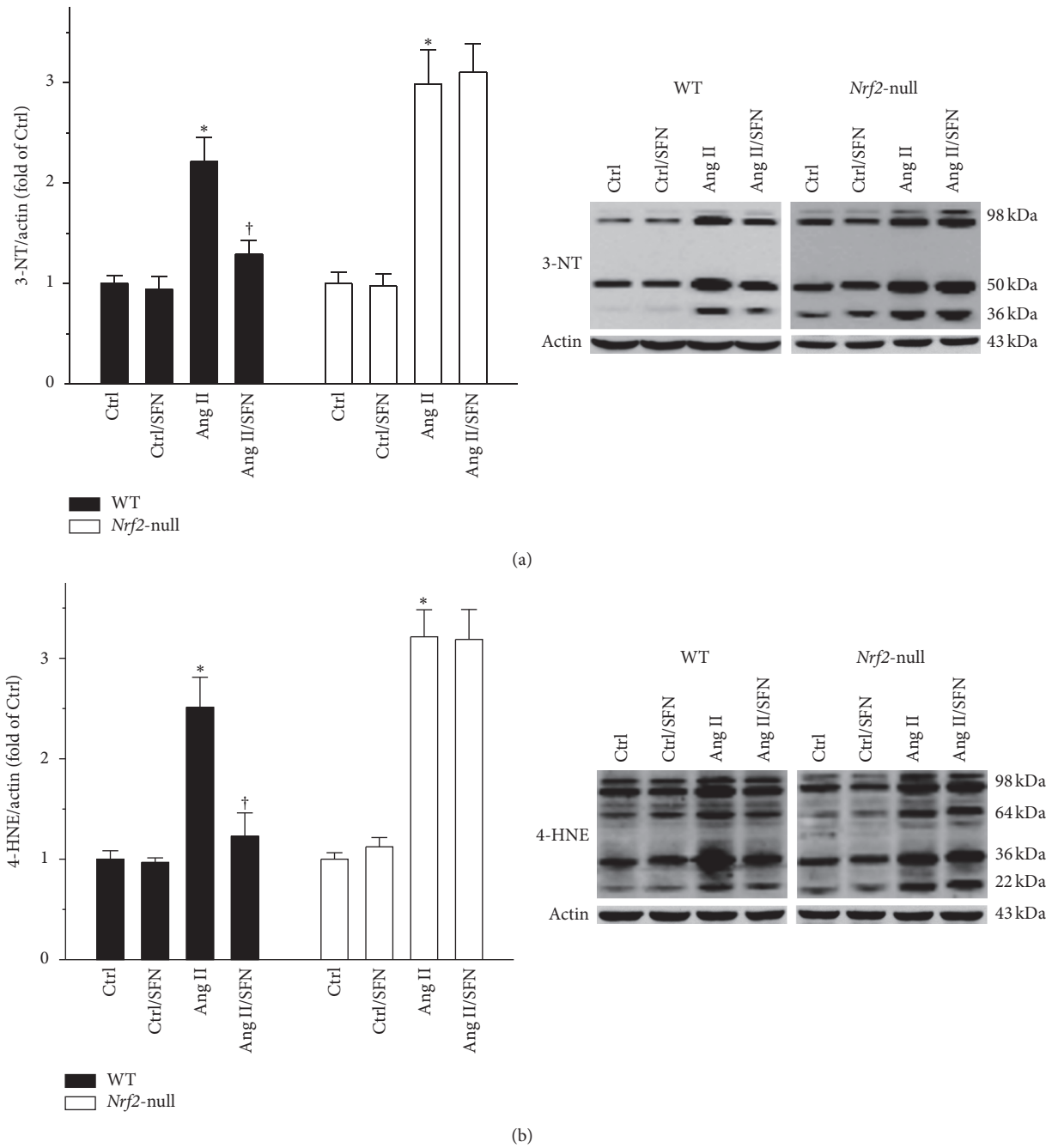

Figure 5: NRF2 played a key role in SFN protection against Ang II-induced testicular oxidative stress. The status of testicular oxidative damage was shown by measuring protein levels of (a) 3-NT and (b) 4-HNE. Data were normalised by respective Ctrl and presented as means ± SD ($n = 5$). $^{*}p < 0.05$ versus Ctrl; $^{\dagger}p < 0.05$ versus Ang II.

multiple sclerosis [48]. The possible reasons for the failure of bardoxolone methyl may be the application in an inappropriate stage of disease, the lack of specificity, and interactions between medicines [49, 50]. Although SFN has been tested in many clinical trials [45], none of these was related to testicular diseases. Moreover, very few studies focused on the effect of SFN on testicular diseases in animal models. Thus, there remains an urgent need to test the effect of SFN on various models of testicular diseases, especially the ones with oxidative stress as the main mechanism.

In summary, the present study indicates, for the first time, that Ang II may exert a detrimental function in inducing testicular apoptotic cell death. Other findings suggest that NRF2 is required for SFN protection against Ang II-induced testicular injury.

Abbreviations

3-NT: 3-Nitrotyrosine
4-HNE: 4-Hydroxynonenal

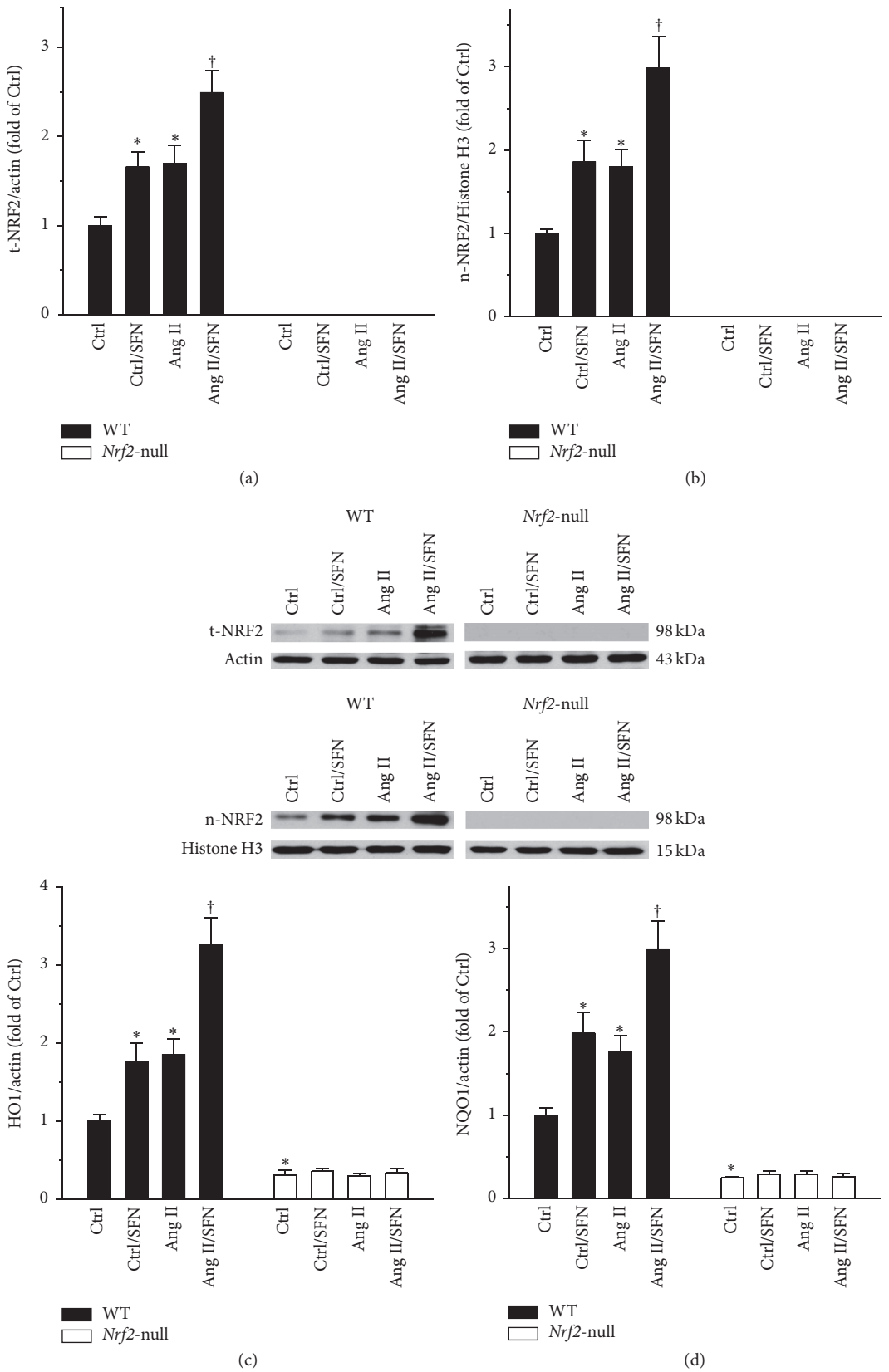

Figure 6: *Nrf2* gene deletion led to a complete loss of SFN function in activating testicular antioxidant gene transcription. *Nrf2* gene expression and function were determined by measuring protein levels of (a) t-NRF2 and (b) n-NRF2, along with (c) *Ho1* and (d) *Nqo1* mRNAs. t-NRF2, total NRF2; n-NRF2, nuclear NRF2. Data were normalised by WT Ctrl and presented as means ± SD ($n = 5$). $^{*}p < 0.05$ versus Ctrl; $^{\dagger}p < 0.05$ versus Ang II.

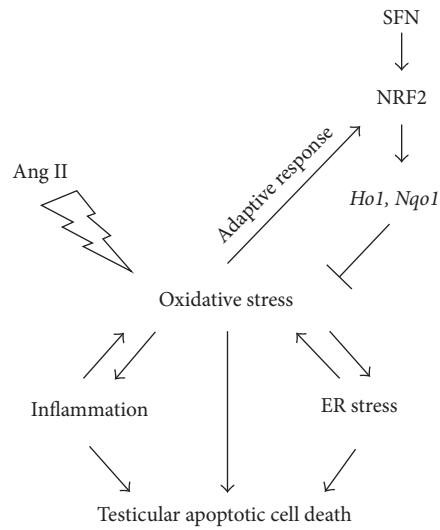

Figure 7: Possible mechanisms for SFN prevention of Ang II-induced testicular apoptotic cell death. Ang II-induced oxidative stress, inflammation, and ER stress contribute to testicular apoptotic cell death. The increased oxidative stress activated NRF2 and the transcription of its downstream target genes *Ho1* and *Nqo1*, as an adaptive mechanism for defence. Ang II-induced testicular damage could further be alleviated by SFN, via the activation of the NRF2 antioxidant signalling.

Actin:	β-Actin
Ang II:	Angiotensin II
ATF4:	Activating transcription factor 4
Bax:	Bcl-2-associated X protein
Bcl-2:	B-cell lymphoma 2
BIP:	Binding immunoglobulin protein
CHOP:	C/EBP homologous protein
DTT:	Dithiothreitol
ER:	Endoplasmic reticulum
HO1:	Heme oxygenase 1
IL-6:	Interleukin 6
NRF2:	Nuclear factor (erythroid-derived 2)-like 2
NQO1:	NAD(P)H dehydrogenase (quinone 1)
SFN:	Sulforaphane
TNF-α:	Tumor necrosis factor-α
VCAM-1:	Vascular cell adhesion molecule-1
WT:	Wild type.

Competing Interests

The authors declare that there is no conflict of interests associated with this article.

Acknowledgments

This work was supported in part by the Natural Science Foundation of Jilin Province (20160101117JC and CZZR2014021) to Yonggang Wang; the Norman Bethune Program of Jilin University (2015438) and the National Natural Science Foundation of China (81600573) to Hao Wu; and the National Institutes of Health grant (1R01DK 091338-01A1) to Lu Cai.

References

[1] M. Chehab, A. Madala, and J. C. Trussell, "On-label and off-label drugs used in the treatment of male infertility," *Fertility and Sterility*, vol. 103, no. 3, pp. 595–604, 2015.

[2] A. B. Atkinson, J. J. Brown, R. Fraser et al., "Angiotensin II and renal hypertension in dog, rat and man: effect of converting enzyme inhibition," *Clinical and Experimental Hypertension*, vol. 2, no. 3-4, pp. 499–524, 1980.

[3] J. T. Fitzsimons, "Angiotensin II in the control of hypovolaemic thirst and sodium appetite," *Canadian Journal of Physiology and Pharmacology*, vol. 58, no. 5, pp. 441–444, 1980.

[4] T. Kono, F. Ikeda, F. Oseko, H. Imura, S. Shimbo, and J. Endo, "Angiotensin II analogue and essential hypertension," *Nippon Rinsho*, vol. 37, no. 10, pp. 3503–3510, 1979.

[5] M. Gianzo, I. Muñoa-Hoyos, I. Urizar-Arenaza et al., "Angiotensin II type 2 receptor is expressed in human sperm cells and is involved in sperm motility," *Fertility and Sterility*, vol. 105, no. 3, pp. 608–616, 2016.

[6] F. Rossi, A. Ferraresi, P. Romagni, L. Silvestroni, and V. Santiemma, "Angiotensin II stimulates contraction and growth of testicular peritubular myoid cells in vitro," *Endocrinology*, vol. 143, no. 8, pp. 3096–3104, 2002.

[7] H. Welter, A. Huber, S. Lauf et al., "Angiotensin II regulates testicular peritubular cell function via AT1 receptor: a specific situation in male infertility," *Molecular and Cellular Endocrinology*, vol. 393, no. 1-2, pp. 171–178, 2014.

[8] S. I. Dikalov, R. R. Nazarewicz, A. Bikineyeva et al., "Nox2-induced production of mitochondrial superoxide in angiotensin II-mediated endothelial oxidative stress and hypertension," *Antioxidants and Redox Signaling*, vol. 20, no. 2, pp. 281–294, 2014.

[9] S. Kossmann, H. Hu, S. Steven et al., "Inflammatory monocytes determine endothelial nitric-oxide synthase uncoupling and nitro-oxidative stress induced by Angiotensin II," *Journal of Biological Chemistry*, vol. 289, no. 40, pp. 27540–27550, 2014.

[10] Y. Tan, X. Li, S. D. Prabhu et al., "Angiotensin II plays a critical role in alcohol-induced cardiac nitrative damage, cell death, remodeling, and cardiomyopathy in a protein kinase c/nicotinamide adenine dinucleotide phosphate oxidase-dependent manner," *Journal of the American College of Cardiology*, vol. 59, no. 16, pp. 1477–1486, 2012.

[11] J. Yang, Y. Tan, F. Zhao et al., "Angiotensin II plays a critical role in diabetic pulmonary fibrosis most likely via activation of NADPH oxidase-mediated nitrosative damage," *American Journal of Physiology—Endocrinology and Metabolism*, vol. 301, no. 1, pp. E132–E144, 2011.

[12] N. Kaushal and M. P. Bansal, "Selenium variation induced oxidative stress regulates p53 dependent germ cell apoptosis: plausible involvement of HSP70-2," *European Journal of Nutrition*, vol. 48, no. 4, pp. 221–227, 2009.

[13] M. Muratori, L. Tamburrino, S. Marchiani et al., "Investigation on the origin of sperm DNA fragmentation: role of apoptosis, immaturity and oxidative stress," *Molecular Medicine*, vol. 21, pp. 109–122, 2015.

[14] K. Shiraishi, H. Takihara, and H. Matsuyama, "Elevated scrotal temperature, but not varicocele grade, reflects testicular oxidative stress-mediated apoptosis," *World Journal of Urology*, vol. 28, no. 3, pp. 359–364, 2010.

[15] Y. Song, Y. Shi, H. Yu, Y. Hu, Y. Wang, and K. Yang, "P,p′-Dichlorodiphenoxydichloroethylene induced apoptosis of Sertoli cells through oxidative stress-mediated p38 MAPK and mitochondrial pathway," *Toxicology Letters*, vol. 202, no. 1, pp. 55–60, 2011.

[16] Y.-C. Yeh, T.-J. Liu, L.-C. Wang et al., "A standardized extract of Ginkgo biloba suppresses doxorubicin-induced oxidative stress and p53-mediated mitochondrial apoptosis in rat testes," *British Journal of Pharmacology*, vol. 156, no. 1, pp. 48–61, 2009.

[17] B. Chhunchha, N. Fatma, E. Kubo, P. Rai, S. P. Singh, and D. P. Singh, "Curcumin abates hypoxia-induced oxidative stress based-ER stress-mediated cell death in mouse hippocampal cells (HT22) by controlling Prdx6 and NF-κB regulation," *American Journal of Physiology—Cell Physiology*, vol. 304, no. 7, pp. C636–C655, 2013.

[18] C. W. Younce and P. E. Kolattukudy, "MCP-1 causes cardiomyoblast death via autophagy resulting from ER stress caused by oxidative stress generated by inducing a novel zinc-finger protein, MCPIP," *Biochemical Journal*, vol. 426, no. 1, pp. 43–53, 2010.

[19] Y. Gong, J. Wu, Y. Huang, S. Shen, and X. Han, "Nonylphenol induces apoptosis in rat testicular Sertoli cells via endoplasmic reticulum stress," *Toxicology Letters*, vol. 186, no. 2, pp. 84–95, 2009.

[20] Y.-L. Ji, H. Wang, C. Zhang et al., "N-acetylcysteine protects against cadmium-induced germ cell apoptosis by inhibiting endoplasmic reticulum stress in testes," *Asian Journal of Andrology*, vol. 15, no. 2, pp. 290–296, 2013.

[21] Y.-L. Ji, H. Wang, X.-F. Zhao et al., "Crosstalk between endoplasmic reticulum stress and mitochondrial pathway mediates cadmium-induced germ cell apoptosis in testes," *Toxicological Sciences*, vol. 124, no. 2, pp. 446–459, 2011.

[22] P. Lin, F. Chen, J. Sun et al., "Mycotoxin zearalenone induces apoptosis in mouse Leydig cells via an endoplasmic reticulum stress-dependent signalling pathway," *Reproductive Toxicology*, vol. 52, pp. 71–77, 2015.

[23] S.-J. Park, T.-S. Kim, C.-K. Park et al., "hCG-induced endoplasmic reticulum stress triggers apoptosis and reduces steroidogenic enzyme expression through activating transcription factor 6 in Leydig cells of the testis," *Journal of Molecular Endocrinology*, vol. 50, no. 2, pp. 151–166, 2013.

[24] A. Dandekar, R. Mendez, and K. Zhang, "Cross talk between ER stress, oxidative stress, and inflammation in health and disease," *Methods in Molecular Biology*, vol. 1292, pp. 205–214, 2015.

[25] H. Kaneto, "Oxidative stress and ER stress in diabetes," *Japanese Journal of Clinical Medicine*, vol. 69, supplement 1, pp. 171–175, 2011.

[26] T. Jiang, Z. Huang, Y. Lin, Z. Zhang, D. Fang, and D. D. Zhang, "The protective role of Nrf2 in streptozotocin-induced diabetic nephropathy," *Diabetes*, vol. 59, no. 4, pp. 850–860, 2010.

[27] T. Nguyen, P. J. Sherratt, and C. B. Pickett, "Regulatory mechanisms controlling gene expression mediated by the antioxidant response element," *Annual Review of Pharmacology and Toxicology*, vol. 43, pp. 233–260, 2003.

[28] W. Dong, Y. Jia, X. Liu et al., "Sodium butyrate activates NRF2 to ameliorate diabetic nephropathy possibly via inhibition of HDAC," *Journal of Endocrinology*, vol. 232, no. 1, pp. 71–83, 2017.

[29] B. N. Nakamura, G. Lawson, J. Y. Chan et al., "Knockout of the transcription factor NRF2 disrupts spermatogenesis in an age-dependent manner," *Free Radical Biology and Medicine*, vol. 49, no. 9, pp. 1368–1379, 2010.

[30] H. Zheng, S. A. Whitman, W. Wu et al., "Therapeutic potential of Nrf2 activators in streptozotocin-induced diabetic nephropathy," *Diabetes*, vol. 60, no. 11, pp. 3055–3066, 2011.

[31] H. Wu, L. Kong, Y. Cheng et al., "Metallothionein plays a prominent role in the prevention of diabetic nephropathy by sulforaphane via up-regulation of Nrf2," *Free Radical Biology & Medicine*, vol. 89, pp. 431–442, 2015.

[32] Y. Wang, Z. Zhang, W. Guo et al., "Sulforaphane reduction of testicular apoptotic cell death in diabetic mice is associated with the upregulation of Nrf2 expression and function," *American Journal of Physiology—Endocrinology and Metabolism*, vol. 307, no. 1, pp. E14–E23, 2014.

[33] Y. Bai, W. Cui, Y. Xin et al., "Prevention by sulforaphane of diabetic cardiomyopathy is associated with up-regulation of Nrf2 expression and transcription activation," *Journal of Molecular and Cellular Cardiology*, vol. 57, no. 1, pp. 82–95, 2013.

[34] Q. Liu, G. Wang, G. Zhou et al., "Angiotensin II-induced p53-dependent cardiac apoptotic cell death: its prevention by metallothionein," *Toxicology Letters*, vol. 191, no. 2-3, pp. 314–320, 2009.

[35] G. Zhou, X. Li, D. W. Hein et al., "Metallothionein suppresses angiotensin II-induced nicotinamide adenine dinucleotide phosphate oxidase activation, nitrosative stress, apoptosis, and pathological remodeling in the diabetic heart," *Journal of the American College of Cardiology*, vol. 52, no. 8, pp. 655–666, 2008.

[36] N. Ben Halima, A. Ben Slima, I. Moalla et al., "Protective effects of oat oil on deltamethrin-induced reprotoxicity in male mice," *Food and Function*, vol. 5, no. 9, pp. 2070–2077, 2014.

[37] A. T. Farag, A. H. Radwan, M. H. Eweidah, R. H. Elmazoudy, and A. E.-K. El-Sebae, "Evaluation of male-mediated reproductive toxic effects of methamidophos in the mouse," *Andrologia*, vol. 44, no. 2, pp. 116–124, 2012.

[38] L. Cai, J. Wang, Y. Li et al., "Inhibition of superoxide generation and associated nitrosative damage is involved in metallothionein prevention of diabetic cardiomyopathy," *Diabetes*, vol. 54, no. 6, pp. 1829–1837, 2005.

[39] Y. Wang, W. Feng, W. Xue et al., "Inactivation of GSK-3β by metallothionein prevents diabetes-related changes in cardiac energy metabolism, inflammation, nitrosative damage, and remodeling," *Diabetes*, vol. 58, no. 6, pp. 1391–1402, 2009.

[40] H. Wu, S. Zhou, L. Kong et al., "Metallothionein deletion exacerbates intermittent hypoxia-induced renal injury in mice," *Toxicology Letters*, vol. 232, no. 2, pp. 340–348, 2015.

[41] H. Wu, L. Kong, Y. Tan et al., "C66 ameliorates diabetic nephropathy in mice by both upregulating NRF2 function via increase in miR-200a and inhibiting miR-21," *Diabetologia*, vol. 59, no. 7, pp. 1558–1568, 2016.

[42] A. Azenabor, A. O. Ekun, and O. Akinloye, "Impact of inflammation on male reproductive tract," *Journal of Reproduction and Infertility*, vol. 16, no. 3, pp. 123–129, 2015.

[43] E. J. Calabrese, G. Dhawan, R. Kapoor, I. Iavicoli, and V. Calabrese, "HORMESIS: a fundamental concept with widespread biological and biomedical applications," *Gerontology*, vol. 62, no. 5, pp. 530–535, 2015.

[44] E. J. Calabrese, "Hormesis: changing view of the dose-response, a personal account of the history and current status," *Mutation Research - Reviews in Mutation Research*, vol. 511, no. 3, pp. 181–189, 2002.

[45] C. A. Houghton, R. G. Fassett, and J. S. Coombes, "Sulforaphane: translational research from laboratory bench to clinic," *Nutrition Reviews*, vol. 71, no. 11, pp. 709–726, 2013.

[46] P. E. Pergola, M. Krauth, J. W. Huff et al., "Effect of bardoxolone methyl on kidney function in patients with T2D and stage 3b-4 CKD," *American Journal of Nephrology*, vol. 33, no. 5, pp. 469–476, 2011.

[47] E. T. Hall and V. Bhalla, "Is there a sweet spot for nrf2 activation in the treatment of diabetic kidney disease?" *Diabetes*, vol. 63, no. 9, pp. 2904–2905, 2014.

[48] R. Gold, L. Kappos, D. L. Arnold et al., "Placebo-controlled phase 3 study of oral BG-12 for relapsing multiple sclerosis," *New England Journal of Medicine*, vol. 367, pp. 1098–1107, 2012.

[49] D. H. Ellison, "Bardoxolone methyl in type 2 diabetes and advanced chronic kidney disease," *New England Journal of Medicine*, vol. 370, no. 18, pp. 1768–1769, 2014.

[50] D. D. Zhang, "Bardoxolone brings Nrf2-based therapies to light," *Antioxidants and Redox Signaling*, vol. 19, no. 5, pp. 517–518, 2013.

Hindawi Publishing Corporation
Oxidative Medicine and Cellular Longevity
Volume 2017, Article ID 6093903, 8 pages
http://dx.doi.org/10.1155/2017/6093903

Research Article

Dimethyl Fumarate Induces Glutathione Recycling by Upregulation of Glutathione Reductase

Christina Hoffmann,[1] Michael Dietrich,[2] Ann-Kathrin Herrmann,[1] Teresa Schacht,[1] Philipp Albrecht,[2] and Axel Methner[1]

[1]*Focus Program Translational Neuroscience (FTN), Rhine Main Neuroscience Network (rmn²) and Department of Neurology, University Medical Center of the Johannes Gutenberg University Mainz, Mainz, Germany*
[2]*Department of Neurology, Heinrich Heine Universität Düsseldorf, Düsseldorf, Germany*

Correspondence should be addressed to Axel Methner; axel.methner@gmail.com

Received 15 June 2016; Revised 5 November 2016; Accepted 16 November 2016; Published 1 January 2017

Academic Editor: Albena Dinkova-Kostova

Neuronal degeneration in multiple sclerosis has been linked to oxidative stress. Dimethyl fumarate (DMF) is an effective oral therapeutic option shown to reduce disease activity and progression in patients with relapsing-remitting multiple sclerosis. DMF activates the transcription factor nuclear factor erythroid 2-related factor 2 (NRF2) leading to increased synthesis of the major cellular antioxidant glutathione (GSH) and prominent neuroprotection *in vitro*. We previously demonstrated that DMF is capable of raising GSH levels even when glutathione synthesis is inhibited, suggesting enhanced GSH recycling. Here, we found that DMF indeed induces glutathione reductase (GSR), a homodimeric flavoprotein that catalyzes GSSG reduction to GSH by using NADPH as a reducing cofactor. Knockdown of GSR using a pool of *E. coli* RNase III-digested siRNAs or pharmacological inhibition of GSR, however, also induced the antioxidant response rendering it impossible to verify the suspected attenuation of DMF-mediated neuroprotection. However, in cystine-free medium, where GSH synthesis is abolished, pharmacological inhibition of GSR drastically reduced the effect of DMF on glutathione recycling. We conclude that DMF increases glutathione recycling through induction of glutathione reductase.

1. Introduction

While an increasing number of therapeutic options have been developed to prevent the acute inflammatory insults in multiple sclerosis (MS) there is an urgent need for an effective treatment for the chronic neuronal degeneration occurring afterwards. This is of special importance as this degeneration is thought to be a major factor driving the development of chronic disability in these patients. A promising target for therapeutic interventions is oxidative stress which is prominently involved in neurodegeneration in MS [1–3]. Dimethyl fumarate (DMF) is an effective oral therapeutic, which reduces disease activity and progression in patients with relapsing-remitting MS [4] and psoriasis [5]. DMF and its active metabolite monomethyl fumarate (MMF) [6–8] exert a number of immunomodulatory effects involving increased apoptosis of T cells stimulated with interleukin-(IL-) 2 or anti-CD3 antibodies [9], inhibition of translocation to the nucleus of the nuclear factor kappa B1/p50 (NF-kB1) induced by the cytokines tumor necrosis factor α and IL-1α [10], and an increased production of protective T helper 2 cytokines IL-4 and IL-5 in CD2/CD8 monoclonal antibody-stimulated peripheral blood mononuclear cells [11]. Besides these immunomodulatory actions, DMF has a prominent antioxidative activity; it first induces short-lived oxidative stress by scavenging the major intracellular antioxidant glutathione (GSH) [12–15]. This results in stabilization and increased levels of the transcription factor nuclear factor erythroid 2-related factor 2 (NRF2) by means of Kelch-like ECH-associated protein 1 (KEAP1) which normally targets Nrf2 for ubiquitination and degradation but loses this ability in response to electrophiles and oxidants [16,

17]. NRF2 then translocates to the nucleus and binds to antioxidant response elements in the promoters of protective genes such as heme-oxygenase-1 [18] and NADPH-quinone-oxidoreductase-1 (NQO1) [19]. This in turn increases the intracellular concentration of GSH [18, 19], rendering the cells more resistant to oxidative stress.

We recently investigated the concentration and time dependence of DMF-mediated protection in neuronal cells and showed that neuroprotective concentrations of DMF depress cytokine production of splenocytes without exerting apoptosis. Neuroprotection was investigated in a model of endogenous oxidative stress, where extracellular glutamate blocks the glutamate-cystine antiporter system Xc^- leading to deprivation of cystine and its reduced form cysteine, the rate-limiting substrate for the synthesis of GSH. The subsequent GSH depletion leads to accumulation of reactive oxygen species and cell death by oxidative stress (recently reviewed in [20]). In these neuroprotection assays, the active metabolite MMF was similarly effective but required much longer incubation times to become active [21]. Our results suggest that low doses of DMF and MMF may bring about resistance against oxidative stress and immunomodulation without a need for T cell apoptosis. One important finding of this study was that DMF was still able to raise GSH levels, when the rate-limiting enzyme in glutathione synthesis, glutamate-cysteine ligase, was inhibited or system Xc^- activity abrogated by incubation in cysteine-free medium [22]. Therefore DMF can still exert protection, when *de novo* glutathione synthesis is blocked, suggesting enhanced GSH recycling.

The key enzyme that mediates the recycling of GSH is the glutathione reductase (GSR), a homodimeric flavoprotein that catalyzes GSSG reduction to GSH by using NADPH as a reducing cofactor. The GSR promoter contains an antioxidant response element [23], making it a likely candidate for the observed effect. In this contribution, we quantified GSR induction in response to DMF and evaluated the effect of GSR knockdown and pharmacological inhibition on cell death caused by endogenous oxidative stress.

2. Materials and Methods

2.1. Material. DMF was obtained from Sigma Aldrich and solubilized in dimethyl sulfoxide (DMSO). Cell culture dishes were from Greiner Bio-One. DMEM cell culture medium, sterile phosphate buffers saline, penicillin, streptomycin, L-glutamic acid, L-glutamine 200 mM (100x), sodium pyruvate 10 mM, and Opti-Mem® (1x) were from Gibco Life Technologies. Cell Titer Blue was from Promega. Lipofectamine® RNAiMAX™ reagent was from Invitrogen by Life Technologies and (S)-4-carboxyphenylglycine from TOCRIS.

2.2. Cell Culture, Viability Assays, and Glutathione Measurement. We used the hippocampal mouse cell line HT22 which lacks ionotropic glutamate receptors. The cell line had initially been generated as a subclone of the HT4 line [24] selected for a higher susceptibility to glutamate toxicity [25]. HT22 cells were cultured as described [26] and viability quantitated 24 h after glutamate addition by the Cell Titer Blue (CTB) assay (Promega) and normalized to vehicle treatment. Total glutathione was measured enzymatically as described previously [26] and normalized to cellular protein measured by the bicinchoninic acid-based method (Pierce). Glutathione released into the cell culture medium was also quantitated enzymatically after 4 h in cystine-free medium and normalized to total cellular protein; 1,3-bis[2-chloroethyl]-2-nitrosourea (BCNU; Carmustine) was solubilized in ethanol, which was also used as the vehicle control. (S)-4-Carboxyphenylglycine was solubilized in NaOH, which was also used as the vehicle control. Cystine-free medium was prepared by using DMEM, high glucose, w/o glutamine, methionine, cystine supplemented with 1% sodium pyruvate (100 mM), 2% L-glutamine (200 mM), and 3% L-methionine.

2.3. siRNA Transfection. Mission® esiRNA against mouse KIF11, FLUC, and mouse GSR, L-methionine, and BCNU were obtained from Sigma Aldrich. Transfections were performed with Lipofectamine according to the manufacturer's protocol (Life technologies). Briefly, cells were transfected with 1600 ng esiRNA in 24-well plates and replated 48 h later in a density of 2500 cells per well into 96-well plates.

2.4. Immunoblotting. Immunoblotting was performed as previously described [26] using antibodies against GSR (N-Term) antibody (1 : 1000; Antikoerper-online.de, ABIN406391) and anti-actin antibody (1 : 4000; Millipore MAB1501). Secondary antibodies were anti-rabbit IgG (H + L) (DyLight™ 800 Conjugate) and anti-mouse IgG (H + L) (DyLight™ 680 Conjugate) from Cell Signaling Technology™ (1 : 30000).

2.5. Quantitative Real-Time PCR. RNA extraction, reverse transcription, and quantitative real-time PCR were performed as previously described [26] using Fam/Dark-quencher probes from the Universal Probe Library™ (Roche) or individually designed Fam/Tamra probes (MWG). Beta-actin and HPRT served as endogenous control genes and showed no differential expression after incubation with DMF. Primer and probe sequences can be obtained from the authors.

2.6. Statistical Analysis. Statistical analysis was performed using spreadsheet (Microsoft Excel) and Prism (Graphpad) software. Multiple group analyses were conducted with two-way ANOVA and Bonferroni or Dunnett's *post hoc* test, comparison of two groups with two-tailed t-test. p values <0.05 were considered significant.

3. Results and Discussion

3.1. Cytoprotective Concentrations of DMF Induce the Expression of Glutathione Reductase. We first reproduced our findings that DMF protects against glutamate toxicity and found that 5 and 10 μM DMF induced a robust protection within 24 h (Figure 1(a)) as previously described. This protection involved an increase in GSH content even in conditions where no GSH can be synthesized because of a lack of the

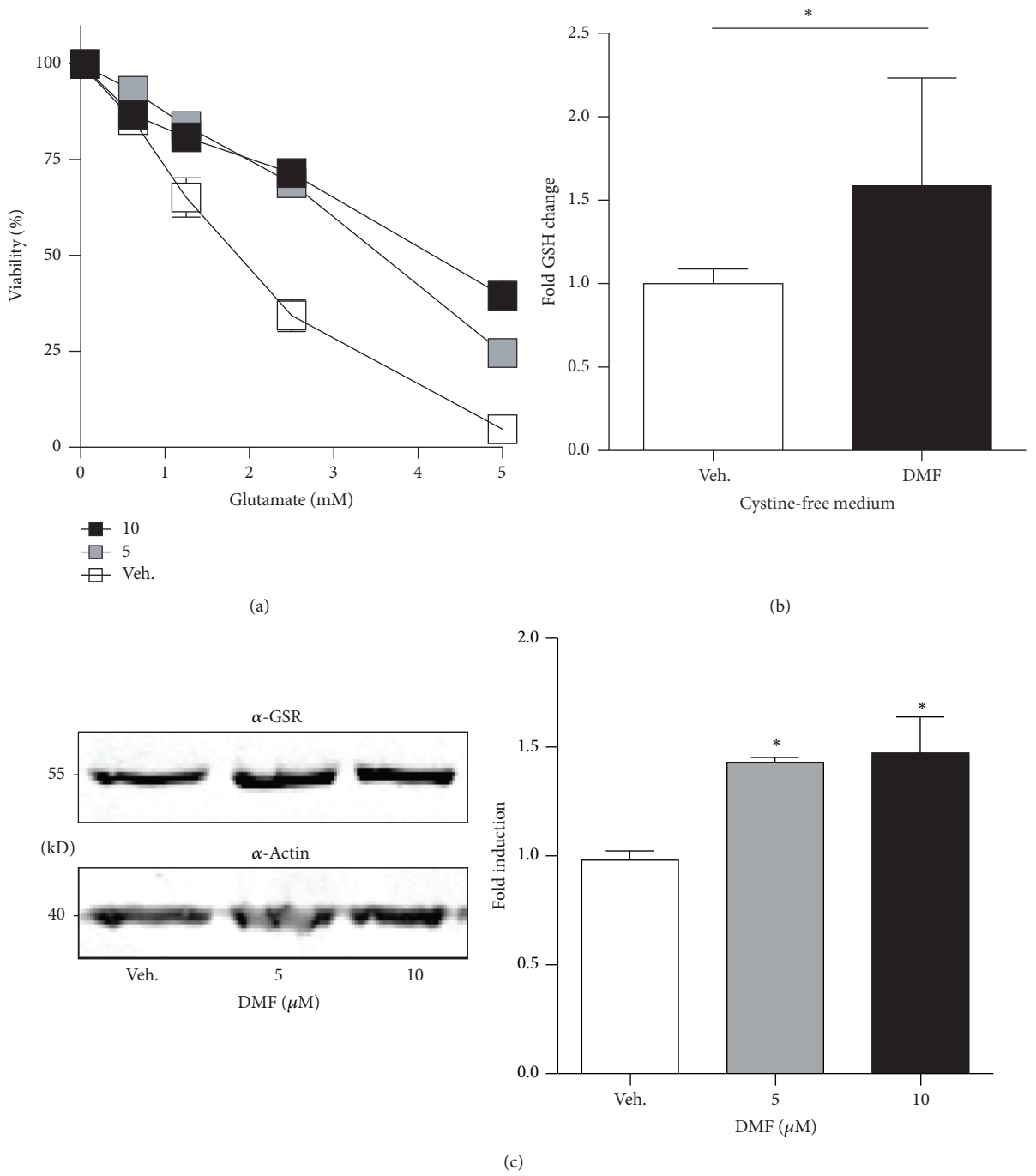

Figure 1: Cytoprotective concentrations of DMF induce the expression of glutathione reductase. (a) HT22 cells were treated for 24 h with the indicated concentrations of DMF before addition of glutamate. Viability was quantified 24 h later by the CTB assay. (b) DMF still elevates cellular GSH when GSH synthesis is blocked by incubation in cystine-free medium for another 24 h before intracellular GSH was measured enzymatically. (c) Cells were treated with DMF for 24 h and the abundance of GSR was quantitated by immunoblotting. Actin served as loading control. Molecular mass is indicated. The bar graphs represent the means ± SD of three independent experiments, $^{*}p < 0.05$, two-way ANOVA, and Tukey's *post hoc* test.

essential building block cystine (Figure 1(b)). This indicates that the increase in GSH observed here is due to an increase in glutathione recycling. In line with this, we indeed observed an increase in the abundance of GSR in cells treated with the protective concentrations of DMF, 5 and 10 μM, as shown by immunoblotting with an antibody specific for GSR and compared to β-actin as loading control (Figure 1(c)). DMF therefore induces the expression of the key enzyme involved in GSH recycling, GSR.

3.2. Identification of Small Interfering RNAs against GSR. To clarify the contribution of GSR to the protection conferred by DMF we decided to knockdown GSR with endoribonuclease-prepared small interfering inhibitory RNAs (esiRNAs) and pools of siRNAs resulting from cleavage of long double-stranded RNA with *Escherichia coli* RNase III. We transfected HT22 cells with esiRNA against GSR or against luciferase as control. After 24 h, 10 μM DMF or vehicle was added and after again 24 h protein lysates were used for immunoblotting with antibodies against GSR or actin as loading control. Untransfected cells treated with DMF or vehicle served as additional controls. The esiRNA against GSR indeed completely abolished GSR expression (Figure 2(a)). DMF was not able to induce GSR expression in the presence of GSR-specific esiRNAs whereas GSR was still expressed in the presence of esiRNA directed against luciferase. We concluded that esiRNA-induced knockdown could serve as a tool to elucidate the contribution of GSR to DMF-mediated protection against oxidative stress.

3.3. Knockdown of GSR Boosts the Protective Effect of DMF by Inducing a Synergistic Set of Antioxidant Response Genes. We transfected the cells with esiRNA against GSR and control esiRNA in 6-well-plates. 24 h later the cells were treated with DMF or vehicle and again 24 h replated into 96-well-plates where they were then exposed to 10 mM glutamate for an additional 24 h. We observed two things; first, esiRNA against GSR induced a protection by itself and second, this even boosted the protection conferred by 10 μM DMF (Figure 2(b)). We hypothesized that the lack of GSR over 48 h before the additional treatment with glutamate probably also induces the antioxidant response synergistically to DMF which increases nuclear Nrf2 protein levels [21].

To clarify the observed synergistic effect of the combination of DMF and GSR knockdown, we quantitated the expression of genes belonging to the antioxidant response battery in DMF- and siGSR-treated cells and their respective controls. This indeed proved that both treatments result in the induction of a synergistic set of antioxidant transcripts. Only the catalytic subunit of the glutamate-cysteine ligase (GCLC) and peroxiredoxin 1 (PRDX1) was upregulated in both sets, whereas glutathione *S*-transferase omega 1 (GSTO1) and heme-oxygenase 1 (HO-1) were downregulated in DMF-treated but upregulated in siGSR-treated cells. NADPH-quinone-oxidoreductase-1 (NQO1) and xCT (also known as SLC7A11) showed the opposite pattern (Figure 2(c)).

3.4. Pharmacological Inhibition of Glutathione Reductase Is Also Protective When Preincubated for 24 h. BCNU (Carmustine) is an antitumor, DNA-alkylating agent, which inhibits cellular glutathione reductase activity [27]. A pharmacological agent should theoretically inhibit GSR without delay and allow a more precise analysis of the contribution of glutathione recycling in the protective effect of DMF with the important caveat of less specificity because most inhibitors inhibit more than one enzyme. BCNU concentration-dependently provoked cell death in HT22 cells with an LD50 of approximately 200 μM (Figure 3(a)). As expected, much lower concentrations of 10 and 100 μM again elicited a protection (Figure 3(b)) again mediated by the induction of some antioxidant transcripts, most prominently the cystine-glutamate antiporter xCT (SLC7A11), HO-1, and NQO1 (Figure 3(c)).

We then tried to attenuate the protective effect of DMF preincubation by a simultaneous exposure of the cells to glutamate, which in these cells inhibits cystine import and therefore leads to glutathione depletion, and BCNU. We observed only a very minor, not statistically significant reduction in viability in cells treated with 100 μM BCNU. Cells not pretreated with DMF but exposed to glutamate and BCNU, in contrast, were significantly more prone to cell death (Figure 3(d)). This means that DMF even protects against a combined assault with an agent that inhibits *de novo* glutathione synthesis, glutamate, and glutathione recycling, BCNU, suggesting additional, not yet known protective mechanisms induced by DMF. At a higher concentration of BCNU, 200 μM, an antiproliferative effect prevailed (Figure 3(d)).

3.5. Pharmacological Inhibition of Glutathione Reductase Inhibits the Positive Effect of DMF on Glutathione Recycling in Cystine-Free Medium. We concluded from these experiments that we could only study the inhibitory effect of BCNU on DMF-mediated glutathione recycling under conditions where (1) *de novo* glutathione synthesis is inhibited and (2) the time of incubation with BCNU is not long enough to allow the induction of gene transcription. We therefore pretreated cells with 10 μM DMF which increased GSH concentration in both normal medium and cystine-free medium as shown in Figure 1(b) and as previously reported [21]. The presence of BCNU for 4 h in the cystine-free medium, however, completely abolished the GSH recycling mediated by DMF (Figure 4). These experiments prove that part of the positive effect of DMF on glutathione content is indeed mediated via increased glutathione recycling.

4. Conclusions

Our major finding is that DMF indeed increases glutathione recycling by induction of GSR. Our studies were hampered by the fact that both knockdown and inhibition of GSR induced a strong antioxidant response by itself. To study the effect of GSR inhibition on glutathione recycling alone, incubation in cystine-free medium can be used to block the

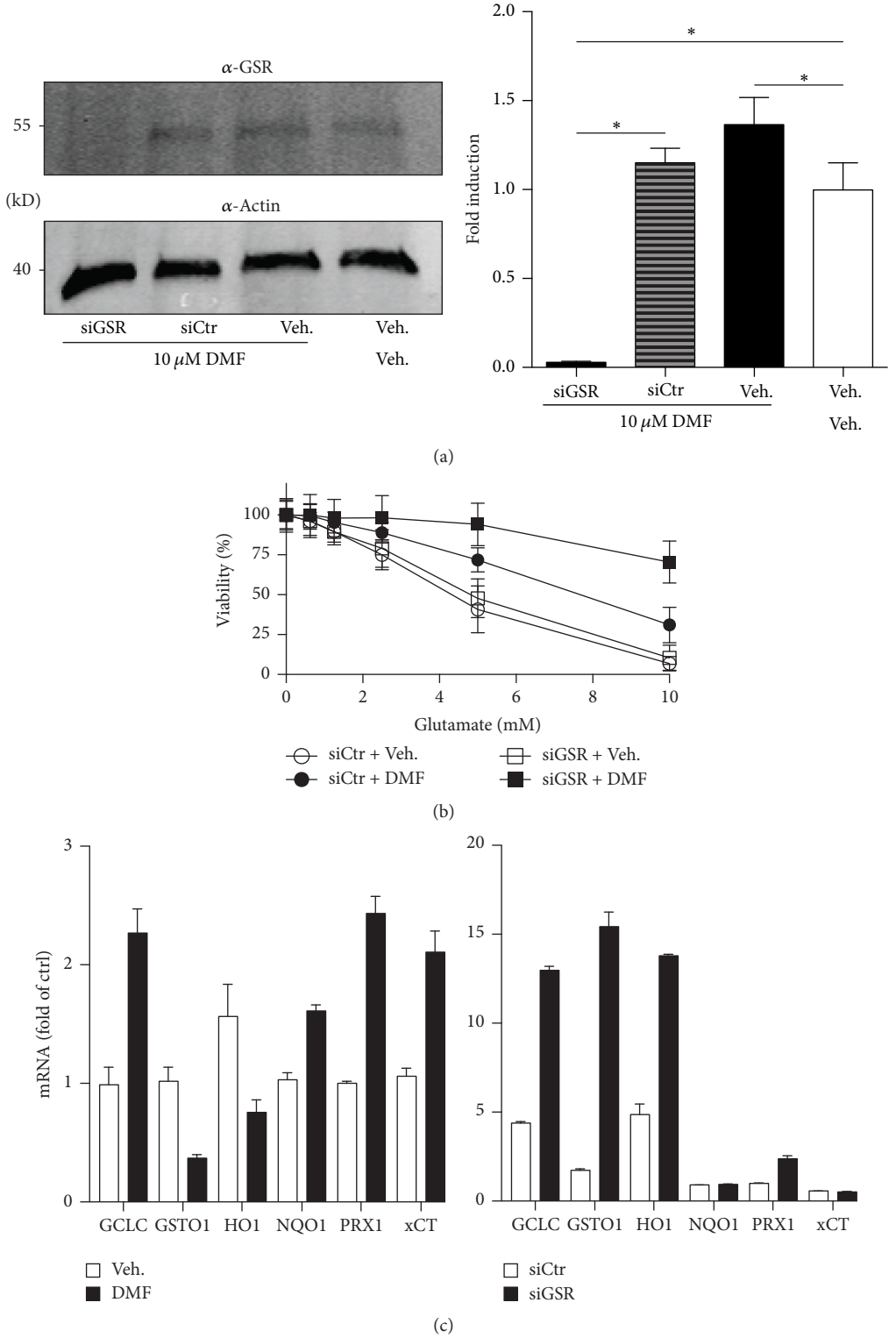

Figure 2: Knockdown of GSR boosts the protective effect of DMF by inducing a synergistic set of antioxidant response genes. (a) Cells were transfected with siRNAs against GSR (siGSR) or luciferase (siCtr) 24 h before addition of 10 μM DMF for an additional 24 h. The same amount of protein lysates was blotted and stained with antibodies against GSR or actin as loading control. The molecular weight is indicated. The bar graphs represent the means ± SEM normalized to vehicle of 3 different blots. (b) DMF was added 24 h after transfection of the indicated siRNAs and 10 mM glutamate 24 h after DMF. Viability was quantified by CTB assays again 24 h later. The bar graphs represent the mean ± SEM of three experiments done in triplicate. (c) DMF treatment or siGSR transfection induces mRNA expression of a synergistic set of transcripts involved in the antioxidant response. Cells were treated for 24 h with 10 μM DMF or vehicle or prepared 48 h after transfection with siGSR and siCtrl and mRNA quantitated by real-time PCR using *β-actin* and *hprt* as endogenous controls. $^*P < 0.05$, two-way ANOVA, and Tukey's *post hoc* test.

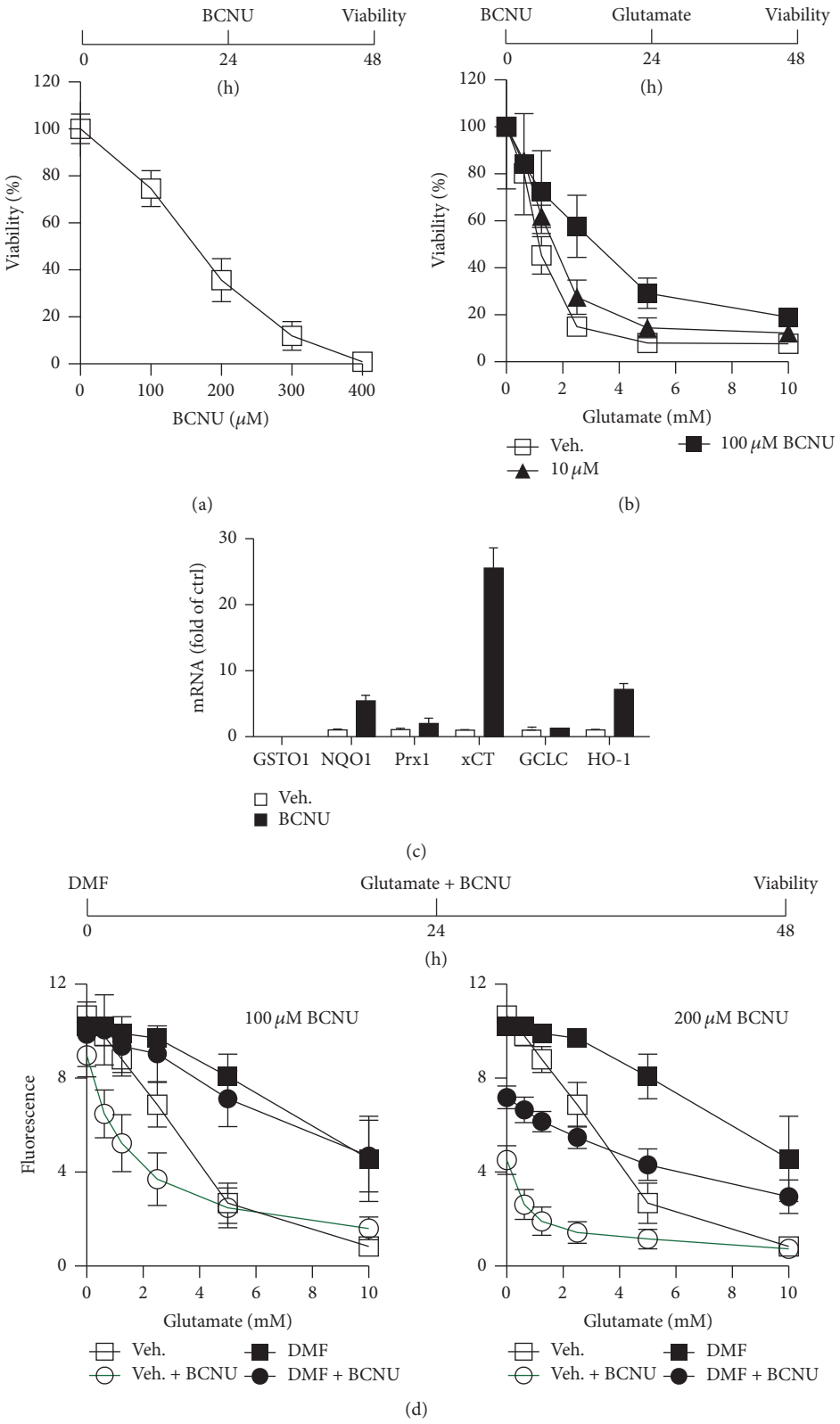

Figure 3: Pharmacological inhibition of glutathione reductase with BCNU is also protective when preincubated for 24 h. HT22 cells were (a) treated for 24 h with the indicated concentrations of BCNU or (b) pretreated with the indicated concentrations of BCNU for 24 h before addition of glutamate at the indicated concentrations for another 24 h. Afterwards, viability was quantified by the CTB assay (a and b). (c) Cells were treated for 24 h with 50 μM BCNU or vehicle and mRNA quantitated by real-time PCR using β-*actin* and *hprt* as endogenous controls. (d) HT22 cells were treated with 10 μM DMF for 24 h before simultaneous addition of BCNU and glutamate in the indicated concentrations. Viability was quantified 24 h later by the CTB assay.

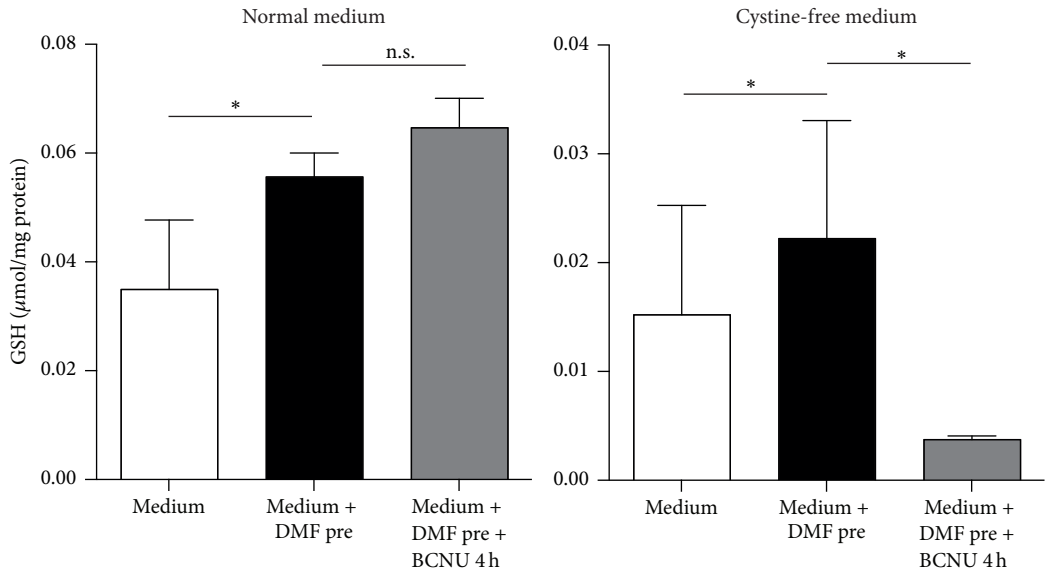

Figure 4: Pharmacological inhibition of glutathione reductase inhibits glutathione recycling in cystine-free medium. DMF still elevates cellular GSH when GSH synthesis is blocked by incubation in cystine-free medium. HT22 cells were treated for 24 h with 10 μM DMF (black bars) or vehicle (white bars) and then exposed to cystine-free medium for another 4 h in the presence of 50 μM BCNU (grey bars) before intracellular GSH was measured enzymatically. Graphs of all experiments represent the means ± SD of three independent experiments performed in triplicate. $^{*}p < 0.05$, two-way ANOVA, and Tukey's *post hoc* test.

de novo synthesis of GSH and avoid confounding effects of GSR inhibition.

Abbreviations

BSO: Buthionine sulfoximine
CTB: Cell Titer Blue
DMF: Dimethyl fumarate
DMSO: Dimethyl sulfoxide
GCLC: Glutamate-cysteine ligase, catalytic subunit
GSH: Glutathione
MS: Multiple sclerosis
NF-κB: Nuclear factor kappa B
Nrf2: Erythroid 2-related factor 2
NQO1: NADPH-quinone-oxidoreductase-1
S4-CPG: (S)-4-Carboxyphenylglycine.

Competing Interests

The authors declare that they have no competing interests.

Authors' Contributions

Philipp Albrecht and Axel Methner conceived the study and participated in its design and coordination, performed the statistical analysis, and wrote the manuscript. Christina Hoffmann, Ann-Kathrin Herrmann, and Teresa Schacht carried out cell viability assays, immunoblots, Michael Dietrich glutathione measurements, and quantitative real-time PCR experiments. All authors critically revised and approved the final manuscript. Philipp Albrecht and Axel Methner are equally contributing last authors.

Acknowledgments

This work was supported by an unrestricted research grant by Biogen to Axel Methner.

References

[1] A. Compston and A. Coles, "Multiple sclerosis," *The Lancet*, vol. 372, no. 9648, pp. 1502–1517, 2008.

[2] R. E. Gonsette, "Neurodegeneration in multiple sclerosis: the role of oxidative stress and excitotoxicity," *Journal of the Neurological Sciences*, vol. 274, no. 1-2, pp. 48–53, 2008.

[3] K.-A. Nave and B. D. Trapp, "Axon-glial signaling and the glial support of axon function," *Annual Review of Neuroscience*, vol. 31, pp. 535–561, 2008.

[4] L. Kappos, R. Gold, D. H. Miller et al., "Efficacy and safety of oral fumarate in patients with relapsing-remitting multiple sclerosis: a multicentre, randomised, double-blind, placebo-controlled phase IIb study," *The Lancet*, vol. 372, no. 9648, pp. 1463–1472, 2008.

[5] U. Mrowietz, J. C. Szepietowski, R. Loewe et al., "Efficacy and safety of LAS41008 (dimethyl fumarate) in adults with moderate-to-severe chronic plaque psoriasis: a randomized, double-blind, Fumaderm®- and placebo-controlled trial (BRIDGE)," *British Journal of Dermatology*, 2016.

[6] M. R. Yazdi and U. Mrowietz, "Fumaric acid esters," *Clinics in Dermatology*, vol. 26, no. 5, pp. 522–526, 2008.

[7] S. Dibbert, B. Clement, T. Skak-Nielsen, U. Mrowietz, and M. Rostami-Yazdi, "Detection of fumarate-glutathione adducts in the portal vein blood of rats: Evidence for rapid dimethylfumarate metabolism," *Archives of Dermatological Research*, vol. 305, no. 5, pp. 447–451, 2013.

[8] N. H. R. Litjens, J. Burggraaf, E. Van Strijen et al., "Pharmacokinetics of oral fumarates in healthy subjects," *British Journal of Clinical Pharmacology*, vol. 58, no. 4, pp. 429–432, 2004.

[9] F. Treumer, K. Zhu, R. Gläser, and U. Mrowietz, "Dimethylfumarate is a potent inducer of apoptosis in human T cells," *Journal of Investigative Dermatology*, vol. 121, no. 6, pp. 1383–1388, 2003.

[10] M. Vandermeeren, S. Janssens, H. Wouters et al., "Dimethylfumarate is an inhibitor of cytokine-induced nuclear translocation of NF-κB1, but not RelA in normal human dermal fibroblast cells," *Journal of Investigative Dermatology*, vol. 116, no. 1, pp. 124–130, 2001.

[11] R. De Jong, A. C. Bezemer, T. P. L. Zomerdijk, T. van de Pouw-Kraan, T. H. M. Ottenhoff, and P. H. Nibbering, "Selective stimulation of T helper 2 cytokine responses by the anti-psoriasis agent monomethylfumarate," *European Journal of Immunology*, vol. 26, no. 9, pp. 2067–2074, 1996.

[12] T. J. Schmidt, M. Ak, and U. Mrowietz, "Reactivity of dimethyl fumarate and methylhydrogen fumarate towards glutathione and N-acetyl-L-cysteine—preparation of S-substituted thiosuccinic acid esters," *Bioorganic & Medicinal Chemistry*, vol. 15, no. 1, pp. 333–342, 2007.

[13] M. M. Schmidt and R. Dringen, "Fumaric acid diesters deprive cultured primary astrocytes rapidly of glutathione," *Neurochemistry International*, vol. 57, no. 4, pp. 460–467, 2010.

[14] K. D. Held, E. R. Epp, S. Awad, and J. E. Biaglow, "Postirradiation sensitization of mammalian cells by the thiol-depleting agent dimethyl fumarate," *Radiation Research*, vol. 127, no. 1, pp. 75–80, 1991.

[15] L. A. Dethlefsen, C. M. Lehman, J. E. Biaglow, and V. M. Peck, "Toxic effects of acute glutathione depletion by buthionine sulfoximine and dimethylfumarate on murine mammary carcinoma cells," *Radiation Research*, vol. 114, no. 2, pp. 215–224, 1988.

[16] L. Baird, D. Llères, S. Swift, and A. T. Dinkova-Kostova, "Regulatory flexibility in the Nrf2-mediated stress response is conferred by conformational cycling of the Keap1-Nrf2 protein complex," *Proceedings of the National Academy of Sciences of the United States of America*, vol. 110, no. 38, pp. 15259–15264, 2013.

[17] L. E. Tebay, H. Robertson, S. T. Durant et al., "Mechanisms of activation of the transcription factor Nrf2 by redox stressors, nutrient cues, and energy status and the pathways through which it attenuates degenerative disease," *Free Radical Biology and Medicine*, vol. 88, pp. 108–146, 2015.

[18] S. X. Lin, L. Lisi, C. Dello Russo et al., "The anti-inflammatory effects of dimethyl fumarate in astrocytes involve glutathione and haem oxygenase-1," *ASN Neuro*, vol. 3, no. 2, pp. 75–84, 2011.

[19] R. A. Linker, D.-H. Lee, S. Ryan et al., "Fumaric acid esters exert neuroprotective effects in neuroinflammation via activation of the Nrf2 antioxidant pathway," *Brain*, vol. 134, no. 3, pp. 678–692, 2011.

[20] P. Albrecht, J. Lewerenz, S. Dittmer, R. Noack, P. Maher, and A. Methner, "Mechanisms of oxidative glutamate toxicity: the glutamate/cystine antiporter system xc- as a neuroprotective drug target," *CNS & Neurological Disorders—Drug Targets*, vol. 9, pp. 373–382, 2010.

[21] P. Albrecht, I. Bouchachia, N. Goebels et al., "Effects of dimethyl fumarate on neuroprotection and immunomodulation," *Journal of Neuroinflammation*, vol. 9, article 163, 2012.

[22] P. Albrecht, I. Bouchachia, C. Zimmermann et al., "Effects of dimethyl fumarate on neuroprotection and immunomodulation," *Journal of Neuroinflammation*, vol. 9, article 163, 2012.

[23] C. J. Harvey, R. K. Thimmulappa, A. Singh et al., "Nrf2-regulated glutathione recycling independent of biosynthesis is critical for cell survival during oxidative stress," *Free Radical Biology and Medicine*, vol. 46, no. 4, pp. 443–453, 2009.

[24] B. H. Morimoto and D. E. Koshland Jr., "Induction and expression of long- and short-term neurosecretory potentiation in a neural cell line," *Neuron*, vol. 5, no. 6, pp. 875–880, 1990.

[25] J. B. Davis and P. Maher, "Protein kinase C activation inhibits glutamate-induced cytotoxicity in a neuronal cell line," *Brain Research*, vol. 652, no. 1, pp. 169–173, 1994.

[26] J. Lewerenz, P. Albrecht, M.-L. T. Tien et al., "Induction of Nrf2 and xCT are involved in the action of the neuroprotective antibiotic ceftriaxone *in vitro*," *Journal of Neurochemistry*, vol. 111, no. 2, pp. 332–343, 2009.

[27] K. P. Rice, P. G. Penketh, K. Shyam, and A. C. Sartorelli, "Differential inhibition of cellular glutathione reductase activity by isocyanates generated from the antitumor prodrugs Cloretazine™ and BCNU," *Biochemical Pharmacology*, vol. 69, no. 10, pp. 1463–1472, 2005.

Hindawi Publishing Corporation
Oxidative Medicine and Cellular Longevity
Volume 2016, Article ID 5720574, 10 pages
http://dx.doi.org/10.1155/2016/5720574

Research Article

Conservation of the Nrf2-Mediated Gene Regulation of Proteasome Subunits and Glucose Metabolism in Zebrafish

Vu Thanh Nguyen,[1,2] Yuji Fuse,[1,2] Junya Tamaoki,[1,3] Shin-ichi Akiyama,[4,5] Masafumi Muratani,[6] Yutaka Tamaru,[5] and Makoto Kobayashi[1]

[1]*Department of Molecular and Developmental Biology, Faculty of Medicine, University of Tsukuba, Tsukuba 305-8575, Japan*
[2]*Doctoral Program in Biomedical Sciences, Graduate School of Comprehensive Human Sciences, University of Tsukuba, Tsukuba 305-8575, Japan*
[3]*College of Biological Sciences, University of Tsukuba, Tsukuba 305-8575, Japan*
[4]*Division of Nephrology, Department of Internal Medicine, Nagoya University Graduate School of Medicine, Nagoya 466-8550, Japan*
[5]*Department of Life Sciences, Graduate School of Bioresources, Mie University, Tsu 514-8507, Japan*
[6]*Department of Genome Biology, Faculty of Medicine, University of Tsukuba, Tsukuba 305-8575, Japan*

Correspondence should be addressed to Makoto Kobayashi; makobayash@md.tsukuba.ac.jp

Received 26 August 2016; Revised 9 November 2016; Accepted 22 November 2016

Academic Editor: Thomas Kensler

The Keap1-Nrf2 system is an evolutionarily conserved defense mechanism against oxidative and xenobiotic stress. Besides the exogenous stress response, Nrf2 has been found to regulate numerous cellular functions, including protein turnover and glucose metabolism; however, the evolutionary origins of these functions remain unknown. In the present study, we searched for novel target genes associated with the zebrafish Nrf2 to answer this question. A microarray analysis of zebrafish embryos that overexpressed Nrf2 revealed that 115 candidate genes were targets of Nrf2, including genes encoding proteasome subunits and enzymes involved in glucose metabolism. A real-time quantitative PCR suggested that the expression of 3 proteasome subunits (*psma3*, *psma5*, and *psmb7*) and 2 enzymes involved in glucose metabolism (*pgd* and *fbp1a*) were regulated by zebrafish Nrf2. We thus next examined the upregulation of these genes by an Nrf2 activator, diethyl maleate, using Nrf2 mutant zebrafish larvae. The results of real-time quantitative PCR and whole-mount in situ hybridization showed that all of these 5 genes were upregulated by diethyl maleate treatment in an Nrf2-dependent manner, especially in the liver. These findings implied that the Nrf2-mediated regulation of the proteasome subunits and glucose metabolism is evolutionarily conserved among vertebrates.

1. Introduction

The Keap1-Nrf2 system is a mechanism that protects cells against xenobiotic and oxidative stress. Under conditions of stress, transcription factor Nrf2 transactivates a wide array of genes, which perform a range of functions, including (but not limited to) the encoding of antioxidant proteins, glutathione-conjugating enzymes, and xenobiotic transporters. This confers an inducible defense against stressors [1, 2]. Although these genes have been extensively studied as Nrf2 targets, there is increasing evidences to show that Nrf2 activates a wider gene set than was initially considered [3]. Nrf2 regulates the protein turnover by inducing proteasome subunits to confer protective effects against chronic diseases [4] and modifies cellular metabolic processes, for example, the pentose phosphate pathway, which provides NADPH and purine nucleotides that are essential for the redox homeostasis and cellular proliferation [5, 6]. Because of this multifunctionality, Nrf2 research has become an emerging topic in the medical field [7, 8].

The zebrafish has become a popular model vertebrate in basic medical science [9, 10]. Although it is convenient to use lower vertebrate models for medical research, there is always some concern as to whether the findings are applicable to human medicine. We have investigated the Keap1-Nrf2 system using the zebrafish as a model and revealed that the

regulation of the system is based on a similar molecular mechanism to mammals [11–15]. Moreover, an analysis of the Nrf2 mutant zebrafish strain, *nrf2a*^{fh318}, revealed that the protective role against oxidative and xenobiotic stress was conserved in the zebrafish [16, 17]. The lineup of the target genes in the zebrafish, which provides the defense function, is also being clarified from recent studies [18]. Our previous study [19] and the study of Hahn et al. [20] reported the performance of microarray analyses using zebrafish larvae treated with potent Nrf2 inducers, diethyl maleate (DEM) and *tert*-butylhydroquinone (tBHQ), respectively, and found that canonical Nrf2 targets, such as detoxification and antioxidative enzymes were conserved in zebrafish. However, it is still unclear whether the Nrf2-mediated regulation of cellular pathways other than antioxidation and detoxification, for example, protein turnover and glucose metabolism, is conserved among vertebrates or whether it is only present in higher vertebrates.

In the present study, we searched for novel target genes for zebrafish Nrf2 to answer this question. We performed a microarray analysis of zebrafish embryos that overexpressed Nrf2, which was a different approach from previous reports [19, 20]. The analysis revealed genes encoding proteasome subunits and enzymes involved in glucose metabolism, suggesting that the Nrf2-mediated regulation of both protein turnover and glucose metabolism is evolutionarily conserved among vertebrates.

2. Materials and Methods

2.1. Zebrafish and Chemical Treatments. The wild-type (AB) and *nrf2a*^{fh318} mutant [16] zebrafish strains were used in the present study. The *nrf2a*^{fh318} strain was maintained by PCR-based genotyping, as described in Fuse et al. [17]. Embryos were obtained by natural mating. For DEM treatment, the larvae were placed in 3 cm culture dishes at 4 days post-fertilization (dpf) and treated with 100 μM DEM for 6 h (Wako, Osaka, Japan). All of the experiments were performed according to methods that were approved by the Animal Experiment Committee of the University of Tsukuba.

2.2. Microarray Analysis. A DNA microarray analysis was performed using custom-made 16 K MZH chips (GPL14379), as described previously [19]. Biological experiments were carried out in triplicate and microarray analyses were conducted in duplicate or triplicate for each biological experiment. For the overexpression of zebrafish *nrf2a*, capped *nrf2a* RNA was synthesized from pCS2nrf2 [11] using an SP6 mMESSAGE mMACHINE in vitro transcription kit (Ambion, Austin, TX). One hundred pg of mRNA was injected into a 1-cell stage embryo by an IM300 microinjector (Narishige, Tokyo, Japan). At 8 h after injection, the embryos were collected and homogenized with QIAzol reagent (Qiagen, Hilden, Germany) and stored at −80°C. A dual-color ratio methodology was applied to compare *nrf2a* RNA-injected embryos with uninjected embryos (Control), according to the manufacturer's protocol for the AceGene DNA microarray (Hitachi Solutions, Tokyo, Japan). Total RNA was extracted according to the manufacturer's instructions for QIAzol reagent (Qiagen), in combination with the clean-up protocol of the RNeasy Mini Kit (Qiagen). Amino-allyl-modified RNA was synthesized using the amino-allyl RNA amplification kit (Sigma-Aldrich, St. Louis, MO) and labeled with monoreactive Cy3 and Cy5 dyes (GE Healthcare, Little Chalfont, UK). The hybridized MZH chips were scanned using the Affymetrix 428 array scanner (Affymetrix, Santa Clara, CA). The microarray data were processed from raw data image files with Affymetrix Jaguar (Affymetrix) and were analyzed using per-chip normalization. The processed data were subsequently imported into Excel (Microsoft, Redmond, WA) to compare expression profiles of two samples (injected versus uninjected with *nrf2a* mRNA). Genes whose expression was affected by the Nrf2a overexpression were selected based on cut-off values of >1.5-fold up or >1.5-fold down, without considering their significance. A biological pathway analysis was performed using the Reactome database (http://www.reactome.org/). We have deposited the raw data at Gene Expression Omnibus (GEO) under accession number GSE86174, and we can confirm all details are Minimum Information About a Microarray Experiment compliant.

2.3. Real-Time PCR. Total RNA from *nrf2a*-overexpressing embryos and DEM-treated larvae was prepared according to the procedure that was performed in the microarray analysis. cDNA was synthesized using ReverTra Ace qPCR RT Master Mix (Toyobo, Osaka, Japan) according to the manufacturer's instructions. A quantitative PCR (qPCR) was performed using a 7500 Fast Real-Time PCR System (Thermo Fisher Scientific, Waltham, MA) with THUNDERBIRD SYBR qPCR Mix (Toyobo). The specific primers are listed in Table S1 in Supplementary Material available online at http://dx.doi.org/10.1155/2016/5720574. The expression level of each gene was normalized to the level of *ef1α*.

2.4. In Situ Hybridization Analysis. A whole-mount in situ hybridization analysis was performed as described previously [21]. To construct pKSpsma3, pKSpsma5, pKSpsmb7, pKSpgd, and pKSfbp1a, PCR fragments were amplified with primers shown in Table S2 using cDNA synthesized from zebrafish larvae (4 dpf), and ligated with pBluescript II KS+ vector using a DNA Ligation Kit Ver.1 (Takara, Otsu, Japan). Plasmids were linearized by restriction enzymes (pKSpsma3, pKSpsmb7, and pKSpgd: *Bam*HI; pKSpsma5: *Eco*RI; pKSfbp1a: *Spe*I) and transcribed with T3 RNA polymerase (Roche Diagnostics, Indianapolis, IN) in the presence of DIG RNA labeling mix (Roche Diagnostics) to make RNA probes. The larvae were photographed using an MZ16 microscope (Leica, Wetzlar, Germany) equipped with a DP73 digital camera (Olympus, Tokyo, Japan), followed by PCR-based genotyping.

2.5. Statistical Analysis. The gene expression levels derived from the real-time PCRs were compared using the two-tailed Student's *t*-test. *P* values of <0.05 were considered to indicate statistical significance.

Table 1: The pathways activated in *nrf2a*-overexpressing embryos.

p value	Pathway name	Genes
$5.27E-7$	Detoxification of reactive oxygen species	*txn*, *gstp1*, *prdx1*, *gsr*, *gpx1b*, *prdx5*, *gpx1a*
$5.22E-5$	Glutathione conjugation	*gclc*, *gsto2*, *gstp1*, *gclm*, *gsta.1*
$6.47E-4$	Reduction of cytosolic Ca^{++} levels	*atp2b2*, *calm3a*
$7.86E-4$	Apoptosis	*lmna*, *tradd*, ***psma3***, ***psmb7***, ***psma5***, *tp53bp2a*, *kpna1*, *prkcdb*
$1.04E-3$	Programmed cell death	*lmna*, *tradd*, ***psma3***, ***psmb7***, ***psma5***, *tp53bp2a*, *kpna1*, *prkcdb*
$5.09E-3$	Degradation of GLI1 by the proteasome	*tpk1*, ***psma3***, ***psmb7***, ***psma5***
$5.09E-3$	GLI3 is processed to GLI3R by the proteasome	*tpk1*, ***psma3***, ***psmb7***, ***psma5***
$5.09E-3$	Degradation of GLI2 by the proteasome	*tpk1*, ***psma3***, ***psmb7***, ***psma5***
$5.99E-3$	Gluconeogenesis	*pcxb*, *fbp1a*, *pck1*, *tpk1*
$7.01E-3$	CaM pathway	*tpk1*, *calm3a*, *prkcdb*

Bold genes encode proteasome subunits.

3. Results

3.1. The Identification of Novel Target Genes for Zebrafish Nrf2 by a Microarray Analysis. To search for the novel target genes of zebrafish Nrf2, we performed a microarray analysis of zebrafish embryos overexpressing Nrf2. In vitro synthesized mRNA of *nrf2a*, the functional ortholog of mammalian Nrf2 in zebrafish, was injected into 1-cell stage of zebrafish embryos, and the gene expression in the injected embryos at 8 h after the injection was examined using 16 K MZH chips, which contain 16,399 probes [19]. In total, 115 genes were found to be upregulated more than 1.5-fold by the overexpression of *nrf2a* (Table S3).

The lineup of upregulated genes in the microarray of *nrf2a*-overexpressing embryos was further analyzed using the Reactome database to determine the biological functions that could be influenced by these upregulated genes (Table 1). Besides antioxidation and glutathione conjugation, proteasome-related pathways were listed, due to the upregulation of the 3 genes encoding the proteasome subunits, *psma3*, *psma5,* and *psmb7* (proteasome subunits $\alpha 3$, $\alpha 5$, and $\beta 7$, resp.). It should be noted that none of the genes encoding the proteasome subunits, including these 3 genes, have been identified in previous microarray analyses [19, 20].

3.2. Proteasome Subunits Were Regulated by Zebrafish Nrf2. To validate the microarray results, we performed a real-time qPCR. *nrf2a*-overexpressing embryos were prepared in the same way as in the microarray analysis. Overexpression of *nrf2a* in mRNA-injected embryos was confirmed by a real-time qPCR (Figure S1, 75.5-fold higher compared to uninjected embryos). As shown in Figure 1(a), *psma3* was significantly induced by the overexpression of *nrf2a* (1.51-fold). *psma5* and *psmb7* also tended to be weakly induced by the overexpression of *nrf2a* (1.28- and 1.18-fold, resp.). These results suggest that, similarly to mammals [4], some of the proteasome subunit genes are targets of Nrf2 in the zebrafish.

We then tested whether the expression of 3 proteasome subunit genes is induced by DEM in an Nrf2-dependent manner by a real-time qPCR. Although DEM did not significantly induce any of proteasome subunit genes at 6 h (Figure 1(b)), *psmb7* was induced after 12 h exposure (Figure 1(c)) in wild-type larvae (1.59-fold) with statistical significance, while the induction in $nrf2a^{fh318/fh318}$ mutant (1.33-fold) was weaker than that of wild-type. *psma3* and *psma5* were also tended to be induced after 12 h exposure to DEM both in wild-type larvae (1.49- and 1.47-fold, resp.) and in $nrf2a^{fh318/fh318}$ mutant larvae (1.27- and 1.63-fold, resp.).

We speculated that the reason of this unclear Nrf2-dependency was due to ubiquitous basal expression of proteasome subunit genes. Thus, we next performed whole-mount in situ hybridization to evaluate tissue-restricted induction of the proteasome subunit genes, since many Nrf2 target genes showed gill-, liver- or nose-specific induction in zebrafish larvae [19]. As we expected, the expression of all three subunit genes was induced in the liver of wild-type and heterozygous mutant ($nrf2a^{fh318/+}$) larvae after 12 h exposure to DEM (Figure 2). This liver-specific induction was not observed in homozygous mutant siblings ($nrf2a^{fh318/fh318}$). These results suggest that Nrf2 regulates the gene expression levels of proteasome subunits in zebrafish, especially in the liver.

3.3. Zebrafish Nrf2 Regulates Enzymes That Are Involved in Glucose Metabolism. It is noteworthy that many high-ranked genes in the present microarray analysis were also identified in the previous microarray analyses using DEM- or tBHQ-treated larvae (see Table S3, gray highlighted genes) [19, 20]. This observation indicates that these 27 overlapping genes may be strong candidates for zebrafish Nrf2 targets (Figure 3(a), indicated genes; Table S3, gray highlighted). We therefore analyzed these genes using the Reactome database to search for novel biological pathways that are related to zebrafish Nrf2 (Table 2). As a result, the "Metabolism" pathway was listed within the top 10 categories, in addition to the pathways related to glutathione conjugation and antioxidation. Three catabolic enzymes that are involved in glucose metabolism were included in the "Metabolism" pathway: *pck1* (phosphoenolpyruvate carboxykinase 1), *pcxb* (pyruvate carboxylase b), and *pgd* (phosphogluconate dehydrogenase). Furthermore, looking back on the lineup of genes that were upregulated by the overexpression of *nrf2a* (Table S3), two more related genes were found: *taldo1* (transaldolase 1) and *fbp1a* (fructose-1,6-bisphosphatase 1a).

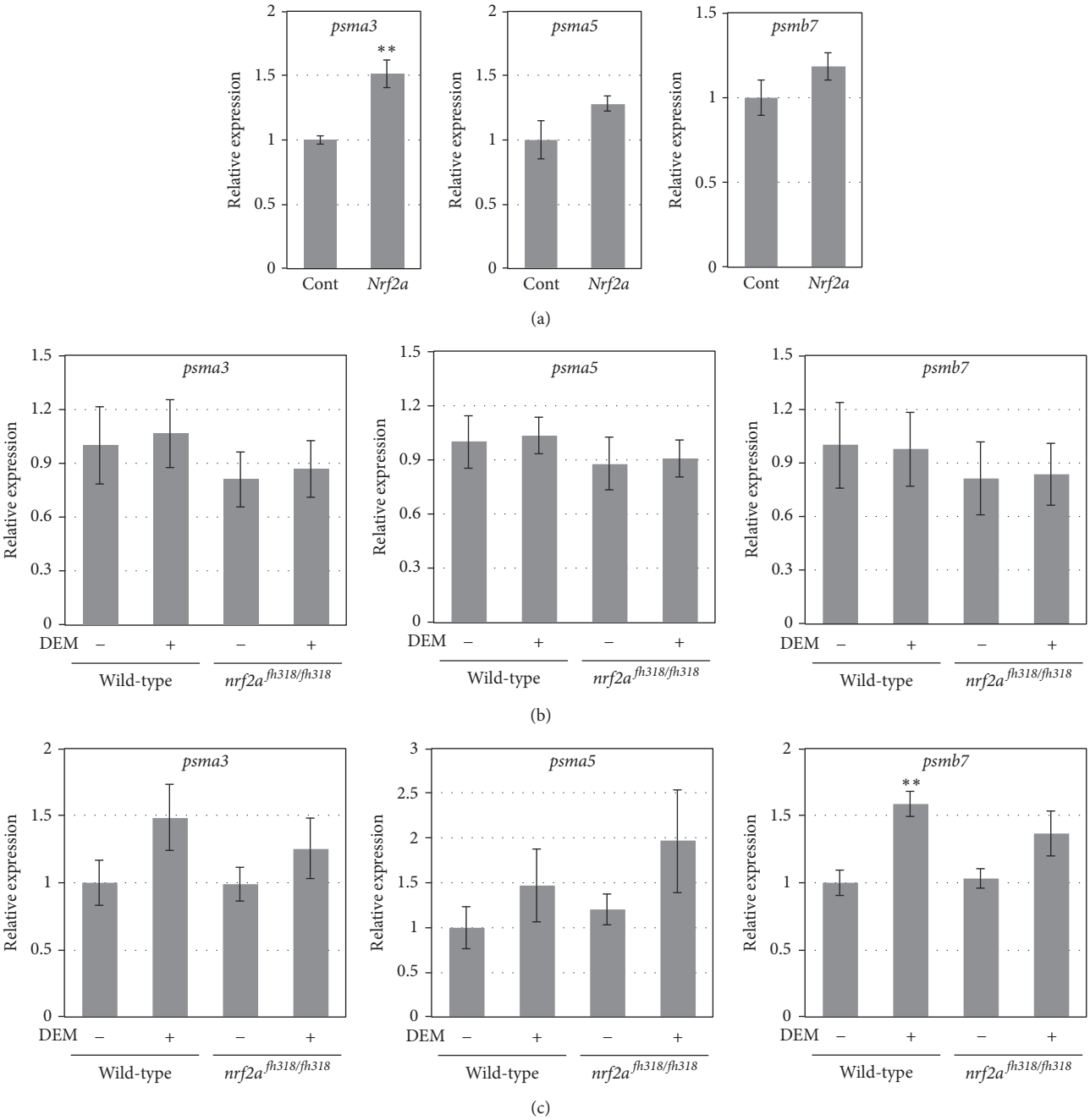

Figure 1: The expression of the proteasome subunit genes. (a) The gene expression of the indicated proteasome subunits in 8 h postfertilization (hpf) wild-type embryos injected with or without 100 pg of *nrf2a* mRNA at the 1-cell stage was analyzed by a real-time qPCR. Total RNA was extracted from 30 embryos for each sample. The expression of each gene was normalized to that of *ef1α* (means ± SEM), and the value in uninjected control was set to 1. Asterisks denote statistical significance (Control versus *nrf2a* overexpression, $^{**}P < 0.01$; Student's *t*-test, $n = 6$ for each group). (b) and (c) The gene expression of the indicated proteasome subunits in 4 dpf wild-type or $nrf2a^{fh318/fh318}$ mutant larvae that were treated (or not treated) with 100 μM DEM for 6 h (b) and 12 h (c) was analyzed by a real-time qPCR. The expression of each gene was normalized to that of *ef1α* (means ± SEM), and the value in untreated wild-type control was set to 1.

To confirm the Nrf2-dependent upregulation of these genes, we next carried out a real-time qPCR using *nrf2a*-overexpressing embryos. The result indicated that the expression levels of *pgd* and *fbp1a* (1.40- and 2.76-fold, resp.), but not *pck1*, *pcxb,* and *taldo1* (1.21-, 0.75-, and 0.70-fold, resp.), were significantly upregulated by the overexpression of *nrf2a* (Figure 3(b)). For *pgd* and *fbp1a*, we further analyzed the gene expression in DEM-treated larvae. As shown in Figure 3(c), the DEM treatment induced the expression of both *pgd* and *fbp1a* in wild-type larvae (5.85- and 2.18-fold, resp.), and

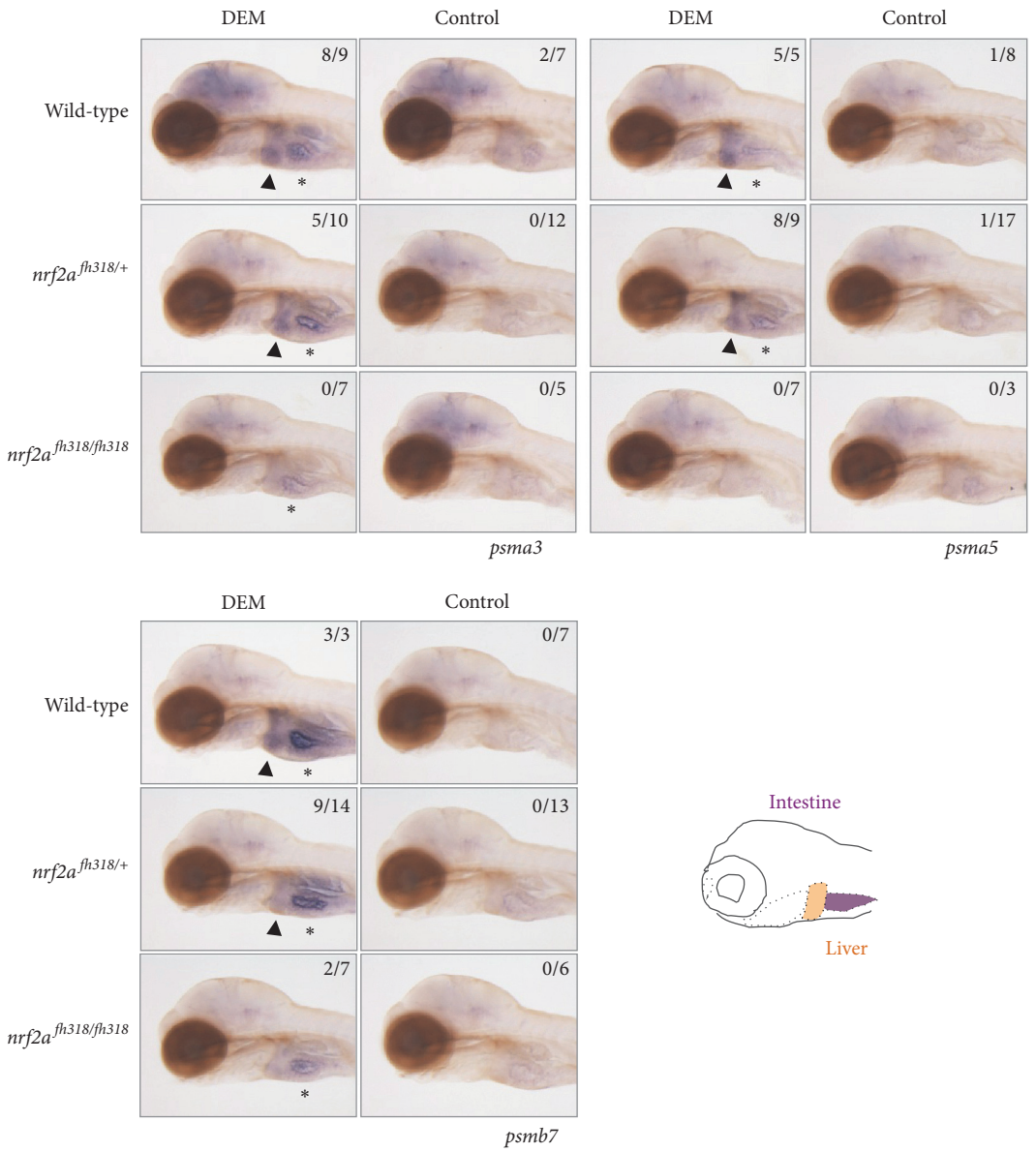

Figure 2: The induction profiles of proteasome subunit genes. Whole-mount in situ hybridization was performed to analyze the induction profiles of *psma3*, *psma5*, and *psmb7* using 4 dpf *nrf2a*^{fh318} mutant larvae treated with or without 100 μM DEM for 12 h. The arrowheads indicate positive expression in the liver, and asterisks denote the basal expression in the intestine. The numbers in each picture indicate the positive/tested larvae.

the induction was weaker in homozygous *nrf2a*^{fh318} mutant larvae (2.15- and 1.20-fold, resp.), suggesting clear genetic evidence of Nrf2-dependent regulation.

Induction profiles of these two genes were further analyzed by in situ hybridization (Figure 4). In wild-type and *nrf2a*^{fh318} heterozygous mutant larvae, *pgd* was induced specifically in the liver after treatment with DEM for 6 h, while no induction was observed in *nrf2a*^{fh318} homozygous mutant. *fbp1a* was also induced by DEM in the liver, and this induction was stronger in wild-type and heterozygous mutant compared with homozygous mutant. Weak DEM-induced expression of *fbp1a* was also observed in the gills, but this induction was independent of *nrf2a* genotypes. These results indicate that the Keap1-Nrf2 system, at least in part, regulates the transcription of these enzymes involved in glucose metabolism.

3.4. The Identification of Other Target Genes for Zebrafish Nrf2. The microarray data offered several more candidates for the conserved Nrf2 target gene in zebrafish. We selected 6 genes from the 27 overlapping genes (see Figure 3(a) and Table S3) identified in the current and previous microarray analyses and analyzed their expression using a real-time qPCR. The genes that were selected included *gclm* (glutamate-cysteine

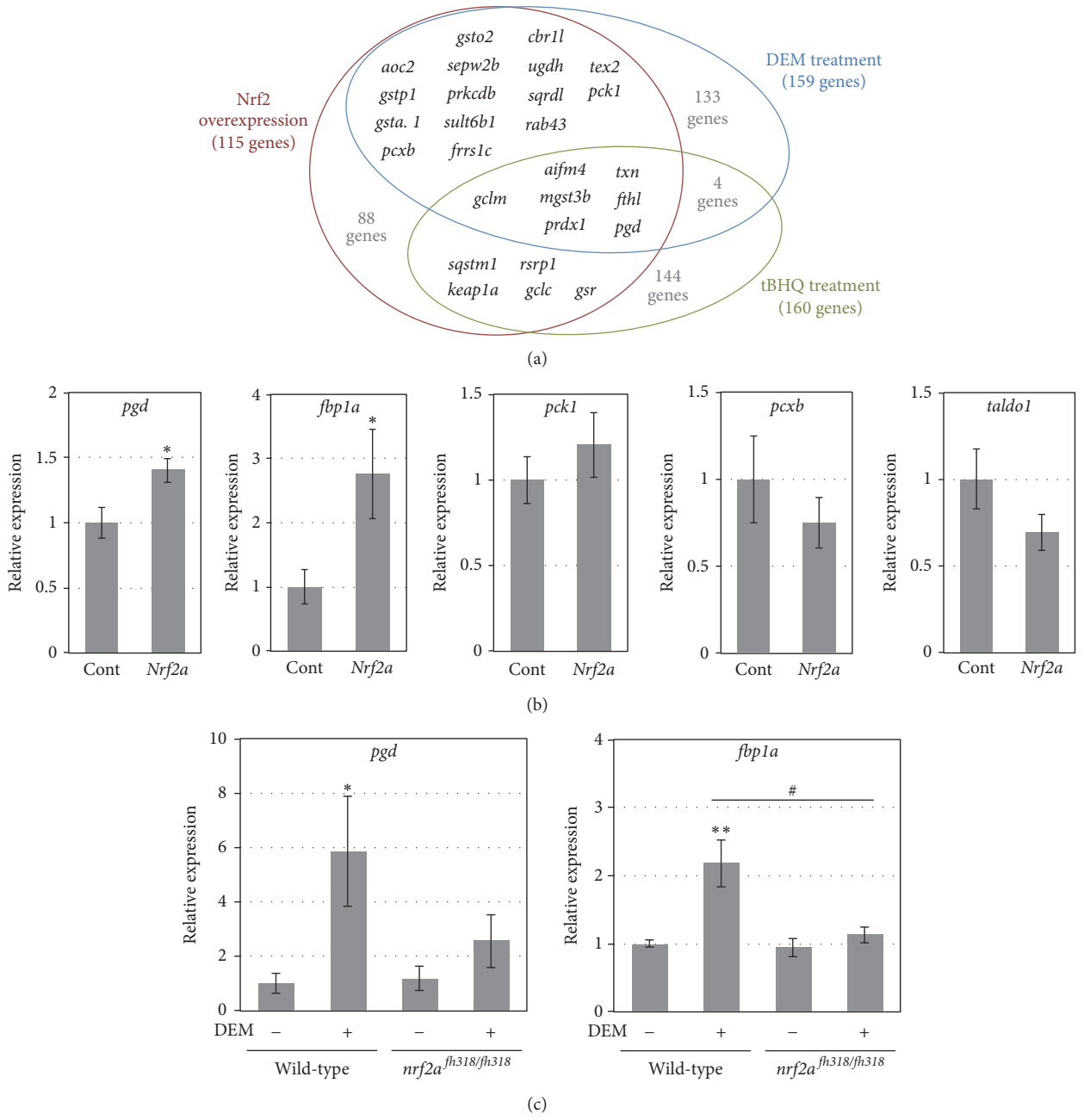

Figure 3: The expression of glucose metabolism-related genes. (a) The upregulated gene lineups from the three microarray experiments were compared. The data of DEM- or tBHQ-treated zebrafish larvae are from Nakajima et al. [19] and Hahn et al. [20], respectively. Numbers in parentheses and in the Venn diagrams denote the numbers of genes which belong to each category. The names of 27 overlapping genes were displayed. (b) The gene expression of the indicated enzymes related to glucose metabolism in 8 hpf wild-type embryos injected with or without 100 pg of *nrf2a* mRNA at the 1-cell stage was analyzed by a real-time qPCR. Asterisks denote statistical significance (Control versus *nrf2a* overexpression, $^{*}P < 0.05$; Student's *t*-test, $n = 6$ for each group). (c) The gene expression of the indicated enzymes related to glucose metabolism in 4 dpf wild-type or *nrf2a*$^{fh318/fh318}$ mutant larvae treated with or without 100 μM DEM for 6 h was analyzed by a real-time qPCR. Asterisks and hash marks denote statistical significance (DEM+ versus DEM−, $^{*}P < 0.05$ and $^{**}P < 0.01$; wild-type versus *nrf2a*$^{fh318/fh318}$, $^{\#}P < 0.05$; Student's *t*-test, $n = 6$ for each group).

ligase, modifier subunit), *gsto2* (glutathione *S*-transferase omega 2), *gsr* (glutathione reductase), *sqstm1* (sequestosome 1), and *keap1a* (kelch-like ECH-associated protein 1a), together with a well-studied *nrf2a* target, *gstp1* (glutathione *S*-transferase pi 1). As shown in Figure 5(a), *gclm*, *gsto2 gsr,* and *gstp1* were upregulated by the overexpression of *nrf2a* (1.98-, 9.10-, 3.12-, and 6.39-fold, resp.), while *sqstm1* and *keap1a* were only slightly induced (1.28- and 1.21-fold, resp.). The expression of these genes was further investigated in the DEM-treated embryos (Figure 5(b)). All of the genes were

Table 2: The pathways activated in both *nrf2a*-overexpressing embryos and DEM/tBHQ-treated larvae.

p value	Pathway name	Genes
3.33*E* − 9	Glutathione conjugation	*gclc*, *gsto2*, *gstp1*, *gclm*, *gsta.1*
4.13*E* − 7	Phase II conjugation	*gclc*, *gsto2*, *gstp1*, *ugdh*, *gclm*, *gsta.1*
7.44*E* − 7	Detoxification of reactive oxygen species	*txn*, *gstp1*, *prdx1*, *gsr*
8.26*E* − 7	Biological oxidations	*gclc*, *gstp1*, *gsto2*, *aoc2*, *ugdh*, *gclm*, *gsta.1*
1.39*E* − 3	Vitamin C (ascorbate) metabolism	*gsto2*
1.78*E* − 3	Sulfur amino acid metabolism	*gclc*, *sqrdl*, *gclm*
4.77*E* − 3	TP53 regulates metabolic genes	*txn*, *prdx1*, *gsr*
6.76*E* − 3	Glutathione synthesis and recycling	*gclc*, *gclm*
8.46*E* − 3	Cellular responses to stress	*txn*, *gstp1*, *prdx1*, *gsr*
8.83*E* − 3	Metabolism	*gclc*, ***pck1***, *gstp1*, *sqrdl*, *txn*, *gsta.1*, *gsr*, ***pcxb***, *gsto2*, *aoc2*, ***pgd***, *ugdh*, *gclm*

Bold genes encode enzymes related to the glucose metabolism process.

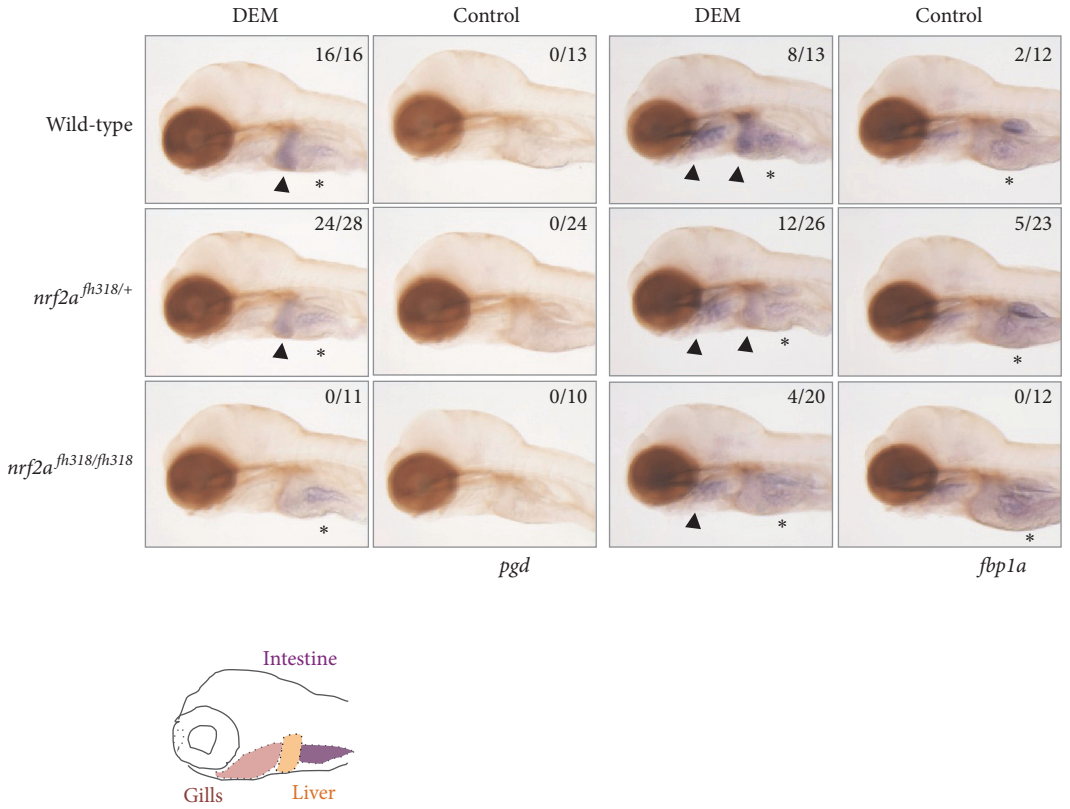

Figure 4: The induction profiles of glucose metabolism-related genes. Whole-mount in situ hybridization was performed to analyze the induction profile of *pgd* and *fbp1a* using 4 pdf *nrf2a*^{fh318} mutant larvae treated with or without 100 μM DEM for 6 h. The arrowheads indicate positive expression in the liver and gills, and asterisks denote the basal expression in the intestine. The numbers in each picture indicate the positive expression in the liver/tested larvae.

strongly induced by DEM in wild-type larvae (*gclm*, 6.37-fold; *gsto2*, 3.99-fold; *gsr*, 9.40-fold; *gstp1*, 5.88-fold; *sqstm1*, 5.44-fold; *keap1a*, 1.72-fold); the induction was weaker, except for *keap1a*, in *nrf2a*$^{fh318/fh318}$ mutant larvae (*gclm*, 2.80-fold; *gsto2*, 2.08-fold; *gsr*, 6.69-fold; *gstp1*, 1.94-fold; *sqstm1*, 2.35-fold; *keap1a*, 2.10-fold). The results suggest that these genes are target genes for zebrafish Nrf2.

In our microarray analysis, we also found 55 genes that were downregulated by the overexpression of *nrf2a* (Table S4). None of these genes, except *hesx1*, was identified in the previous DEM- or tBHQ-based microarray analyses (25 and 82 genes, resp.) [19, 20]. More importantly, we could not find genes associated with fatty acid metabolism or inflammation—recent studies have implied that these functions are

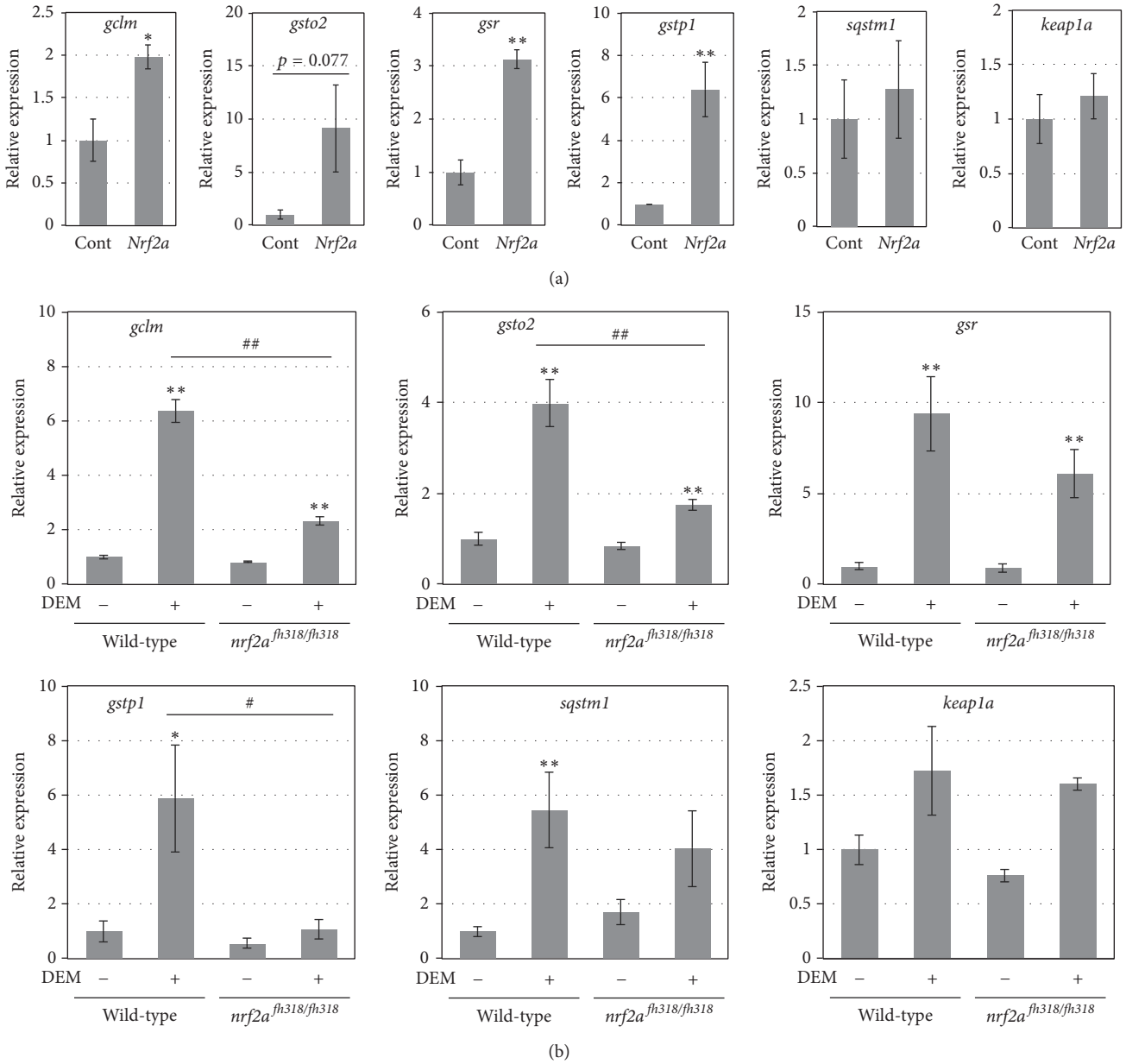

Figure 5: The expression of other candidate genes for zebrafish Nrf2 targets. (a) The expression of the indicated genes in 8 hpf wild-type embryos injected with or without 100 pg of *nrf2a* mRNA at the 1-cell stage was analyzed by a real-time qPCR. Asterisks denote statistical significance (Control versus *nrf2a* overexpression, $^{*}P < 0.05$ and $^{**}P < 0.01$; Student's *t*-test, $n = 6$ for each group). (b) The expression of the indicated genes in 4 dpf wild-type or $nrf2a^{fh318/fh318}$ mutant larvae treated with or without 100 μM DEM for 6 h was analyzed by a real-time qPCR. Asterisks and hash marks denote statistical significance (DEM+ versus DEM−, $^{*}P < 0.05$ and $^{**}P < 0.01$; wild-type versus $nrf2a^{fh318/fh318}$, $^{\#}P < 0.05$ and $^{\#\#}P < 0.01$; Student's *t*-test, $n = 6$ for each group).

negatively regulated by Nrf2 [5, 22, 23]. The evolutional conservation related to the Nrf2-dependent negative regulation of some types of genes remains unclear.

4. Discussion

In the present study, we found that the three proteasome subunits in the 20S core particle were regulated by zebrafish Nrf2, one of which (*psmb7*) has a trypsin-like protease activity; the others (*psma3* and *psma5*) comprise the α ring structure [24]. In mammals, multiple subunits of proteasome have also been shown to be regulated by Nrf2 at the transcriptional level [4], suggesting the presence of a conserved regulatory mechanism among vertebrates. Consistent with the report by Kwak et al. [4], which showed the transcriptional induction of proteasome subunits in mice liver after treatment with D3T, an Nrf2-activating antioxidant, induction was observed dominantly in the liver of zebrafish larvae. Although most Nrf2

target genes tested in zebrafish larvae showed the induction in the nose and gills in addition to the liver [19], proteasome subunit genes were induced only in the liver. The molecular basis of this liver specificity together with their slow induction should be characterized in the future. As the Nrf2-dependent upregulation of the proteasome function is suggested to be important in the defense against oxidative stress, endoplasmic reticulum stress, and senescence [25–27], it is anticipated that the regulatory context should be clarified for medical applications. The zebrafish model can also provide a good model for further study.

Enzymes related to glucose metabolism were also targeted by Nrf2 in zebrafish. Phosphogluconate dehydrogenase (Pgd) is an enzyme that converts 6-phosphogluconate to ribulose 5-phosphate in the oxidative branch of the pentose phosphate pathway, which produces NADPH as well as purine nucleotides [28]. The Nrf2-dependent upregulation of *pgd* has also been demonstrated in mice [6]. The upregulation of *pgd* may confer protection against stressors by augmenting the supply of NADPH, an essential cofactor for redox homeostasis [5], and the activation of nucleotide biosynthesis through the pentose phosphate pathway, which may lead to the metabolic remodeling in cancer cells [6]. The zebrafish has recently emerged as an important model in cancer biology [29, 30]. It will be worthwhile to study the Nrf2-dependent metabolic remodeling that takes place in carcinogenesis using zebrafish. In addition to *pgd*, the Nrf2-depedent transcriptional regulation of fructose-1,6-bisphosphatase (Fbp), an enzyme that converts fructose 1,6-bisphosphate to fructose 6-phosphate in gluconeogenesis, was observed specifically in the liver. Further study on the mechanism underlying this liver-specific induction will provide an important clue to understand the biological significance of Nrf2-dependent regulation of glucose metabolism.

In the present microarray analysis, the cut-off value for significant upregulation by the overexpression of *nrf2a* was set at a 1.5-fold change instead of a 2-fold change in the previous studies [19, 20]. It was effective, since 4 out of 6 genes, as we validated the microarray data by a real-time qPCR with statistical significance, showed less than 2-fold change in the microarray analysis (see Figure S2 and Table S3). A correlation in the fold changes between microarray and real-time qPCR data was relatively poor; thus, it is worthwhile to pick up not only high-ranked genes in the microarray analysis but also low-ranked genes for further analyses.

The unique point of the present study is that genes were screened using *nrf2a*-overexpressing embryos. A major approach for the microarray-based screening of Nrf2-target genes is the use of cells/tissues/animals treated with Nrf2-activating compounds [31–33] as is the case for the previous screen studies that used zebrafish [19, 20]. Another approach is the use of Keap1 knockout cells/tissues [5, 34]. Since Keap1 is an E3 ubiquitin ligase that targets Nrf2, the disruption of its gene increases the stability of Nrf2 and leads to the constitutive activation of Nrf2. A study by Yates et al. [22] which compared sets of genes upregulated by treatment with a potent Nrf2-activating compound (CDDO-Im) with those upregulated by liver-specific Keap1 knockout is of particular interest. Keap1-knockout activated Nrf2-dependent transcription more strongly than the pharmacological activation; as a result greater numbers of Nrf2-regulated genes were detected [22]. It is possible that similar effects were observed in the overexpression method of the present study.

5. Conclusions

In conclusion, we found novel Nrf2-target genes in zebrafish by a microarray analysis using *nrf2a*-overexpressing zebrafish embryos. The basal expression levels of proteasome subunits were revealed to be regulated by zebrafish Nrf2. In addition, enzymes involved in the pentose phosphate pathway and gluconeogenesis were found to be under Nrf2-dependent transcriptional control. These results suggest that the Nrf2-mediated regulation of the genes related to protein turnover and glucose metabolism, at least a part of them, was evolutionarily conserved in vertebrates.

Competing Interests

The authors declare that they have no competing interests.

Authors' Contributions

Vu Thanh Nguyen and Yuji Fuse contributed equally to this work.

Acknowledgments

The authors thank Masayuki Yamamoto for valuable suggestions and Hiroshi Kaneko, Li Li, Yaeko Nakajima-Takagi, Tadayuki Tsujita, and Takeshi Wakasa for experimental help. This work was supported by Grants-in-Aids from the Ministry of Education, Science, Sports and Culture of Japan (to Makoto Kobayashi) (21659043, 24590340, 25118705, 26116705, and 26520101) and the grant from the Yamazaki Spice Promotion Foundation.

References

[1] T. Suzuki and M. Yamamoto, "Molecular basis of the Keap1–Nrf2 system," *Free Radical Biology and Medicine*, vol. 88, pp. 93–100, 2015.

[2] M. Kobayashi and M. Yamamoto, "Nrf2-Keap1 regulation of cellular defense mechanisms against electrophiles and reactive oxygen species," *Advances in Enzyme Regulation*, vol. 46, no. 1, pp. 113–140, 2006.

[3] J. D. Hayes and A. T. Dinkova-Kostova, "The Nrf2 regulatory network provides an interface between redox and intermediary metabolism," *Trends in Biochemical Sciences*, vol. 39, no. 4, pp. 199–218, 2014.

[4] M.-K. Kwak, N. Wakabayashi, J. L. Greenlaw, M. Yamamoto, and T. W. Kensler, "Antioxidants enhance mammalian proteasome expression through the Keap1-Nrf2 signaling pathway," *Molecular and Cellular Biology*, vol. 23, no. 23, pp. 8786–8794, 2003.

[5] K. C. Wu, J. Y. Cui, and C. D. Klaassen, "Beneficial role of Nrf2 in regulating NADPH generation and consumption," *Toxicological Sciences*, vol. 123, no. 2, pp. 590–600, 2011.

[6] Y. Mitsuishi, K. Taguchi, Y. Kawatani et al., "Nrf2 redirects glucose and glutamine into anabolic pathways in metabolic reprogramming," *Cancer Cell*, vol. 22, no. 1, pp. 66–79, 2012.

[7] D. V. Chartoumpekis, N. Wakabayashi, and T. W. Kensler, "Keap1/Nrf2 pathway in the frontiers of cancer and non-cancer cell metabolism," *Biochemical Society Transactions*, vol. 43, pp. 639–644, 2015.

[8] T. Suzuki, H. Motohashi, and M. Yamamoto, "Toward clinical application of the Keap1-Nrf2 pathway," *Trends in Pharmacological Sciences*, vol. 34, no. 6, pp. 340–346, 2013.

[9] C. A. MacRae and R. T. Peterson, "Zebrafish as tools for drug discovery," *Nature Reviews Drug Discovery*, vol. 14, no. 10, pp. 721–731, 2015.

[10] J. B. Phillips and M. Westerfield, "Zebrafish models in translational research: tipping the scales toward advancements in human health," *Disease Models and Mechanisms*, vol. 7, no. 7, pp. 739–743, 2014.

[11] M. Kobayashi, K. Itoh, T. Suzuki et al., "Identification of the interactive interface and phylogenic conservation of the Nrf2-Keap1 system," *Genes to Cells*, vol. 7, no. 8, pp. 807–820, 2002.

[12] Y. Takagi, M. Kobayashi, L. Li, T. Suzuki, K. Nishikawa, and M. Yamamoto, "MafT, a new member of the small Maf protein family in zebrafish," *Biochemical and Biophysical Research Communications*, vol. 320, no. 1, pp. 62–69, 2004.

[13] T. Suzuki, Y. Takagi, H. Osanai et al., "Pi-class glutathione S-transferase genes are regulated by Nrf2 through an evolutionarily conserved regulatory element in zebrafish," *Biochemical Journal*, vol. 388, no. 1, pp. 65–73, 2005.

[14] L. Li, M. Kobayashi, H. Kaneko, Y. Nakajima-Takagi, Y. Nakayama, and M. Yamamoto, "Molecular evolution of Keap1: two Keap1 molecules with distinctive intervening region structures are conserved among fish," *Journal of Biological Chemistry*, vol. 283, no. 6, pp. 3248–3255, 2008.

[15] M. Kobayashi, L. Li, N. Iwamoto et al., "The antioxidant defense system Keap1-Nrf2 comprises a multiple sensing mechanism for responding to a wide range of chemical compounds," *Molecular and Cellular Biology*, vol. 29, no. 2, pp. 493–502, 2009.

[16] K. Mukaigasa, L. T. P. Nguyen, L. Li, H. Nakajima, M. Yamamoto, and M. Kobayashi, "Genetic evidence of an evolutionarily conserved role for Nrf2 in the protection against oxidative stress," *Molecular and Cellular Biology*, vol. 32, no. 21, pp. 4455–4461, 2012.

[17] Y. Fuse, V. T. Nguyen, and M. Kobayashi, "Nrf2-dependent protection against acute sodium arsenite toxicity in zebrafish," *Toxicology and Applied Pharmacology*, vol. 305, pp. 136–142, 2016.

[18] M. E. Hahn, A. R. Timme-Laragy, S. I. Karchner, and J. J. Stegeman, "Nrf2 and Nrf2-related proteins in development and developmental toxicity: insights from studies in zebrafish (*Danio rerio*)," *Free Radical Biology and Medicine*, vol. 88, pp. 275–289, 2015.

[19] H. Nakajima, Y. Nakajima-Takagi, T. Tsujita et al., "Tissue-restricted expression of Nrf2 and its target genes in zebrafish with gene-specific variations in the induction profiles," *PLoS ONE*, vol. 6, no. 10, Article ID e26884, 2011.

[20] M. E. Hahn, A. G. McArthur, S. I. Karchner et al., "The transcriptional response to oxidative stress during vertebrate development: effects of *tert*-butylhydroquinone and 2,3,7,8-tetrachlorodibenzo-*p*-dioxin," *PLoS ONE*, vol. 9, no. 11, Article ID e113158, 2014.

[21] Y. Fuse, H. Nakajima, Y. Nakajima-Takagi, O. Nakajima, and M. Kobayashi, "Heme-mediated inhibition of Bach1 regulates the liver specificity and transience of the Nrf2-dependent induction of zebrafish heme oxygenase 1," *Genes to Cells*, vol. 20, no. 7, pp. 590–600, 2015.

[22] M. S. Yates, Q. T. Tran, P. M. Dolan et al., "Genetic versus chemoprotective activation of Nrf2 signaling: overlapping yet distinct gene expression profiles between Keap1 knockout and triterpenoid-treated mice," *Carcinogenesis*, vol. 30, no. 6, pp. 1024–1031, 2009.

[23] E. H. Kobayashi, T. Suzuki, R. Funayama et al., "Nrf2 suppresses macrophage inflammatory response by blocking proinflammatory cytokine transcription," *Nature Communications*, vol. 7, Article ID 11624, 2016.

[24] R. J. Tomko Jr. and M. Hochstrasser, "Molecular architecture and assembly of the eukaryotic proteasome," *Annual Review of Biochemistry*, vol. 82, pp. 415–445, 2013.

[25] A. M. Pickering, R. A. Linder, H. Zhang, H. J. Forman, and K. J. A. Davies, "Nrf2-dependent induction of proteasome and Pa28$\alpha\beta$ regulator are required for adaptation to oxidative stress," *The Journal of Biological Chemistry*, vol. 287, no. 13, pp. 10021–10031, 2012.

[26] S. Lee, E.-G. Hur, I.-G. Ryoo, K.-A. Jung, J. Kwak, and M.-K. Kwak, "Involvement of the Nrf2-proteasome pathway in the endoplasmic reticulum stress response in pancreatic β-cells," *Toxicology and Applied Pharmacology*, vol. 264, no. 3, pp. 431–438, 2012.

[27] S. Kapeta, N. Chondrogianni, and E. S. Gonos, "Nuclear erythroid factor 2-mediated proteasome activation delays senescence in human fibroblasts," *Journal of Biological Chemistry*, vol. 285, no. 11, pp. 8171–8184, 2010.

[28] A. Stincone, A. Prigione, T. Cramer et al., "The return of metabolism: biochemistry and physiology of the pentose phosphate pathway," *Biological Reviews*, vol. 90, no. 3, pp. 927–963, 2015.

[29] R. M. White, "Cross-species oncogenomics using zebrafish models of cancer," *Current Opinion in Genetics and Development*, vol. 30, pp. 73–79, 2015.

[30] J. Yen, R. M. White, and D. L. Stemple, "Zebrafish models of cancer: progress and future challenges," *Current Opinion in Genetics and Development*, vol. 24, no. 1, pp. 38–45, 2014.

[31] R. K. Thimmulappa, K. H. Mai, S. Srisuma, T. W. Kensler, M. Yamamoto, and S. Biswal, "Identification of Nrf2-regulated genes induced by the chemopreventive agent sulforaphane by oligonucleotide microarray," *Cancer Research*, vol. 62, no. 18, pp. 5196–5203, 2002.

[32] M.-K. Kwak, N. Wakabayashi, K. Itoh, H. Motohashi, M. Yamamoto, and T. W. Kensler, "Modulation of gene expression by cancer chemopreventive dithiolethiones through the Keap1-Nrf2 pathway. Identification of novel gene clusters for cell survival," *The Journal of Biological Chemistry*, vol. 278, no. 10, pp. 8135–8145, 2003.

[33] R. Hu, C. Xu, G. Shen et al., "Identification of Nrf2-regulated genes induced by chemopreventive isothiocyanate PEITC by oligonucleotide microarray," *Life Sciences*, vol. 79, no. 20, pp. 1944–1955, 2006.

[34] H. Okawa, H. Motohashi, A. Kobayashi, H. Aburatani, T. W. Kensler, and M. Yamamoto, "Hepatocyte-specific deletion of the *keap1* gene activates Nrf2 and confers potent resistance against acute drug toxicity," *Biochemical and Biophysical Research Communications*, vol. 339, no. 1, pp. 79–88, 2006.

Hindawi Publishing Corporation
Oxidative Medicine and Cellular Longevity
Volume 2016, Article ID 8694641, 9 pages
http://dx.doi.org/10.1155/2016/8694641

Research Article

Nuclear Factor (Erythroid-Derived)-Related Factor 2-Associated Retinal Pigment Epithelial Cell Protection under Blue Light-Induced Oxidative Stress

Kei Takayama,[1] Hiroki Kaneko,[1] Keiko Kataoka,[1] Reona Kimoto,[1] Shiang-Jyi Hwang,[1,2] Fuxiang Ye,[1,3] Yosuke Nagasaka,[1] Taichi Tsunekawa,[1] Toshiyuki Matsuura,[1] Norie Nonobe,[1] Yasuki Ito,[1] and Hiroko Terasaki[1]

[1]*Department of Ophthalmology, Nagoya University Graduate School of Medicine, Nagoya 466-8550, Japan*
[2]*Laboratory of Bell Research Center-Department of Obstetrics and Gynecology Collaborative Research, Nagoya University Graduate School of Medicine, Nagoya 466-8550, Japan*
[3]*Department of Ophthalmology, Shanghai First People's Hospital, Shanghai Jiao Tong University School of Medicine, Shanghai 200240, China*

Correspondence should be addressed to Hiroki Kaneko; h-kaneko@med.nagoya-u.ac.jp

Received 28 May 2016; Revised 29 July 2016; Accepted 25 August 2016

Academic Editor: Ian Copple

Purpose. It is a matter of increasing concern that exposure to light-emitting diodes (LED), particularly blue light (BL), damages retinal cells. This study aimed to investigate the retinal pigment epithelium (RPE) damage caused by BL and to elucidate the role of nuclear factor (erythroid-derived)-related factor 2 (Nrf2) in the pathogenesis of BL-induced RPE damage. *Methods*. ARPE-19, a human RPE cell line, and mouse primary RPE cells from wild-type and *Nrf2* knockout ($Nrf2^{-/-}$) mice were cultured under blue LED exposure (intermediate wavelength, 450 nm). Cell death rate and reactive oxygen species (ROS) generation were measured. TUNEL staining was performed to detect apoptosis. Real-time polymerase chain reaction was performed on *NRF2* mRNA, and western blotting was performed to detect Nrf2 proteins in the nucleus or cytoplasm of RPE cells. *Results*. BL exposure increased cell death rate and ROS generation in ARPE-19 cells in a time-dependent manner; cell death was caused by apoptosis. Moreover, BL exposure induced *NRF2* mRNA upregulation and Nrf2 nuclear translocation in RPE. Cell death rate was significantly higher in RPE cells from $Nrf2^{-/-}$ mice than from wild-type mice. *Conclusions*. The Nrf2 pathway plays an important role in protecting RPE cells against BL-induced oxidative stress.

1. Introduction

Age-related macular degeneration (AMD) leads to blindness, accounting for approximately 9% of blindness cases worldwide. There are approximately 30 million patients with AMD, of whom > 0.5 million have become blind [1]. AMD can be divided into two categories: wet and dry AMD [2]. In wet AMD, choroidal neovascularization breaks the retinal pigment epithelium (RPE) through to the neural retina, causing the leakage of fluid, lipids, and blood; these changes lead to fibrous scarring and antivascular endothelial growth factor drugs are approved for wet AMD treatment [3–5]. In dry AMD, progressive geographic atrophy of RPE occurs, followed by severe damage of the photoreceptors. Severe irreversible blindness from AMD is caused by these advanced forms [6, 7].

AMD may have a multifactorial pathogenesis [8] and is characterized by photoreceptor cell death [9–14]. Several factors, such as smoking, obesity, eating habits, and light exposure, particularly blue light (BL) exposure, play important roles in the progression of AMD [15–18]. BL exposure causes an increase in the reactive oxygen species (ROS), which may result in structural damage and decreased viability of retinal cells. It also causes RPE apoptosis via oxidative stress and mitochondrial damage [19–21].

One of the most important antioxidation pathways is the nuclear factor (erythroid-derived)-like 2 (Nrf2) pathway. Nrf2 is a 65 kDa molecule with a basic leucine zipper structure [22]. Without oxidative stress, Nrf2 in its inactive state is bound to Kelch-like ECH-associated protein 1 (Keap1) in the cytoplasm [23]. When cells are exposed to oxidative stress, the active site cysteine residues of Keap1 are oxidized, preventing Keap1 from interacting with *NRF2*. With Nrf2 accumulation in the cytoplasm, Nrf2 moves to the nucleus and binds to the antioxidant response element [24]. Nrf2 also serves as the master regulator of a highly coordinated antioxidant response in RPE cells [25]. Several studies demonstrated that antioxidative factors prevent RPE cells from being damaged by oxidative stress [26–34]. Some antioxidative factors also upregulate Nrf2 signaling. RPE damage may be prevented by these antioxidative factors via the upregulation of Nrf2 signaling. However, little is known regarding whether Nrf2 signaling activation is directly involved in RPE protection. Moreover, to the best of our knowledge, the direct relationship between BL exposure and Nrf2 signaling in RPE cells has not been well elucidated.

Nrf2 knockout ($Nrf2^{-/-}$) mice have been used in studies on systemic and ocular diseases. In ophthalmology, there are some studies regarding simulating diabetic retinopathy, ischemic retinopathy, and macular degeneration [32, 35–40]. $Nrf2^{-/-}$ mice developed ocular pathology similar to AMD [35]. Moreover, primary RPE cells from $Nrf2^{-/-}$ mice are susceptible to oxidative stress [32]. However, to the best of our knowledge, no studies have focused on $Nrf2^{-/-}$ RPE cells exposed to BL. Therefore, in this study, we prepared primary RPE cells from $Nrf2^{-/-}$ mice and investigated the direct involvement of *Nrf2* signaling in BL-induced RPE cell damage.

2. Materials and Methods

2.1. Cell Culture, Primary Cell Preparation, and BL Exposure. ARPE-19, a human RPE cell line, was purchased from the American Type Culture Collection (Rockville, MD, USA), and primary human RPE (hRPE) cell line was purchased from Lonza (Walkersville, MD, USA). Cells were grown in colorless Dulbecco's modified Eagle's medium (DMEM) premixed with Ham's F-12 (1 : 1 ratio, Sigma-Aldrich) and supplemented with 10% fetal bovine serum and the antibiotics streptomycin/penicillin G (Sigma-Aldrich) [13, 14]. Primary mouse RPE cells were collected from the wild-type and $Nrf2^{-/-}$ mice, as previously described [41, 42]. In brief, mouse eyecups were washed with sterile PBS, and flatmounts were created. The retina was gently removed to allow RPE layer to be on the surface of the flatmount. The RPE eyecups were rinsed in a chelating agent (Versene, Invitrogen), and RPE cells were enzymatically dislodged by 2% Dispase (Roche Diagnostics). Dislodged RPE cells were collected and cultured in DMEM containing antibiotics at 37°C containing 5% CO_2. Animal studies were approved by the Institutional Animal Care and Use Committee of the Nagoya University Graduate School of Medicine. All procedures involving animals were conducted according to the Association for Research in Vision and Ophthalmology Statement for the Use of Animals in Ophthalmic and Vision Research. $Nrf2^{-/-}$ mice were provided by RIKEN BRC through the National Bio-Resource Project of MEXT, Japan [43]. The cells were cultured in the dark or under BL (Zensui LED Lamp Blue™; Zensui Inc., Japan; peak wavelength: 450 μm, 1,200 lux).

2.2. LDH Assay and ROS Measurement. The cell death rate was evaluated by measuring the lactate dehydrogenase (LDH) activities using the Cytotoxicity Detection Kit PLUS (Roche Diagnostics, Mannheim, Germany). The supernatant of the culture medium, which contained LDH secreted from dead cells, was collected, followed by the addition of Triton X-100 in the medium to release intracellular LDH from the surviving cells. After measuring the LDH activities in the culture supernatant and medium, the proportions of dead cells among the total cells were calculated. Oxidative stress on BL exposure was evaluated with respect to the amount of ROS, measured using the OxiSelect™ ROS assay kit (Cell Biolabs. Co., Japan). In brief, after BL exposure, the assay was terminated by adding cell lysis buffer, and fluorescence intensity was measured at 493 nm (ex)/523 nm (em) using a fluorescent plate reader at each time point.

2.3. Cell Morphology and TUNEL Staining. Morphological changes of ARPE-19 cells exposed to BL were visualized using a phase-contrast microscope (FSX-100; Olympus, Tokyo, Japan). TUNEL-positive apoptotic cells were detected, as previously described [14, 44]. In brief, after 24 h of BL exposure, the cells were fixed with 2% PFA for 20 min at room temperature on the chambered cell culture slides. The cells were stained with the *In Situ* Cell Death Detection kit (Roche Diagnostics, Mannheim, Germany) and 0.3 mg/mL 4′,6-diamidino-2-phenylindole (Invitrogen, Carlsbad, CA, USA) for 1 h. The stained cells were then observed using a Bio Imaging Navigator fluorescence microscope (BZ-9000; Keyence, Osaka, Japan). The number of TUNEL-positive cells was calculated from images obtained with a 20x lens (537 × 710 μm). The average number of TUNEL-positive cells observed in three independent areas was calculated per well (n = number of wells) [14].

2.4. Protein and RNA Isolation. For total protein collection, the cultured human and mouse cells were lysed in RIPA buffer (Sigma-Aldrich) with a protease inhibitor cocktail (Roche Diagnostics, Indianapolis, IN, USA). The lysate was centrifuged at 15,000 ×g for 15 min at 4°C, and the supernatant was collected. Protein concentrations were determined using the Bradford Assay Kit (Bio-Rad, Hercules, CA, USA) with bovine serum albumin as the standard. To measure Nrf2 abundance in the nucleus, ARPE-19 cells were treated with NE-PER Nuclear and Cytoplasmic Extraction Kit (Pierce, Rockford, IL, USA) as previously described [41]. For real-time polymerase chain reaction (RT-PCR) analyses, total RNA was purified using the Qiagen RNeasy Mini Kit (Qiagen, Hilden, Germany), according to the manufacturer's protocol; the RNA concentration and quality were assessed using the

NanoDrop ND-1000 spectrophotometer (NanoDrop Technologies, Rockland, DE, USA) [13].

2.5. Quantitative Reverse Transcription-PCR (RT-PCR). The total RNA was reverse transcribed using the Transcriptor Universal cDNA Master Kit (Roche Diagnostics), starting with 2 μg of total RNA from each sample [13]. RT-PCR was performed using the Thunderbird Probe qPCR Mix (Toyobo Life Science, Osaka, Japan) and Gene Expression Assay containing primers and an FAM dye-labeled TaqMan probe for detecting human *NRF2* (HS00965961-g1; Applied Biosystems, USA) and eukaryotic 18S rRNA (Hs_99999901_s1; Applied Biosystems) that is available for human 18S rRNA [12]. PCR cycles consisted of a predenaturation step at 95°C for 2 min followed by 40 cycles of denaturing steps at 95°C for 15 s and annealing and extending steps at 60°C for 60 s. The relative expressions of the target genes were determined using the $2^{-\Delta\Delta Ct}$ method.

2.6. Western Blotting. Western blotting was performed as previously described [13, 14]. In brief, proteins (50 μg) from ARPE-19 cells were run on SDS precast gels (Wako, Osaka, Japan) and were transferred to PVDF membranes. The transferred membranes were washed with TBS-T (0.05 M Tris, 0.138 M NaCl, 0.0027 M KCl, pH = 8.0, and 0.05% Tween 20; Sigma-Aldrich) and then blocked with 5% nonfat dry milk/TBS-T at room temperature for 2 h. The membranes were then incubated with the rabbit antibody against NRF2 (1 : 100; Santa Cruz Biotechnology) at 4°C overnight. Total protein loading was assessed by immunoblotting using β-actin (1 : 3000: Cell Signaling), and nuclear protein loading was assessed by immunoblotting using lamin B (rabbit, 1 : 200; Santa Cruz Biotechnology) [45]. HRP-linked secondary antibody was used (1 : 3,000, Invitrogen) at RT for 1 h. The signal was visualized with enhanced chemiluminescence (ECL plus; GE Healthcare, Piscataway, NJ, USA) and captured using ImageQuant LAS-4000 Imager (GE Healthcare).

2.7. Outcomes and Statistical Analysis. Cell death rate, ROS generation, and RT-PCR of Nrf2 mRNA were statistically analyzed using the Mann-Whitney U test. P values of <0.05 were considered to be statistically significant.

3. Results

First, we examined whether BL exposure induced ROS generation and RPE cell death. BL exposure caused ARPE-19 cells to release LDH. The values of BL-induced/total LDH were 12.0% ± 4.2% (n = 4), 14.4% ± 5.9% (n = 4), 25.3% ± 5.8% (n = 4), and 27.7% ± 5.7% (n = 4) at 1, 2, 4, and 6 h after BL exposure, respectively. Among these values, there were significant increases at 4 h (P = 0.012) and 6 h (P = 0.0012) compared with the value at 1 h after BL exposure. In contrast, the values of BL-free/total LDH were 10.6% ± 3.8% (n = 4), 10.6% ± 2.3% (n = 4), 11.6% ± 2.0% (n = 4), and 11.8% ± 4.8% (n = 4) at 1, 2, 4, and 6 h after the onset of treatment, respectively. Among these values, there were also significant differences at 4 h (P = 0.014) and 6 h (P = 0.0057) compared with those without BL exposure. These findings also showed that ARPE-19 cell death was promoted by BL exposure in a time-dependent manner. This was confirmed by the LDH results from ARPE-19 cells not exposed to BL (Figure 1(a)). BL exposure also induced ROS generation in ARPE-19 cells in a time-dependent manner. ROS generation was significantly higher at 4 h (1.10 ± 0.05, n = 5, P = 0.027), 6 h (1.32 ± 0.11, n = 5, P = 0.043), and 24 h (22.4 ± 3.2, n = 5, P < 0.001) than at 1 h (1.0 ± 0.06, n = 5) after BL exposure (Figure 1(b)). Compared with ARPE-19 cells at 24 h after the onset of the treatment without BL exposure (control, 1.00 ± 0.10, n = 8), ARPE-19 cells exposed to BL generated significantly higher amounts of ROS (Figure 1(c); 14.8 ± 2.1, n = 8, P < 0.001). In hRPE cells, the values of BL-induced/total LDH were 9.5% ± 2.9% (n = 4), 8.6% ± 5.9% (n = 4), 16.4% ± 6.7% (n = 4), and 22.3% ± 5.7% (n = 4) at 1, 2, 4, and 6 h after BL exposure, respectively. Among these values, there were significant increases at 4 h (P = 0.034) and 6 h (P = 0.0011) compared with the value at 1 h after BL exposure. In contrast, the values of BL-free/total LDH were 9.4% ± 4.4% (n = 4), 9.5% ± 4.1% (n = 4), 11.2% ± 1.6% (n = 4), and 9.4% ± 4.4% (n = 4) at 1, 2, 4, and 6 h after the onset of treatment, respectively. Among these values, there were significant differences at 4 h (P = 0.048) and 6 h (P < 0.001) compared with those without BL exposure. These findings also showed that hRPE cell death was promoted by BL exposure in a time-dependent manner. This was confirmed by LDH results from hRPE cells not exposed to BL (Figure 1(d)). BL exposure also induced ROS generation in hRPE cells. ROS generation was significantly higher at 4 h (3.23 ± 0.07, n = 8, P < 0.001), 6 h (33.28 ± 0.49, n = 8, P < 0.001), and 24 h (10.54 ± 0.41, n = 8, P < 0.001) than at 1 h (1.0 ± 0.06, n = 8) after BL exposure (Figure 1(e)). Compared with hRPE cells at 24 h after the onset of the treatment without BL exposure (control, 1.00 ± 0.07, n = 8), hRPE cells exposed to BL generated significantly higher amounts of ROS (Figure 1(f); 22.12 ± 0.91, n = 8, P < 0.001).

Moreover, we examined the morphological change of ARPE-19 cells on BL exposure. Under normal condition, ARPE-19 cells showed a spindle shape. However, on BL exposure, these cells shrank and changed to an oval shape. These findings indicated that BL exposure decreased the viability of ARPE-19 cells as previously described (Figure 2) [46]. To clarify more precisely the mechanism of ARPE-19 cell death by BL exposure, we performed TUNEL staining of ARPE-19 cells with and without BL exposure. This staining revealed that numerous ARPE-19 cells were TUNEL-positive at 24 h after BL exposure. These findings indicated that BL exposure-induced ARPE-19 cell death mostly involved apoptosis (Figure 3).

To investigate the involvement of *NRF2* in the effect of BL exposure on ARPE-19 cells, we examined mRNA level and *NRF2* protein expression of ARPE-19 cells with and without BL exposure. Compared with the mRNA level of ARPE-19 cells at the onset of treatment (control, 1.00 ± 0.09, n = 2), the level at 6 h after BL exposure was significantly higher (Figure 4(a); 7.24 ± 3.74, n = 8, P = 0.042). *NRF2* mRNA level was increased by BL exposure, whereas it did not significantly increase in the absence of BL exposure from 0 to 6 h after the onset of treatment. Nrf2 protein

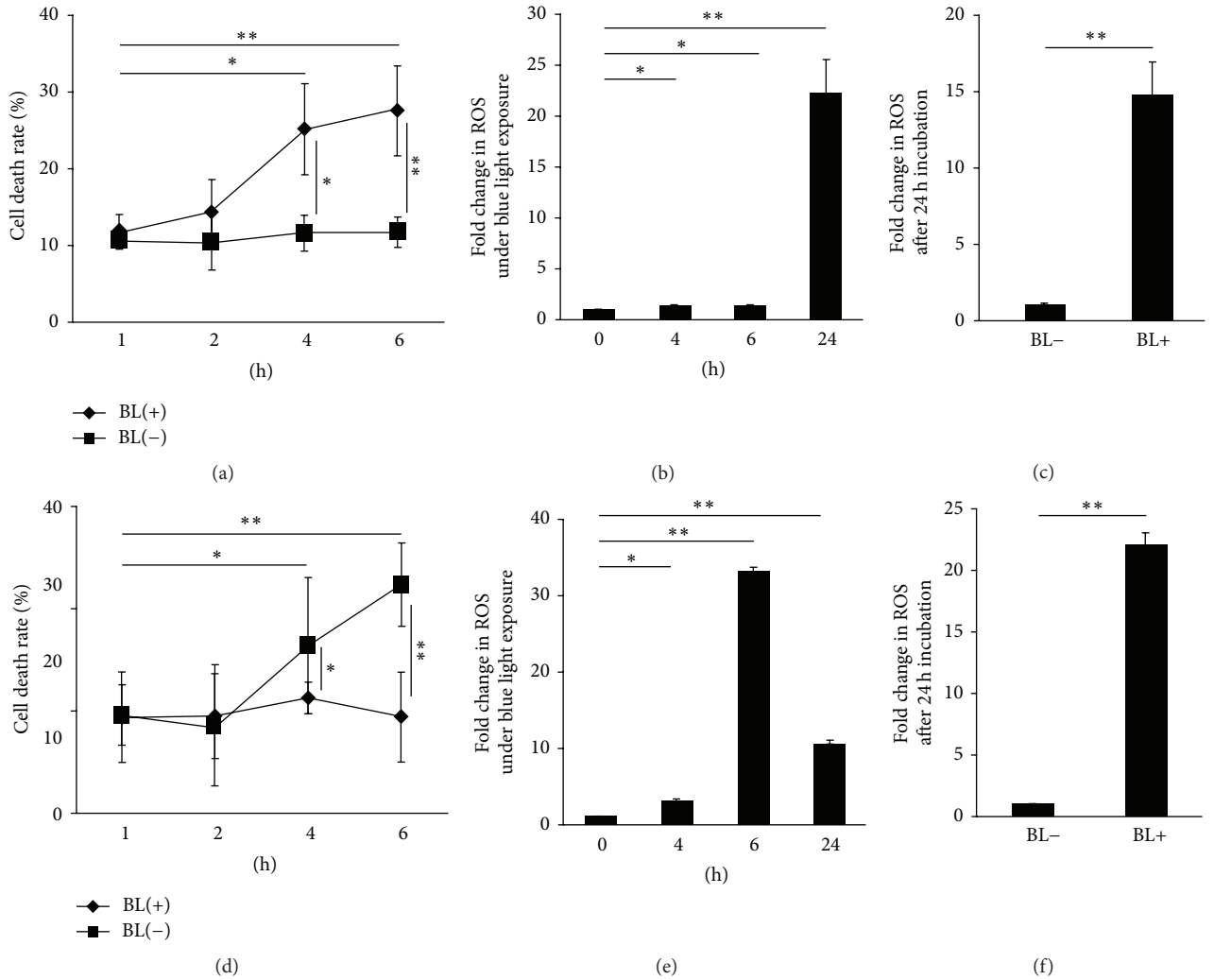

Figure 1: Increases in cell death rate and ROS generation in ARPE-19 cells and human RPE (hRPE) cells with or without BL exposure. (a) BL exposure increased the cell death rate and (b) ROS generation in ARPE-19 cells exposed to BL in a time-dependent manner. (c) ROS reactivity in ARPE-19 cells was significantly higher with BL exposure than without BL exposure 24 h later. (d) BL exposure increased the cell death rate and (e) ROS generation in hRPE cells exposed to BL. (f) ROS reactivity in hRPE cells was significantly higher with BL exposure than without BL exposure 24 h later. $^{*}P < 0.05$; $^{**}P < 0.01$.

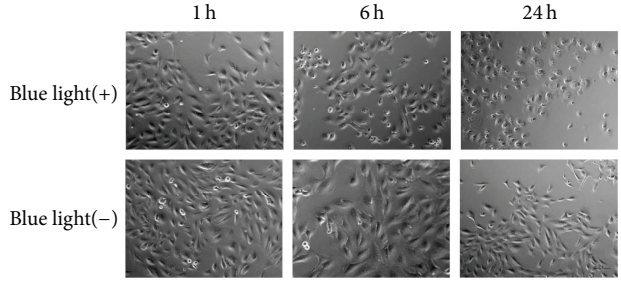

Figure 2: Morphological changes of ARPE-19 cells with or without blue light (BL) exposure. ARPE-19 cells changed to an oval shape and shrank upon BL exposure in a time-dependent manner (1, 6, and 24 h), whereas only minor changes were shown in those without BL exposure. Scale bar = 100 μm.

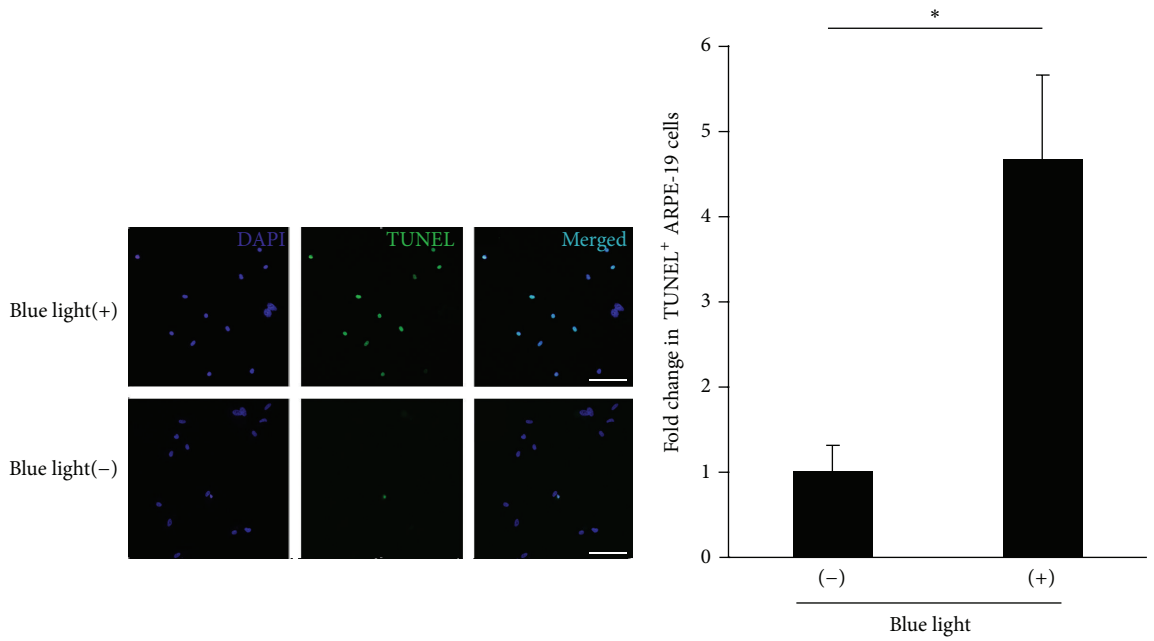

Figure 3: Detection of apoptosis in ARPE-19 cells at 24 h with or without BL exposure. (a) TUNEL (green) staining showed that, 24 h after BL exposure, ARPE-19 cells showed TUNEL positivity, reflecting apoptosis, by BL exposure. (b) There was a significant increase (4.67-fold) in the number of TUNEL-positive RPE cells with BL exposure compared to those without BL exposure. DAPI indicates the nucleus. Scale bar = 100 μm. $^{*}P < 0.01$.

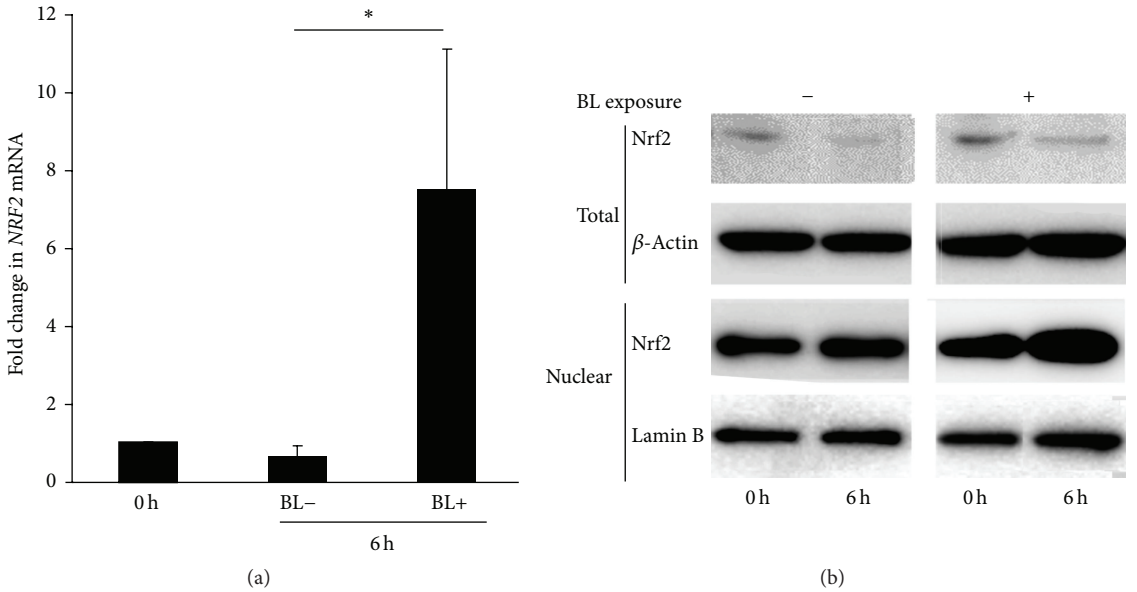

Figure 4: Nrf2 abundance in ARPE-19 cells with blue light (BL) exposure. (a) BL exposure increased *NRF2* mRNA level in ARPE-19 cells and showed a significant difference at 6 h compared with that without BL exposure. (b) Nrf2 protein in the total ARPE-19 cells was decreased at 6 h of exposure, although Nrf2 protein in the nucleus was increased at 6 h of exposure. $^{*}P < 0.05$.

expression from total ARPE-19 cells appeared to be decreased by BL exposure (Figure 4(b)). In an active state, Nrf2 showed nuclear translocation. Therefore, we separately obtained Nrf2 protein from the nucleus of ARPE-19 cells. Nrf2 protein was abundantly expressed in the ARPE-19 nucleus (Figure 4(b)). These results showed that, as a result of BL exposure, Nrf2 in ARPE-19 cells was activated. To shed more light on the importance of Nrf2 activation in BL exposure-induced ARPE-19 cell damage, we collected primary RPE cells from $Nrf2^{-/-}$ and wild-type ($Nrf2^{+/+}$) mice and compared their cell

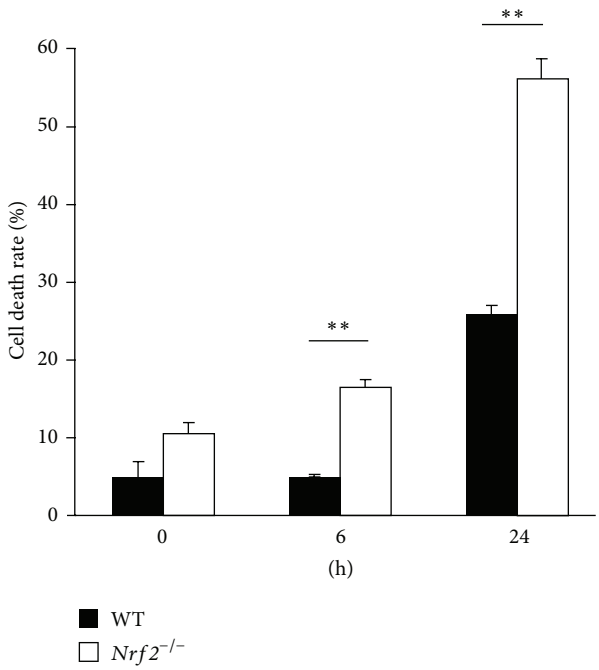

Figure 5: Increased cell death in *Nrf2*$^{-/-}$ RPE cells under blue light (BL) exposure. BL exposure induced more cell death in *Nrf2*$^{-/-}$ RPE cells than in wild-type RPE cells. $^{**}P < 0.01$.

death rates on BL exposure. Under these conditions, death rates of RPE cells from *Nrf2*$^{-/-}$ mice were 16.4 ± 1.1 ($n = 6$) and 56.1±2.8 ($n = 6$) at 6 and 24 h after exposure, respectively. In contrast, death rates of RPE cells from wild-type mice were 5.0 ± 0.1 ($n = 6$) and 25.7 ± 1.4 ($n = 6$) at 6 and 24 h after exposure, respectively. There were significant increases in the death rate in *Nrf2*$^{-/-}$ mouse RPE cells at 6 h ($P < 0.001$) and 24 h ($P < 0.001$) compared with those in wild-type mice (Figure 5). These findings indicated that Nrf2 plays an important role in blocking cell death caused by BL exposure-induced ROS generation.

4. Discussion

Visible light exposure-induced damage in retinal cells occurs through type I (free radical) and type II (oxygen-dependent) mechanisms. Free radicals induce cells to undergo necrosis, whereas oxygen-dependent mechanisms induce them to undergo apoptosis [47]. The mechanism of AMD was considered to involve oxidative stress caused by several factors driving RPE cells to die via apoptosis. BL exposure induces ROS generation, damaging mitochondrial DNA and cell structure; then, RPE cells are forced to enter an apoptotic state [15–17]. In this study, we demonstrated that BL exposure increased ROS generation in RPE cells and induced cell death in a time-dependent manner. In addition, TUNEL staining suggested that apoptotic RPE cell death was caused by BL exposure. To an extent, these findings simulate the pathogenesis of AMD.

ARPE-19 cells have some differences from primary hRPE cells in terms of promoter strength [48], proliferation, and cell death [49]. Previous studies have demonstrated that ARPE-19 cells are stronger and tolerable for oxidative stress compared with primary hRPE cells. In the present study, cell death rate and ROS of primary hRPE cells at 6 h of BL exposure (Figures 1(d) and 1(e)) were higher than those of ARPE-19 cells (Figures 1(a) and 1(b)). It has been previously demonstrated that primary hRPE cells are more sensitive than ARPE-19 cells against BL exposure-derived oxidative stress. On the other hand, ROS generation at 24 h was lower than that at 6 h in primary hRPE cells. This is possibly because primary hRPE cells were killed by 24 h BL exposure, and lower ROS generation was measured from the remaining (smaller number of) cells. Although both cells were damaged by BL exposure-derived ROS in a time-dependent manner, we considered that the use of these cells for this BL exposure study design is suitable.

The Nrf2 pathway is one of the most important pathways for protecting cells against oxidative stress [22]. Without oxidative stress, Nrf2, in its inactive state, is kept in the cytoplasm [23]. When cells are exposed to oxidative stress, this Nrf2 is released from Keap1 and moves to the nucleus where it functions in antioxidative protective mechanisms [24]. Other cells, such as epidermoid carcinoma cells [50] and retinal ganglion cells [51], also showed increased Nrf2 protein expression on BL exposure *in vitro*. These reports suggested that BL exposure increased ROS generation, activated *Nrf2* signaling, and reduced cell viability in a time-dependent manner. In our study, BL exposure of RPE cells increased ROS generation and apoptotic cell death rate in a time-dependent manner. In addition, *Nrf2* mRNA level and Nrf2 protein expression in the nucleus were increased in RPE cells in a time-dependent manner. These findings indicated that BL exposure induces the upregulation of ROS and Nrf2, which are involved in antioxidative protective mechanisms as previously reported.

If the *Nrf2* pathway does not properly function, antioxidative protection would be weaker and oxidative stress would cause severe cell damage. *Nrf2*$^{-/-}$ mice developed ocular pathology similar to the cardinal features of human AMD; deregulated autophagy is a likely mechanistic link between oxidative injury and inflammation [35]. *Nrf2*$^{-/-}$ RPE cells are susceptible to oxidative stress induced by t-butylhydroperoxide [32]. However, these studies did not use light exposure as an oxidative stressor. In dermatology, some studies revealing the relationship between *Nrf2*$^{-/-}$ cells and light exposure have been published [52–55]. Ultraviolet light-irradiated *Nrf2*$^{-/-}$ cells exhibited accelerated photoaging, resulting in the necrosis of irradiated cells, inflammatory cell infiltration, TUNEL-positive apoptotic cell formation, and the accumulation of oxidative DNA products, which are caused by oxidative stress. In this study, *Nrf2*$^{-/-}$ RPE cells died at rates of 10.5%, 16.4%, and 56.1% at 0, 6, and 24 h of BL exposure, respectively. This rate of cell death at 0 h tended to be higher than that of wild-type RPE cells, and the rates at 6 and 24 h were significantly higher than those of the wild-type RPE cells. These findings suggest that *Nrf2*$^{-/-}$ RPE cells are weaker than wild-type RPE cells, and *Nrf2* signaling plays a key protective role against BL-induced oxidative stress.

Previous studies demonstrated that some materials, such as polyphenol, salvianolic acid, 4-acetoxyphenol, 17-beta-estradiol triterpenoid RTA-408, pinosylvin, alpha-mangostin, and coconut water, protect cells against oxidative stress via *Nrf2* signaling. They showed that these materials upregulate Nrf2 protein expression and concluded that these materials protect cells against oxidative stress by increasing Nrf2 protein expression. However, it is unknown whether *Nrf2* protein expression is increased by these materials to rescue cells from oxidative stress or whether the expression is secondarily increased in a manner independent of these materials [26–34]. These materials would be expected to stimulate the *Nrf2* pathway and increase *Nrf2* protein expression to protect cells against oxidative stress.

A limitation of this study is that we examined only an *in vitro* biological change. A previous study used $Nrf2^{-/-}$ mice subjected to direct light exposure *in vivo* and revealed tissue change caused by oxidative stress [54]. Studying the effect of BL exposure on living $Nrf2^{-/-}$ mice will provide us with more precise information regarding the adverse effects of BL exposure on the eyes and the importance of the Nrf2 pathway in protecting eyes during BL exposure.

In conclusion, BL exposure induced ROS generation and caused cell death via apoptosis in RPE cells. The *Nrf2* pathway plays a protective role against oxidative stress on BL exposure. Our findings in this study are meaningful for demonstrating the direct relationship between BL exposure and *Nrf2* signaling, as proved by $Nrf2^{-/-}$ in RPE cells.

Competing Interests

The authors declare that they have no competing interests regarding the publication of this paper.

References

[1] R. Klein and B. E. K. Klein, "The prevalence of age-related eye diseases and visual impairment in aging: current estimates," *Investigative Ophthalmology & Visual Science*, vol. 54, no. 14, pp. ORSF5–ORSF13, 2013.

[2] M. van Lookeren Campagne, J. LeCouter, B. L. Yaspan, and W. Ye, "Mechanisms of age-related macular degeneration and therapeutic opportunities," *The Journal of Pathology*, vol. 232, no. 2, pp. 151–164, 2014.

[3] M. Saito, T. Iida, M. Kano, and K. Itagaki, "Two-year results of combined intravitreal ranibizumab and photodynamic therapy for retinal angiomatous proliferation," *Japanese Journal of Ophthalmology*, vol. 60, no. 1, pp. 42–50, 2016.

[4] Y. Nomura and Y. Yanagi, "Intravitreal aflibercept for ranibizumab-resistant exudative age-related macular degeneration with choroidal vascular hyperpermeability," *Japanese Journal of Ophthalmology*, vol. 59, no. 4, pp. 261–265, 2015.

[5] M. Inoue, K. Kadonosono, A. Arakawa, S. Yamane, and T. Ishibashi, "Long-term outcome of intravitreal pegaptanib sodium as maintenance therapy in Japanese patients with neovascular age-related macular degeneration," *Japanese Journal of Ophthalmology*, vol. 59, no. 3, pp. 173–178, 2015.

[6] L. S. Lim, P. Mitchell, J. M. Seddon, F. G. Holz, and T. Y. Wong, "Age-related macular degeneration," *The Lancet*, vol. 379, no. 9827, pp. 1728–1738, 2012.

[7] J. Ambati and B. J. Fowler, "Mechanisms of age-related macular degeneration," *Neuron*, vol. 75, no. 1, pp. 26–39, 2012.

[8] M. Miyake, M. Saito, K. Yamashiro, T. Sekiryu, and N. Yoshimura, "Complement factor H R1210C among Japanese patients with age-related macular degeneration," *Japanese Journal of Ophthalmology*, vol. 59, no. 5, pp. 273–278, 2015.

[9] F. Ye, H. Kaneko, Y. Nagasaka et al., "Plasma-activated medium suppresses choroidal neovascularization in mice: a new therapeutic concept for age-related macular degeneration," *Scientific Reports*, vol. 5, article 7705, 2015.

[10] A. Takeda, J. Z. Baffi, M. E. Kleinman et al., "CCR3 is a target for age-related macular degeneration diagnosis and therapy," *Nature*, vol. 460, no. 7252, pp. 225–230, 2009.

[11] R. Ijima, H. Kaneko, F. Ye et al., "Interleukin-18 induces retinal pigment epithelium degeneration in mice," *Investigative Ophthalmology & Visual Science*, vol. 55, no. 10, pp. 6673–6678, 2014.

[12] H. Kaneko, F. Ye, R. Ijima et al., "Histamine H4 receptor as a new therapeutic target for choroidal neovascularization in age-related macular degeneration," *British Journal of Pharmacology*, vol. 171, no. 15, pp. 3754–3763, 2014.

[13] F. Ye, H. Kaneko, Y. Hayashi et al., "Malondialdehyde induces autophagy dysfunction and VEGF secretion in the retinal pigment epithelium in age-related macular degeneration," *Free Radical Biology & Medicine*, vol. 94, pp. 121–134, 2016.

[14] A. Matsui, H. Kaneko, S. Kachi et al., "Expression of vascular endothelial growth factor by retinal pigment epithelial cells induced by amyloid-β is depressed by an endoplasmic reticulum stress inhibitor," *Ophthalmic Research*, vol. 55, no. 1, pp. 37–44, 2015.

[15] A. K. Kiser, E. K. Deschler, and G. Dagnelie, "Visual function and performance with blue-light blocking filters in age-related macular degeneration," *Clinical & Experimental Ophthalmology*, vol. 36, no. 6, pp. 514–520, 2008.

[16] A. E. Fletcher, G. C. Bentham, M. Agnew et al., "Sunlight exposure, antioxidants, and age-related macular degeneration," *Archives of Ophthalmology*, vol. 126, no. 10, pp. 1396–1403, 2008.

[17] T. H. Margrain, M. Boulton, J. Marshall, and D. H. Sliney, "Do blue light filters confer protection against age-related macular degeneration?" *Progress in Retinal and Eye Research*, vol. 23, no. 5, pp. 523–531, 2004.

[18] H. R. Taylor, B. Munoz, S. West, N. M. Bressler, S. B. Bressler, and F. S. Rosenthal, "Visible light and risk of age-related macular degeneration," *Transactions of the American Ophthalmological Society*, vol. 88, pp. 163–178, 1990.

[19] M. Kernt, A. Walch, A. S. Neubauer et al., "Filtering blue light reduces light-induced oxidative stress, senescence and accumulation of extracellular matrix proteins in human retinal pigment epithelium cells," *Clinical and Experimental Ophthalmology*, vol. 40, no. 1, pp. e87–e97, 2012.

[20] A. King, E. Gottlieb, D. G. Brooks, M. P. Murphy, and J. L. Dunaief, "Mitochondria-derived reactive oxygen species mediate blue light-induced death of retinal pigment epithelial cells," *Photochemistry and Photobiology*, vol. 79, no. 5, pp. 470–475, 2004.

[21] A. R. Wielgus, R. J. Collier, E. Martin et al., "Blue light induced A2E oxidation in rat eyes-experimental animal model of dry AMD," *Photochemical and Photobiological Sciences*, vol. 9, no. 11, pp. 1505–1512, 2010.

[22] A. Klettner, "Oxidative stress induced cellular signaling in rpe cells," *Frontiers in Bioscience*, vol. 4, pp. 392–411, 2012.

[23] R. Howden, "*Nrf2* and cardiovascular defense," *Oxidative Medicine and Cellular Longevity*, vol. 2013, Article ID 104308, 10 pages, 2013.

[24] A. A. Gupte, C. J. Lyon, and W. A. Hsueh, "Nuclear factor (erythroid-derived 2)-like-2 factor (Nrf2), a key regulator of the antioxidant response to protect against atherosclerosis and nonalcoholic steatohepatitis," *Current Diabetes Reports*, vol. 13, no. 3, pp. 362–371, 2013.

[25] M. M. Sachdeva, M. Cano, and J. T. Handa, "Nrf2 signaling is impaired in the aging RPE given an oxidative insult," *Experimental Eye Research*, vol. 119, pp. 111–114, 2014.

[26] K. Manna, A. Khan, D. Kr Das et al., "Protective effect of coconut water concentrate and its active component shikimic acid against hydroperoxide mediated oxidative stress through suppression of NF-κB and activation of Nrf2 pathway," *Journal of Ethnopharmacology*, vol. 155, no. 1, pp. 132–146, 2014.

[27] W. Liu, Z. Xu, T. Yang et al., "The protective role of tea polyphenols against methylmercury-induced neurotoxic effects in rat cerebral cortex via inhibition of oxidative stress," *Free Radical Research*, vol. 48, no. 8, pp. 849–863, 2014.

[28] H. Zhang, Y.-Y. Liu, Q. Jiang et al., "Salvianolic acid a protects RPE cells against oxidative stress through activation of Nrf2/HO-1 signaling," *Free Radical Biology & Medicine*, vol. 69, pp. 219–228, 2014.

[29] J. Hanus, A. Kolkin, J. Chimienti, S. Botsay, and S. Wang, "4-Acetoxyphenol prevents RPE oxidative stress-induced necrosis by functioning as an NRF2 stabilizer," *Investigative Ophthalmology & Visual Science*, vol. 56, no. 9, pp. 5048–5059, 2015.

[30] C. Zhu, S. Wang, B. Wang et al., "17β-Estradiol up-regulates Nrf2 via PI3K/AKT and estrogen receptor signaling pathways to suppress light-induced degeneration in rat retina," *Neuroscience*, vol. 304, pp. 328–339, 2015.

[31] X. Liu, K. Ward, C. Xavier et al., "The novel triterpenoid RTA 408 protects human retinal pigment epithelial cells against H_2O_2-induced cell injury via NF-E2-related factor 2 (Nrf2) activation," *Redox Biology*, vol. 8, pp. 98–109, 2016.

[32] S. Koinzer, K. Reinecke, T. Herdegen, J. Roider, and A. Klettner, "Oxidative stress induces biphasic ERK1/2 activation in the RPE with distinct effects on cell survival at early and late activation," *Current Eye Research*, vol. 40, no. 8, pp. 853–857, 2015.

[33] A. Koskela, M. Reinisalo, J. M. T. Hyttinen, K. Kaarniranta, and R. O. Karjalainen, "Pinosylvin-mediated protection against oxidative stress in human retinal pigment epithelial cells," *Molecular Vision*, vol. 20, pp. 760–769, 2014.

[34] Y. Fang, T. Su, X. Qiu et al., "Protective effect of alpha-mangostin against oxidative stress induced-retinal cell death," *Scientific Reports*, vol. 6, Article ID 21018, 2016.

[35] Z. Zhao, Y. Chen, J. Wang et al., "Age-related retinopathy in NRF2-deficient mice," *PLoS ONE*, vol. 6, no. 4, Article ID e19456, 2011.

[36] Z. Xu, H. Cho, M. J. Hartsock et al., "Neuroprotective role of Nrf2 for retinal ganglion cells in ischemia-reperfusion," *Journal of Neurochemistry*, vol. 133, no. 2, pp. 233–241, 2015.

[37] Z. Xu, Y. Wei, J. Gong et al., "NRF2 plays a protective role in diabetic retinopathy in mice," *Diabetologia*, vol. 57, no. 1, pp. 204–213, 2014.

[38] N. Himori, K. Yamamoto, K. Maruyama et al., "Critical role of Nrf2 in oxidative stress-induced retinal ganglion cell death," *Journal of Neurochemistry*, vol. 127, no. 5, pp. 669–680, 2013.

[39] T. Kojima, M. Dogru, A. Higuchi et al., "The effect of *Nrf2* knockout on ocular surface protection from acute tobacco smoke exposure: evidence from *Nrf2* knockout mice," *The American Journal of Pathology*, vol. 185, no. 3, pp. 776–785, 2015.

[40] H. Cho, M. J. Hartsock, Z. Xu, M. He, and E. J. Duh, "Monomethyl fumarate promotes Nrf2-dependent neuroprotection in retinal ischemia-reperfusion," *Journal of Neuroinflammation*, vol. 12, no. 1, article 239, 2015.

[41] H. Kaneko, S. Dridi, V. Tarallo et al., "DICER1 deficit induces Alu RNA toxicity in age-related macular degeneration," *Nature*, vol. 471, no. 7338, pp. 325–332, 2011.

[42] D. Yang, S. G. Elner, L.-R. Lin, V. N. Reddy, H. R. Petty, and V. M. Elner, "Association of superoxide anions with retinal pigment epithelial cell apoptosis induced by mononuclear phagocytes," *Investigative Ophthalmology & Visual Science*, vol. 50, no. 10, pp. 4998–5005, 2009.

[43] K. Itoh, T. Chiba, S. Takahashi et al., "An Nrf2/small Maf heterodimer mediates the induction of phase II detoxifying enzyme genes through antioxidant response elements," *Biochemical and Biophysical Research Communications*, vol. 236, no. 2, pp. 313–322, 1997.

[44] F. Ye, T. Zhao, X. Liu et al., "Long-term autophagy and nrf2 signaling in the hippocampi of developing mice after carbon ion exposure," *Scientific Reports*, vol. 5, article 18636, 2015.

[45] B. Dasari, J. R. Prasanthi, G. Marwarha, B. B. Singh, and O. Ghribi, "The oxysterol 27-hydroxycholesterol increases β-amyloid and oxidative stress in retinal pigment epithelial cells," *BMC Ophthalmology*, vol. 10, no. 1, article 22, 2010.

[46] K. Takayama, T. Sato, Y. Karasawa, S. Sato, M. Ito, and M. Takeuchi, "Phototoxicity of indocyanine green and brilliant blue G under continuous fluorescent illumination on cultured human retinal pigment epithelial cells," *Investigative Ophthalmology & Visual Science*, vol. 53, no. 11, pp. 7389–7394, 2012.

[47] R. D. Glickman, "Phototoxicity to the retina: mechanisms of damage," *International Journal of Toxicology*, vol. 21, no. 6, pp. 473–490, 2002.

[48] S. Proulx, S. Landreville, S. L. Guérin, and C. Salesse, "Integrin α5 expression by the ARPE-19 cell line: comparison with primary RPE cultures and effect of growth medium on the α5 gene promoter strength," *Experimental Eye Research*, vol. 79, no. 2, pp. 157–165, 2004.

[49] C. S. Alge, S. M. Hauck, S. G. Priglinger, A. Kampik, and M. Ueffing, "Differential protein profiling of primary versus immortalized human RPE cells identifies expression patterns associated with cytoskeletal remodeling and cell survival," *Journal of Proteome Research*, vol. 5, no. 4, pp. 862–878, 2006.

[50] A. D. Patel, S. Rotenberg, R. L. W. Messer et al., "Blue light activates phase 2 response proteins and slows growth of A431 epidermoid carcinoma xenografts," *Anticancer Research*, vol. 34, no. 11, pp. 6305–6313, 2014.

[51] C. Huang, P. Zhang, W. Wang et al., "Long-term blue light exposure induces RGC-5 cell death in vitro: involvement of mitochondria-dependent apoptosis, oxidative stress, and MAPK signaling pathways," *Apoptosis*, vol. 19, no. 6, pp. 922–932, 2014.

[52] A. Hirota, Y. Kawachi, K. Itoh et al., "Ultraviolet A irradiation induces NF-E2-related factor 2 activation in dermal fibroblasts: protective role in UVA-induced apoptosis," *The Journal of Investigative Dermatology*, vol. 124, no. 4, pp. 825–832, 2005.

[53] A. Hirota, Y. Kawachi, M. Yamamoto, T. Koga, K. Hamada, and F. Otsuka, "Acceleration of UVB-induced photoageing in *nrf2* gene-deficient mice," *Experimental Dermatology*, vol. 20, no. 8, pp. 664–668, 2011.

[54] E. V. Knatko, S. H. Ibbotson, Y. Zhang et al., "Nrf2 activation protects against solar-simulated ultraviolet radiation in mice and humans," *Cancer Prevention Research*, vol. 8, no. 6, pp. 475–486, 2015.

[55] C. L. Saw, M.-T. Huang, Y. Liu, T. O. Khor, A. H. Conney, and A.-N. Kong, "Impact of Nrf2 on UVB-induced skin inflammation/photoprotection and photoprotective effect of sulforaphane," *Molecular Carcinogenesis*, vol. 50, no. 6, pp. 479–486, 2011.

Hindawi Publishing Corporation
Oxidative Medicine and Cellular Longevity
Volume 2016, Article ID 4378461, 9 pages
http://dx.doi.org/10.1155/2016/4378461

Research Article

Apigenin Attenuates Oxidative Injury in ARPE-19 Cells thorough Activation of Nrf2 Pathway

Xinrong Xu,[1] Min Li,[1] Weiwei Chen,[1] Haitao Yu,[2] Yan Yang,[1] and Li Hang[1]

[1]*Department of Ophthalmology, Affiliated Hospital of Nanjing University of Chinese Medicine, Nanjing 210029, China*
[2]*School of Pharmacy, Nanjing University of Chinese Medicine, Nanjing 210023, China*

Correspondence should be addressed to Xinrong Xu; xinrong_xu@aliyun.com

Received 11 June 2016; Accepted 1 August 2016

Academic Editor: Ian Copple

The current study was aimed at evaluating the therapeutic implication of apigenin and to elucidate the underlying mechanism. The *tert*-butyl hydroperoxide (*t*-BHP) at 200 μM was used to induce oxidative stress-associated injury in ARPE-19 cells. Apigenin at concentrations less than 800 μM did not cause cytotoxic effects on ARPE-19 cells. Cell viability assay showed that apigenin at 200 μM significantly promoted cell survival in *t*-BHP-treated ARPE-19 cells. Additionally, apigenin at 100 μM significantly protected ARPE-19 cells from *t*-BHP-induced apoptosis. Molecular examinations demonstrated that apigenin at 400 μM significantly upregulated the mRNA and protein expression of Nrf2 and stimulated its nuclear translocation in ARPE-19 cells treated with or without *t*-BHP. Apigenin 400 μM also significantly elevated the expression of HO-1, NQO1, and GCLM at both mRNA and protein levels in the presence or absence of *t*-BHP. Furthermore, apigenin at 400 μM significantly increased the activities of SOD, CAT, GSH-PX, and T-AOC and reduced the levels of ROS and MDA in *t*-BHP-treated ARPE-19 cells. However, these effects of apigenin were all abolished by being transfected with Nrf2 siRNA. Collectively, our current data indicated that apigenin exerted potent antioxidant properties in ARPE-19 cells challenged with *t*-BHP, which were dependent on activation of Nrf2 signaling.

1. Introduction

Age-related macular degeneration (AMD) represents the leading cause of blindness in the elderly population, and its prevalence increases tremendously with every decade after the age of 50 years all over the world [1]. The early stage of AMD is featured by alterations of retinal pigmented epithelium (RPE) and subretinal deposits between the RPE and Bruch's membrane [2]. AMD can develop to choroidal neovascularization characterized by new blood vessels that invade the macula, which is a rapidly deteriorating stage of AMD, also known as wet AMD [3]. Therefore, vascular endothelial growth factor (VEGF) as the most important regulator of angiogenic network has been considered as a key target for current treatment of wet AMD, and several VEGF inhibitors such as bevacizumab, pegaptanib, or ranibizumab have demonstrated promising therapeutic benefits in clinical context [4]. In addition, dry AMD can slowly progress to geographic atrophy, which is the late-onset form that results in RPE degeneration in the macula [5]. Unfortunately, there are no available treatments for dry AMD so far.

Mounting evidence indicates that oxidative stress plays a key role in the pathogenesis of dry AMD. Oxidative stress refers to cellular or molecular damage caused by reactive oxygen species (ROS), which especially occurs in age-related conditions as a result of disrupted balance between the ROS production and antioxidant defense response [6]. It has been well-established that the transcription factor Nrf2 (nuclear factor erythroid 2-related factor 2) functions as the master regulator of a highly conserved protective molecular response to oxidative stress in mammal cells. Under basal conditions, Nrf2 physically binds to the negative regulator Keap1 for ubiquitination and proteasomal degradation within the cytoplasm, thus limiting Nrf2 activity. However, under oxidative circumstances, Nrf2 is released from Keap1 and translocates into the nucleus, where it binds to antioxidant response elements (AREs), thus activating transcription of its target genes encoding phase II metabolizing enzymes and

antioxidases, including heme oxygenase-1 (HO-1), quinone oxidoreductase-1 (NQO1), glutathione peroxidase (GSH-PX), glutamate-cysteine ligase modifier subunit (GCLM), glutathione, and epoxide hydrolase [7]. There has been evidence that Nrf2-deficient mice developed ocular pathology similar to cardinal features of human AMD and deregulated autophagy is likely a mechanistic link between oxidative injury and inflammation [8]. More understanding of the potential role of Nrf2 in the pathogenesis of dry AMD may provide novel opportunities for therapeutic intervention for the prevention of progression to advanced disease.

Apigenin is a flavonoid compound abundantly present in common fruits, such as grapefruit, and plant-derived beverages and vegetables, such as parsley, onions, oranges, tea, chamomile, and wheat sprouts, and in some seasonings [9]. This compound has been increasingly reported to have various pharmacological activities including anti-inflammation [10], antivirus [11], antioxidation [12], and anticancer [13]. Given the potent antioxidative effects of apigenin, we herein hypothesized that this compound may have therapeutic implication for dry AMD. To this end, *tert*-butyl hydroperoxide (*t*-BHP) was used to establish the oxidative stress-induced cellular model in human RPE cell line ARPE-19, which is isolated from human retinal pigmented epithelium and from stable monolayers exhibiting morphological and functional polarity [14]. ARPE-19 cells have structural and functional properties characteristic of RPE cells *in vivo* and are valuable for *in vitro* studies of RPE physiology. We used this model to examine the protective effects of apigenin and to elucidate the underlying mechanism.

2. Materials and Methods

2.1. Regents and Antibodies. *t*-BHP and apigenin were purchased from Sigma-Aldrich (Saint Louis, MO, USA). The primary antibodies against Nrf2, HO-1, GCL, NQO1, β-actin, and Lamin B and the secondary antibody Goat Anti-Rabbit IgG/HRP used in Western blot analyses were all obtained from Abcam (Cambridge, UK).

2.2. Cell Culture. Human RPE cell line ARPE-19 was purchased from the American Type Culture Collection (USA). ARPE-19 cells were cultured in Dulbecco's modified eagle medium (DMEM; Invitrogen, Grand Island, NY, USA) supplemented with 10% fetal bovine serum (FBS; Sijiqing Biological Engineering Materials Co., Ltd., Hangzhou, China), 100 U/mL penicillin, and 100 mg/mL streptomycin and grown in a 95% air and 5% CO_2 humidified atmosphere at 37°C.

2.3. Establishment of Oxidative Injury Model in ARPE-19 Cells. ARPE-19 cells were seeded in 96-well plates (1×10^4/well) and cultured in DMEM with 10% FBS for 24 h. Cells were treated with *t*-BHP at concentrations of 50, 100, 200, 300, 400, and 500 μM for 24 h. Then the medium was replaced with 100 μL phosphate buffered saline containing 0.5 mg/mL 3-(4,5-dimethylthiazol-2-yl)-2,5-diphenyl tetrazolium bromide (MTT) incubating at 37°C for 4 h. Next, dimethylsulfoxide of 200 μL was added to dissolve the crystals. The spectrophotometric absorbance at 490 nm was measured by a SPECTRAmax™ microplate spectrophotometer (Molecular Devices, Sunnyvale, CA, USA). Cell growth inhibition curve was drawn and the half-inhibition concentration (IC_{50}) was selected as appropriate concentration of *t*-BHP for establishing oxidative injury model in ARPE-19 cells. Cell growth inhibition rate = (test OD value − blank OD value)/(control OD value − blank OD value) × 100%. Cell survival rate = [1 − (test OD value − blank OD value)/(control OD value − blank OD value)] × 100%. Experiments were performed in triplicate.

2.4. Evaluation of Toxicity of Apigenin in ARPE-19 Cells. ARPE-19 cells were seeded in 96-well plates (1×10^4/well) and cultured in DMEM with 10% FBS for 24 h. Cells were treated with apigenin at concentrations of 10, 50, 100, 200, 400, and 800 μM for 24 h. Cell viability was evaluated using MTT assay as described above. Cell survival rate was calculated to evaluate the cellular toxicity of apigenin. Experiments were performed in triplicate.

2.5. Evaluation of Apigenin Protection of ARPE-19 Cells against Oxidative Injury. ARPE-19 cells were seeded in 96-well plates (1×10^4/well) and cultured in DMEM with 10% FBS for 24 h. Cells were pretreated with apigenin at concentrations of 100, 200, and 400 μM for 6 h. Then cells were additionally treated with *t*-BHP at 200 μM for 24 h. Cell viability was evaluated using MTT assay as described above to evaluate apigenin protection against oxidative injury in ARPE-19 cells. Experiments were performed in triplicate.

2.6. Analyses of Apoptosis. ARPE-19 cells were treated with apigenin at concentrations of 100, 200, and 400 μM for 6 h and then were additionally treated with *t*-BHP at 200 μM for 24 h. Apoptotic rates were determined by flow cytometry using Annexin V-FITC apoptosis assay kits (Nanjing KeyGen Biotech Co., Ltd., Nanjing, China) according to the protocol. Apoptotic cells were defined as the cells situated in the right two quadrants of each plot and the percentages were determined by flow cytometry (FACSCalibur; Becton, Dickinson and Company, Franklin Lakes, NJ, USA). The data were analyzed using the software CELLQuest. Experiments were performed in triplicate.

2.7. Cell Transfection with Nrf2 siRNA. Nrf2 siRNA (Shanghai GenePharma Co. Ltd., Shanghai, China) of 100 pmol was added to 100 μL medium without serum and antibiotics and incubated at room temperature for 5 min. The final concentration of Nrf2 siRNA was 100 nM. Lipofectamine 2000 reagent (Invitrogen, USA) of 25 μL was added to 75 μL medium without serum and antibiotics and incubated at room temperature for 5 min. The above two solutions were mixed well at room temperature for 20 min, and about 200 μL transfection complex was obtained. Then the medium of 800 μL without serum and antibiotics was added to the 200 μL transfection complex and mixed well, and the transfection complex solution of 1000 μL was obtained. ARPE-19 cells were incubated with the transfection complex solution at 37°C for 8 h and then were reincubated in complete medium at 37°C for an additional 16 h. Control siRNA (Shanghai

GenePharma Co. Ltd., Shanghai, China) is a nontargeting 20–25 nt siRNA designed as a negative control.

2.8. Determination of Antioxidant System. ARPE-19 cells were treated with apigenin at 400 μM and/or transfected with Nrf2 siRNA for 6 h and then additionally treated with *t*-BHP at 200 μM for 24 h. Cells were broken up by ultrasound treatment and subjected to centrifugation to obtain the supernatant. The activities of superoxide dismutase (SOD), catalase (CAT), GSH-PX, malondialdehyde (MDA), and the total antioxidant capacity (T-AOC) were determined using corresponding enzyme-linked immunosorbent assay kits (Nanjing Jiancheng Bioengineering Institute, Nanjing, China) according to the instructions of the manufacturer. Experiments were performed in triplicate.

2.9. Determination of ROS Level. ARPE-19 cells were treated with apigenin at 400 μM and/or transfected with Nrf2 siRNA for 6 h and then additionally treated with *t*-BHP at 200 μM for 24 h. The fluorescent probe 2′,7′-dichlorodihydrofluorescein diacetate (DCFH-DA) was used to measure the intracellular generation of ROS. ARPE-19 cells were treated with 10 μM DCFH-DA for 20 min at 37°C and then washed three times with medium. Cells were incubated with apigenin at 400 μM and/or transfected with Nrf2 siRNA for 6 h and then additionally treated with *t*-BHP at 200 μM for 24 h. The fluorescence was determined by flow cytometry (FACSCalibur; Becton, Dickinson and Company, Franklin Lakes, NJ, USA) at 488 nm wavelength. Experiments were performed in triplicate.

2.10. Real-Time PCR. Total RNA was isolated from treated cells using Trizol reagent (Sigma, St. Louis, MO, USA) following the protocol provided by the manufacturer. Real-time PCR was performed as described previously [15]. β-actin was used as the invariant control. Fold changes in the mRNA levels of target genes related to β-actin were calculated as suggested by Schmittgen et al. [16]. Experiments were performed in triplicate. The primers of genes (GenScript, Nanjing, China) were as follows: *Nrf2*: (forward) 5′-TGAGGTTTCTTCGGCTACGTT-3′ and (reverse) 5′-CTTCTGTCAGTTTGGCTTCTGG-3′; *HO-1* (forward) 5′-CTGGAGGAGGAGATTGAGCG-3′ and (reverse) 5′-ATGGCTGGTGTGTAGGGGAT-3′; *NQO1* (forward) 5′-GCGTCTGGAGACTGTCTGGG-3′ and (reverse) 5′-CGGCTGGAATGGACTTGC-3′; *GCLM* (forward) 5′-ATCAAACTCTTCATCATCAAC-3′ and (reverse) 5′-GATTAACTCCATCTTCAATAGG-3′; *β-actin* (forward) 5′-CCACACCTTCTACAATGAGC-3′ and (reverse) 5′-GGTCTCAAACATGATCTGGG-3′.

2.11. Western Blot Analyses. Whole cell protein extracts were prepared from treated cells with radioimmunoprecipitation assay buffer containing 150 mM NaCl, 50 mM Tris, 0.1% sodium dodecyl sulphate, 1% Nonidet P-40, and 0.5% deoxycholate supplemented with protease inhibitor phenylmethylsulfonyl fluoride. In examining Nrf2 expression, nuclear proteins and cytoplasmic proteins were separated using a Bioepitope Nuclear and Cytoplasmic Extraction Kit (Bioworld Technology, St. Louis Park, MN, USA) according to the protocol. Proteins (50 μg/well) were separated by SDS-polyacrylamide gel, transferred to a PVDF membrane (Millipore, Burlington, MA, USA), and blocked with 5% skim milk in Tris-buffered saline containing 0.1% Tween 20. Target proteins were detected by corresponding primary antibodies and subsequently by horseradish peroxidase-conjugated secondary antibodies. Protein bands were visualized using chemiluminescence reagent (Millipore, Burlington, MA, USA). Equivalent loading was confirmed using an antibody against β-actin for total proteins and against Lamin B for nuclear proteins. Representative blots were from three independent experiments. The levels of target protein bands were densitometrically determined using Quantity One 4.4.1. The variation in the density of bands was expressed as fold changes compared to the control in the blot after normalization to β-actin or Lamin B.

2.12. Statistical Analysis. Data were presented as mean ± SD, and results were analyzed using SPSS16.0 software. The significance of difference was determined by one-way ANOVA with the *post hoc* Dunnett's test. A value of $P < 0.05$ was considered to be statistically significant.

3. Results

3.1. Apigenin Protects against t-BHP-Induced Oxidative Injury in ARPE-19 Cells. In order to establish an oxidative injury model in ARPE-19 cells, we used MTT assay to determine cell growth in the presence of *t*-BHP, a well-known oxidizing agent. The results showed that *t*-BHP increased the cell growth inhibition rate in a concentration-dependent manner (Figure 1(a)) and that *t*-BHP at 200 μM caused a significant reduction in cell survival rate in ARPE-19 cells (Figure 1(b)). Accordingly, *t*-BHP at 200 μM was used to induce oxidative injury in these cells for subsequent experiments. In addition, we found that apigenin at concentrations up to 800 μM did not apparently affect ARPE-19 cell viability, indicating that apigenin might not have toxic effects on these cells (Figure 1(c)). Next, we observed that apigenin concentration dependently increased cell survival rate in ARPE-19 cells exposed to *t*-BHP (Figure 1(d)). Then apoptosis was examined using flow cytometry, and the results demonstrated that ARPE-19 cells exposed to *t*-BHP had significant apoptotic rate compared to control, but apigenin significantly reduced *t*-BHP-induced apoptosis in APRE-19 cells (Figures 1(e) and 1(f)). Taken together, these data collectively indicated that apigenin protected ARPE-19 cells against *t*-BHP-induced oxidative injury.

3.2. Apigenin Activates Nrf2 and Its Target Genes Involved in Antioxidant System in ARPE-19 Cells. We next examined the role of Nrf2 signaling in apigenin protection of ARPE-19 cells using Nrf2 siRNA-mediated knockout approaches. Real-time PCR analyses demonstrated that Nrf2 mRNA was significantly upregulated by apigenin but was significantly decreased by transfection with Nrf2 siRNA in the presence or absence of apigenin in ARPE-19 cells treated with or without *t*-BHP (Figures 2(a) and 2(b)). Consistently, Western

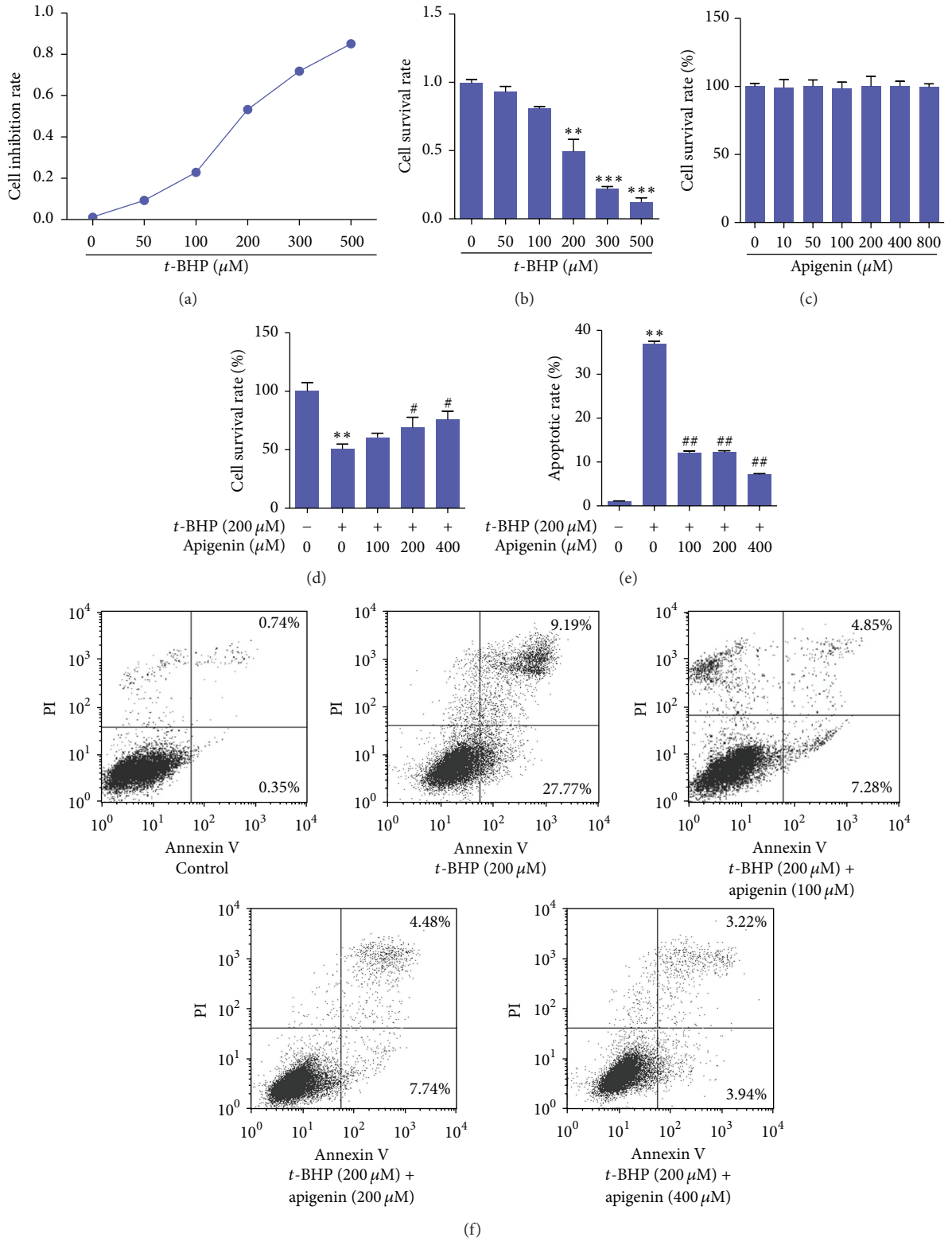

Figure 1: Apigenin protects against *t*-BHP-induced oxidative injury in ARPE-19 cells. (a, b) MTT assay for determining cell inhibition rate and cell survival rate when exposed to *t*-BHP. Significance: $^{**}P < 0.01$ versus control; $^{***}P < 0.001$ versus control. (c) MTT assay for determining whether apigenin had toxic effects on cells. (d) MTT assay for determining the protective effects of apigenin on *t*-BHP-treated cells. Significance: $^{**}P < 0.01$ versus control; $^{\#}P < 0.05$ versus *t*-BHP. (e) Flow cytometry analyses of apoptosis using FITC-labeled Annexin V/PI staining. Significance: $^{**}P < 0.01$ versus control; $^{\#\#}P < 0.01$ versus *t*-BHP. (f) Representative charts of flow cytometry analyses of apoptosis. Cells situated in the right two quadrants of each plot were regarded as apoptotic cells.

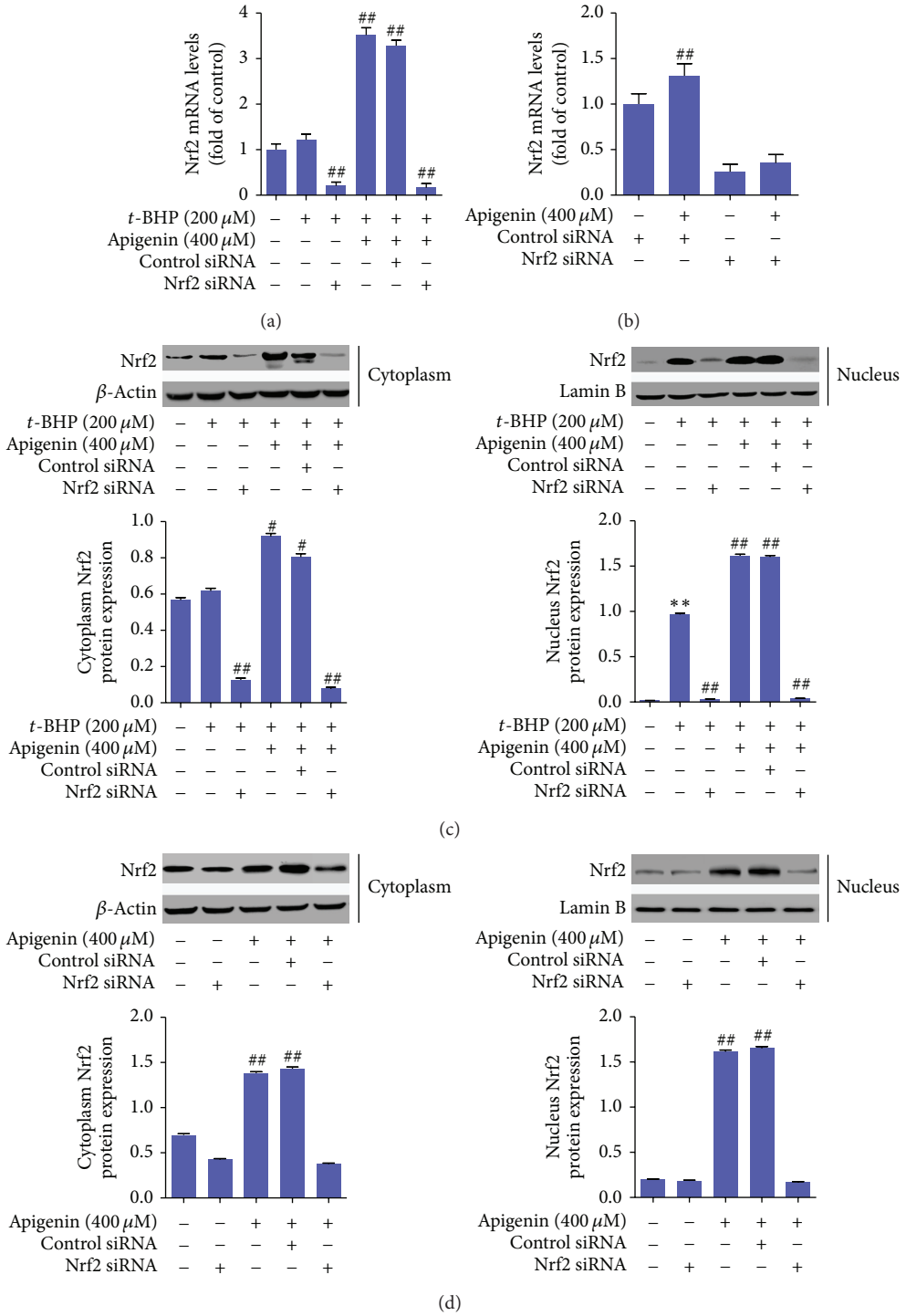

Figure 2: Apigenin upregulates Nrf2 expression and promotes its nuclear translocation in ARPE-19 cells. (a) Real-time PCR analyses of Nrf2 mRNA expression in t-BHP-treated ARPE-19 cells. Significance: $^{\#\#}P < 0.01$ versus t-BHP. (b) Real-time PCR analyses of Nrf2 mRNA expression in ARPE-19 cells in the absence of t-BHP. Significance: $^{\#\#}P < 0.01$ versus control siRNA. (c) Western blot analyses of protein abundance of Nrf2 in cytoplasm and nucleus in t-BHP-treated ARPE-19 cells with quantification. Significance: $^{**}P < 0.01$ versus control, $^{\#}P < 0.05$ versus t-BHP, and $^{\#\#}P < 0.01$ versus t-BHP. (d) Western blot analyses of protein abundance of Nrf2 in cytoplasm and nucleus in ARPE-19 cells in the absence of t-BHP with quantification. Significance: $^{\#\#}P < 0.01$ versus control.

blot analyses revealed that the protein abundance of Nrf2 in both cytoplasm and nucleus was significantly increased by apigenin but was significantly reduced by transfection with Nrf2 siRNA in the presence or absence of apigenin in ARPE-19 cells treated with or without *t*-BHP (Figures 2(c) and 2(d)). These data indicated that apigenin could activate Nrf2 signaling in these cells and that the expression and nuclear translocation of Nrf2 could be effectively inhibited by Nrf2 siRNA. Furthermore, we examined the expression of several target genes of Nrf2, which are critically involved in the antioxidant system within cells. The mRNA expressions of HO-1, NQO1, and glutamate-cysteine ligase modifier subunit (GCLM) were all significantly upregulated by *t*-BHP compared to control. Apigenin elevated their mRNA expression significantly compared to the *t*-BHP-treated cells, but transfection with Nrf2 siRNA resulted in reduced mRNA expression of HO-1, NQO1, and GCLM (Figure 3(a)). Apigenin also significantly increased their mRNA expression in ARPE-19 cells in the absence of *t*-BHP (Figure 3(b)). Western blot analyses showed similar consistent results in ARPE-19 cells in the presence or absence of *t*-BHP at the protein level (Figures 3(c) and 3(d)). Collectively, these data suggested that apigenin increased Nrf2 expression and promoted its nuclear translocation, leading to enhanced expression of its target genes implicated in protection against oxidative-caused injuries in ARPE-19 cells.

3.3. Activation of Nrf2 Is Required for Apigenin to Exert Antioxidative Properties in t-BHP-Treated ARPE-19 Cells. We next evaluated the antioxidative effects of apigenin and their associations with activation of Nrf2 signaling. We measured the activities of a series of phase II metabolizing enzymes and antioxidases in *t*-BHP-treated ARPE-19 cells. The results showed that the enzyme activities of SOD, CAT, and GSH-PX were significantly reduced in *t*-BHP-treated ARPE-19 cells, but apigenin at 400 μM significantly restored the activities of these enzymes. However, the effects of apigenin were significantly abrogated by transfection with Nrf2 siRNA in ARPE-19 cells exposed to *t*-BHP (Figures 4(a)–4(c)). Moreover, the levels of ROS, MDA, and T-AOC, three parameters indicative of oxidative status within cells, were determined. ARPE-19 cells challenged with *t*-BHP exhibited significantly elevated ROS and MDA levels and reduced T-AOC levels. However, apigenin significantly reduced ROS and MDA levels and enhanced T-AOC levels in *t*-BHP-treated ARPE-19 cells, but these effects were apparently abolished by transfection with Nrf2 siRNA (Figures 4(d)–4(f)). Altogether, these results suggested that activation of Nrf2 was required for apigenin to exert antioxidative properties in *t*-BHP-treated ARPE-19 cells.

4. Discussion

Effective therapeutic approaches for dry AMD are urgently needed in current clinical context. Increasing evidence from basic and clinical studies highlights that oxidative injury is critically implicated in the pathogenesis of dry AMD, and thus agents with antioxidative properties may be promising therapeutic options for dry AMD [17]. For example, an Age-Related Eye Disease Study (AREDS) evaluated the effects of several antioxidant agents at pharmacological doses including β-carotene, vitamin C, vitamin E, zinc, and copper on the progression of AMD and visual acuity, demonstrating that administration of antioxidants could result in 25% risk reduction in advanced AMD progression and 19% risk reduction in moderate vision loss within 5 years [18]. In addition, a recent investigation evaluated the safety and efficacy of OT-551, a disubstituted hydroxylamine with antioxidant properties, for the treatment of geographic atrophy, the advanced atrophic form of AMD, and demonstrated that this agent could be beneficial for maintaining visual acuity in AMD patients [19]. In the present study, we demonstrated that the flavonoid compound apigenin was safe for ARPE-19 cells and significantly increased the survival rate and reduced the apoptotic rate in these cells with oxidative injury caused by *t*-BHP. Apigenin at 400 μM, especially, could provide favorable protective effects on ARPE-19 cells against oxidative injury. Our discoveries suggested apigenin as therapeutic candidate for AMD. Moreover, in view of the fact that oxidative stress is most likely an early (and enduring) toxic stimulus, we assumed that apigenin could also serve as a preventing agent for AMD. Given that flavonoids are well-known for their antioxidant properties, we therefore concentrated on the signaling pathways that regulate intracellular redox system in hope of elucidating the mechanisms of apigenin implicated in treatment for AMD.

The transcription factor Nrf2 is widely acknowledged as a key regulator of antioxidative pathways in mammal cells. A large number of studies have established an important link of Nrf2 signaling to the pathogenesis of AMD. Studies showed that Nrf2-deficient mice exhibited remarkable AMD-like retina alterations [8] and that activation of Nrf2 pathway by pharmacological agents could protect ARPE cells against oxidative-caused damage [20, 21]. Our current data demonstrated that *t*-BHP at 200 μM did not apparently alter the transcription of Nrf2 but significantly elevated the nuclear protein abundance of Nrf2 in ARPE cells. Apigenin also potently increased the transcription of nuclear translocation of Nrf2 and upregulated the expression of a series of phase II metabolizing enzymes in *t*-BHP-treated ARPE cells. These data suggested that Nrf2 nuclear translocation occurred in ARPE cells upon oxidative stimulation, leading to the transcription and expression of several phase II metabolizing enzymes, and that apigenin could potently activate Nrf2 signaling in these cells. Consistently, it was reported that apigenin could restore the silenced status of Nrf2 in skin epidermal JB6 P + cells by CpG demethylation coupled with attenuated activities of DNA methyltransferase and histone deacetylases [22]. Apigenin was also found to significantly activate the Nrf2-antioxidant response element-mediated gene expression and induce anti-inflammatory activities in HepG2 cells [23].

We further demonstrated that apigenin had potent antioxidant properties in ARPE cells, because the activities of antioxidant enzymes SOD, CAT, and GSH-PX and the T-AOC levels were significantly enhanced, but the levels of ROS and MDA were significantly reduced by apigenin.

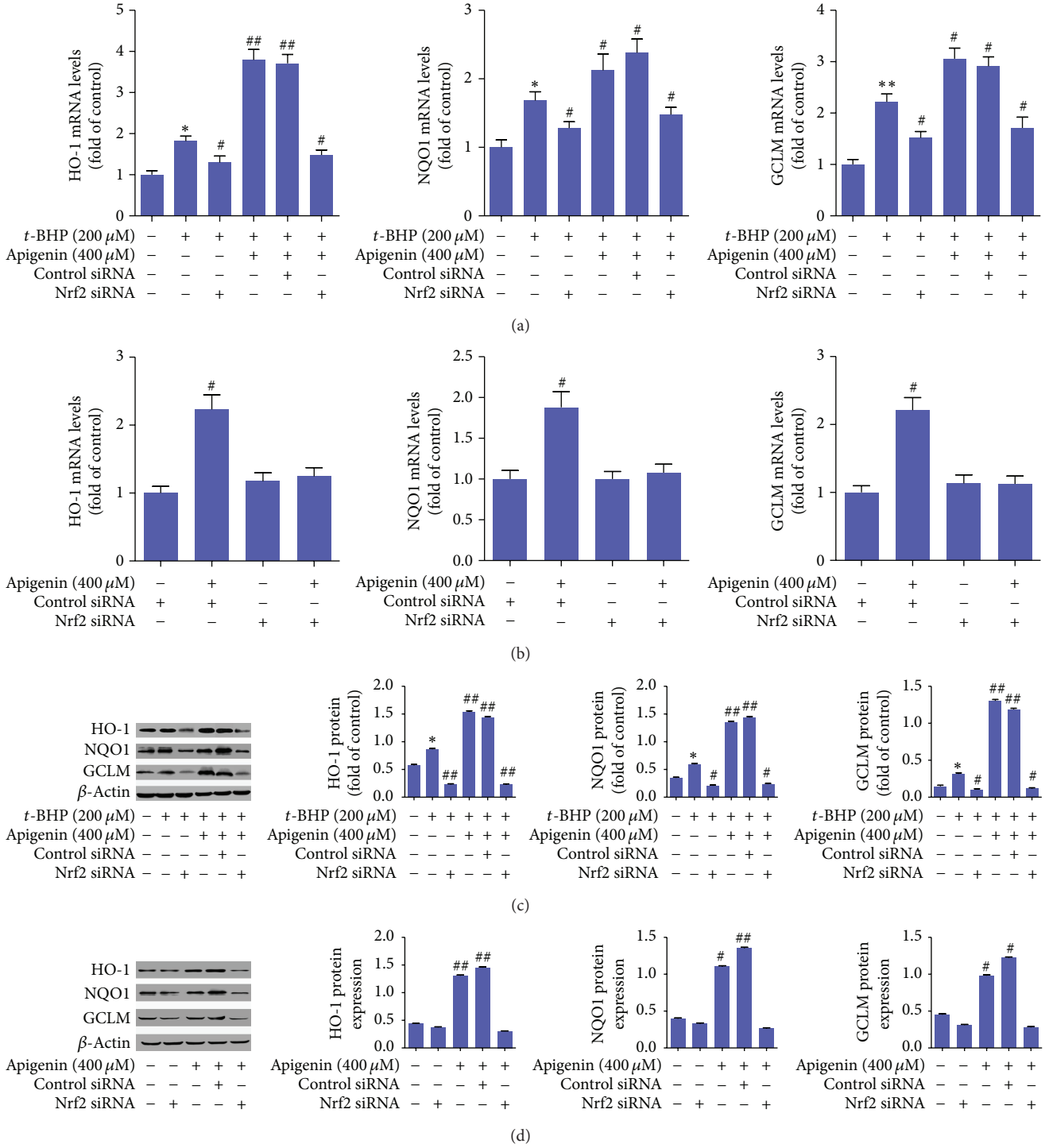

FIGURE 3: Apigenin increases the expression of Nrf2 target genes involved in antioxidant system in ARPE-19 cells. (a) Real-time PCR analyses of the mRNA expression of HO-1, NQO1, and GCLM in t-BHP-treated ARPE-19 cells. Significance: $^{*}P < 0.05$ versus control, $^{**}P < 0.01$ versus control, $^{\#}P < 0.05$ versus t-BHP, and $^{\#\#}P < 0.01$ versus t-BHP. (b) Real-time PCR analyses of the mRNA expression of HO-1, NQO1, and GCLM in ARPE-19 cells in the absence of t-BHP. Significance: $^{\#}P < 0.05$ versus control siRNA. (c) Western blot analyses of protein abundance of HO-1, NQO1, and GCLM in t-BHP-treated ARPE-19 cells with quantification. Significance: $^{*}P < 0.05$ versus control, $^{\#}P < 0.05$ versus t-BHP, and $^{\#\#}P < 0.01$ versus t-BHP. (d) Western blot analyses of protein abundance of HO-1, NQO1, and GCLM in ARPE-19 cells in the absence of t-BHP with quantification. Significance: $^{\#}P < 0.05$ versus control; $^{\#\#}P < 0.01$ versus control.

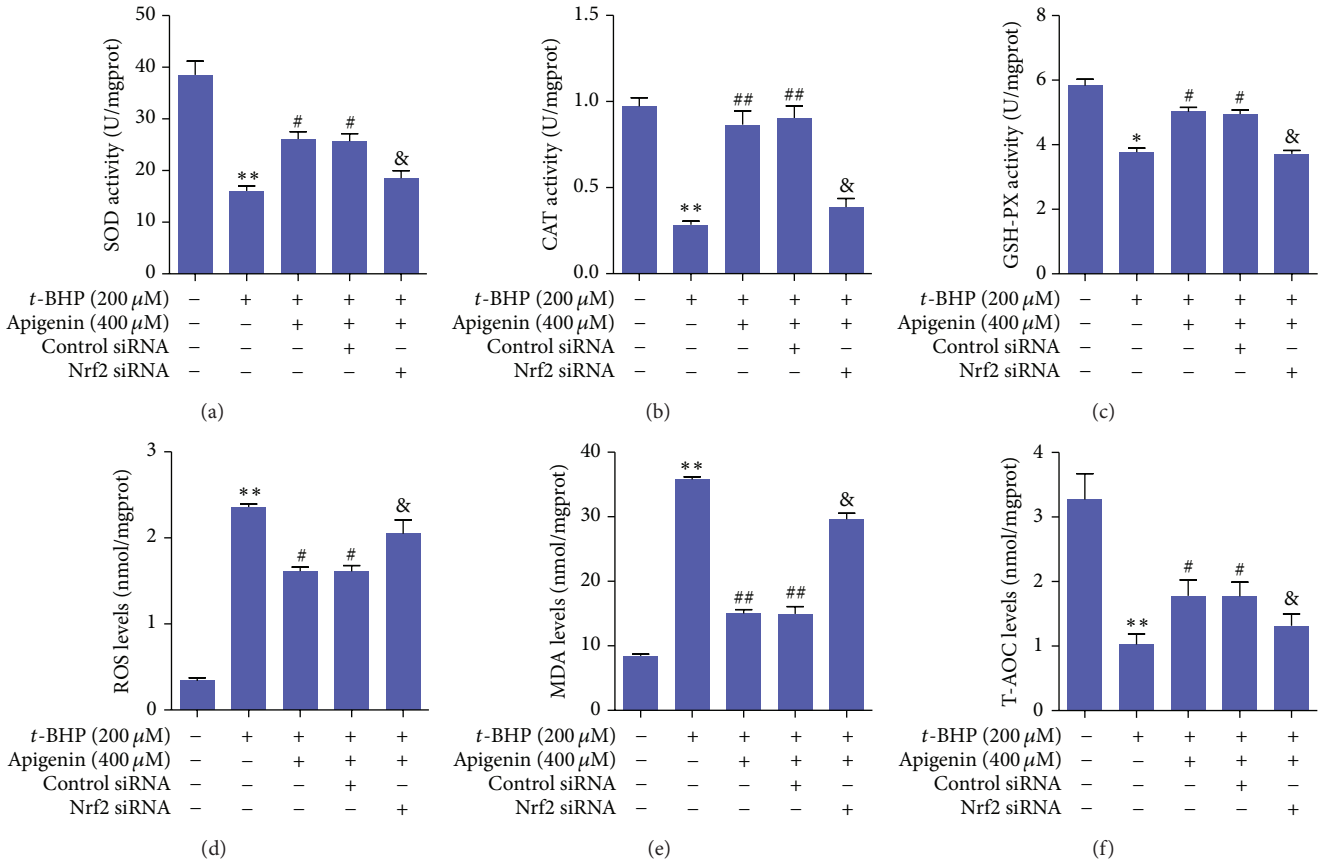

FIGURE 4: Activation of Nrf2 is required for apigenin to exert antioxidative properties in *t*-BHP-treated ARPE-19 cells. ELISA for SOD activity (a), CAT activity (b), GSH-PX activity (c), ROS levels (d), MDA levels (e), and T-AOC levels (f). Significance: $^{*}P < 0.05$ versus control, $^{**}P < 0.01$ versus control, $^{\#}P < 0.05$ versus *t*-BHP, $^{\#\#}P < 0.01$ versus *t*-BHP, and $^{\&}P < 0.05$ versus *t*-BHP + apigenin + control siRNA.

Consistently, the antioxidant effects of apigenin were also demonstrated in many other circumstances. For example, the flavonoid constituents of *Sida cordata*, which are full of apigenin, increased the activity of hepatic antioxidant enzymes including CAT, SOD, POD, GST, GSR, and GSH-Px in rats intoxicated with carbon tetrachloride [24]. The yam peel extracts, in which apigenin is one of the predominant components, could protect rats from liver damage by enhancing the activities of antioxidant enzymes and anti-inflammatory capacity [25]. Our current studies recaptured these results in ARPR-19 cells under oxidative stress, which could be implicated in AMD treatment. Interestingly, we observed that the antioxidant properties of apigenin were dependent on activation of Nrf2 in ARPE-19 cells exposed to *t*-BHP, because loss-of-function approaches with siRNA-mediated Nrf2 knockdown significantly abrogated apigenin upregulation of SOD, CAT, GSH-PX, and T-AOC activities and rescued apigenin downregulation of ROS and MAD levels. These findings indicated that Nrf2 could be a key target molecule for pharmaceutical modulators to protect human retinal epithelial cells against oxidative injury and thus play a beneficial role for AMD treatment. In line with our current data, apigenin was reported to increase Nrf2 expression or activate its function in differentiated PC12 cells [26] and rat primary hepatocytes [27]. However, contrast results also reported that apigenin dramatically reduced Nrf2 expression at both the mRNA and protein levels through downregulation of PI3 K/Akt pathway, leading to a reduction of Nrf2-downstream genes in BEL-7402 cells [28]. Taking these findings together, it was presumed that apigenin regulation of Nrf2 could be dependent on different cell types or pathophysiological contexts. In view of this, we are performing animal studies using Nrf2 knockout mice to validate the apigenin regulation of Nrf2 signaling and the therapeutic effects of apigenin on AMD *in vivo*.

In summary, apigenin exhibited potent protective effects on ARPE-19 cells against *t*-BHP-induced oxidative injury, which were associated with its antioxidant effects dependent on activation of Nrf2 signaling. Our current study strongly indicated that apigenin could be a safe therapeutic option for treatment of dry AMD.

Competing Interests

The authors declare that there are no competing interests regarding the publication of this paper.

Acknowledgments

This work was supported by the Science and Technology Planning Project of Jiangsu Province, China (Grant no. BK20151601), and the Program for Leading Talents of Traditional Chinese Medicine of Jiangsu Province, China (Grant no. LJ200911).

References

[1] R. Klein and B. E. K. Klein, "The prevalence of age-related eye diseases and visual impairment in aging: current estimates," *Investigative Ophthalmology & Visual Science*, vol. 54, no. 14, pp. ORSF5–ORSF13, 2013.

[2] M. A. Zarbin, R. P. Casaroli-Marano, and P. J. Rosenfeld, "Age-related macular degeneration: clinical findings, histopathology and imaging techniques," *Developments in Ophthalmology*, vol. 53, pp. 1–32, 2014.

[3] A. Klettner, A. Kauppinen, J. Blasiak, J. Roider, A. Salminen, and K. Kaarniranta, "Cellular and molecular mechanisms of age-related macular degeneration: from impaired autophagy to neovascularization," *The International Journal of Biochemistry & Cell Biology*, vol. 45, no. 7, pp. 1457–1497, 2013.

[4] A. G. Smith and P. K. Kaiser, "Emerging treatments for wet age-related macular degeneration," *Expert Opinion on Emerging Drugs*, vol. 19, no. 1, pp. 157–164, 2014.

[5] M. Ishikawa, D. Jin, Y. Sawada, S. Abe, and T. Yoshitomi, "Future therapies of wet age-related macular degeneration," *Journal of Ophthalmology*, vol. 2015, Article ID 138070, 10 pages, 2015.

[6] P. S. Mettu, A. R. Wielgus, S. S. Ong, and S. W. Cousins, "Retinal pigment epithelium response to oxidant injury in the pathogenesis of early age-related macular degeneration," *Molecular Aspects of Medicine*, vol. 33, no. 4, pp. 376–398, 2012.

[7] K. Itoh, J. Mimura, and M. Yamamoto, "Discovery of the negative regulator of Nrf2, Keap1: a historical overview," *Antioxidants & Redox Signaling*, vol. 13, no. 11, pp. 1665–1678, 2010.

[8] Z. Zhao, Y. Chen, J. Wang et al., "Age-related retinopathy in NRF2-deficient mice," *PLoS ONE*, vol. 6, no. 4, Article ID e19456, 2011.

[9] S. Shukla and S. Gupta, "Apigenin: a promising molecule for cancer prevention," *Pharmaceutical Research*, vol. 27, no. 6, pp. 962–978, 2010.

[10] R. H. Patil, R. L. Babu, M. Naveen Kumar et al., "Anti-Inflammatory effect of apigenin on LPS-induced pro-inflammatory mediators and AP-1 factors in human lung epithelial cells," *Inflammation*, vol. 39, no. 1, pp. 138–147, 2016.

[11] W. Zhang, H. Qiao, Y. Lv et al., "Apigenin inhibits enterovirus-71 infection by disrupting viral RNA association with trans-acting factors," *PLoS ONE*, vol. 9, no. 10, Article ID e110429, 2014.

[12] A. Andueza, A. García-Garzón, M. Ruiz de Galarreta et al., "Oxidation pathways underlying the pro-oxidant effects of apigenin," *Free Radical Biology & Medicine*, vol. 87, pp. 169–180, 2015.

[13] T.-H. Tseng, M.-H. Chien, W.-L. Lin et al., "Inhibition of MDA-MB-231 breast cancer cell proliferation and tumor growth by apigenin through induction of G2/M arrest and histone H3 acetylation-mediated $p21^{WAF1/CIP1}$ expression," *Environmental Toxicology*, 2016.

[14] K. C. Dunn, A. E. Aotaki-Keen, F. R. Putkey, and L. M. Hjelmeland, "ARPE-19, a human retinal pigment epithelial cell line with differentiated properties," *Experimental Eye Research*, vol. 62, no. 2, pp. 155–169, 1996.

[15] X.-R. Xu, H.-T. Yu, L. Hang, Y. Shao, S.-H. Ding, and X.-W. Yang, "Preparation of naringenin/β-cyclodextrin complex and its more potent alleviative effect on choroidal neovascularization in rats," *BioMed Research International*, vol. 2014, Article ID 623509, 9 pages, 2014.

[16] T. D. Schmittgen, B. A. Zakrajsek, A. G. Mills, V. Gorn, M. J. Singer, and M. W. Reed, "Quantitative reverse transcription-polymerase chain reaction to study mRNA decay: comparison of endpoint and real-time methods," *Analytical Biochemistry*, vol. 285, no. 2, pp. 194–204, 2000.

[17] G. Querques, P. J. Rosenfeld, E. Cavallero et al., "Treatment of dry age-related macular degeneration," *Ophthalmic Research*, vol. 52, no. 3, pp. 107–115, 2014.

[18] C. S. Sackett and S. Schenning, "The age-related eye disease study: the results of the clinical trial," *Insight*, vol. 27, no. 1, pp. 5–7, 2002.

[19] W. T. Wong, W. Kam, D. Cunningham et al., "Treatment of geographic atrophy by the topical administration of OT-551: results of a phase ii clinical trial," *Investigative Ophthalmology and Visual Science*, vol. 51, no. 12, pp. 6131–6139, 2010.

[20] Z. Li, X. Dong, H. Liu et al., "Astaxanthin protects ARPE-19 cells from oxidative stress via upregulation of Nrf2-regulated phase II enzymes through activation of PI3K/AkT," *Molecular Vision*, vol. 19, pp. 1656–1666, 2013.

[21] X.-R. Xu, H.-T. Yu, Y. Yang, L. Hang, X.-W. Yang, and S.-H. Ding, "Quercetin phospholipid complex significantly protects against oxidative injury in ARPE-19 cells associated with activation of Nrf2 pathway," *European Journal of Pharmacology*, vol. 770, pp. 1–8, 2016.

[22] X. Paredes-Gonzalez, F. Fuentes, Z.-Y. Su, and A.-N. T. Kong, "Apigenin reactivates Nrf2 anti-oxidative stress signaling in mouse skin epidermal JB6 P + cells through epigenetics modifications," *The AAPS Journal*, vol. 16, no. 4, pp. 727–735, 2014.

[23] X. Paredes-Gonzalez, F. Fuentes, S. Jeffery et al., "Induction of NRF2-mediated gene expression by dietary phytochemical flavones apigenin and luteolin," *Biopharmaceutics & Drug Disposition*, vol. 36, no. 7, pp. 440–451, 2015.

[24] N. A. Shah, M. R. Khan, B. Ahmad, F. Noureen, U. Rashid, and R. A. Khan, "Investigation on flavonoid composition and anti free radical potential of Sida cordata," *BMC Complementary and Alternative Medicine*, vol. 13, article 276, 2013.

[25] Y.-H. Yeh, Y.-L. Hsieh, and Y.-T. Lee, "Effects of yam peel extract against carbon tetrachloride-induced hepatotoxicity in rats," *Journal of Agricultural and Food Chemistry*, vol. 61, no. 30, pp. 7387–7396, 2013.

[26] H. Guo, S. Kong, W. Chen et al., "Apigenin mediated protection of OGD-evoked neuron-like injury in differentiated PC12 cells," *Neurochemical Research*, vol. 39, no. 11, pp. 2197–2210, 2014.

[27] C.-S. Huang, C.-K. Lii, A.-H. Lin et al., "Protection by chrysin, apigenin, and luteolin against oxidative stress is mediated by the Nrf2-dependent up-regulation of heme oxygenase 1 and glutamate cysteine ligase in rat primary hepatocytes," *Archives of Toxicology*, vol. 87, no. 1, pp. 167–178, 2013.

[28] A.-M. Gao, Z.-P. Ke, J.-N. Wang, J.-Y. Yang, S.-Y. Chen, and H. Chen, "Apigenin sensitizes doxorubicin-resistant hepatocellular carcinoma BEL-7402/ADM cells to doxorubicin via inhibiting PI3K/Akt/Nrf2 pathway," *Carcinogenesis*, vol. 34, no. 8, pp. 1806–1814, 2013.